JIMMA UNIVERSITY

JIMMA INSTITUTE OF TECHNOLOGY

SCHOOL OF ELECTRICAL AND COMPUTER ENGINEERING

GRADUATE PROGRAM IN ELECTRICAL POWER ENGINEERING

TRANSMISSION LINE LOSS MINIMIZATION AND REGULATION OF SYSTEM VOLTAGE USING UPFC (FACTS DEVICES):- CASE STUDY OF SOUTH WESTERN REGION OF ETHIOPIA

By

ALEBACHEW TENNA

THESIS SUBMITTED TO JIMMA UNIVERSITY IN PARTIAL FULFILLMENT OF THE REQUIREMENTS FOR THE DEGREE OF

MASTER OF SCIENCE

IN

ELECTRICAL POWER ENGINEERING

ADVISOR: Dr. ASHAMO ERENGO

CO-ADVISOR: K. SARAVANAN (ASS. PRO.)

January, 2016

Jimma, Ethiopia

JIMMA UNIVERSITY

JIMMA INSTITUTE OF TECHNOLOGY

SCHOOL OF ELECTRICAL AND COMPUTER ENGINEERING

GRADUATE PROGRAM IN ELECTRICAL POWER ENGINEERING

MSc. Thesis

On

TRANSMISSION LINE LOSS MINIMIZATION AND REGULATION OF SYSTEM VOLTAGE USING UPFC (FACTS DEVICES):- CASE STUDY OF SOUTH WESTERN REGION OF ETHIOPIA.

By

ALEBACHEW TENNA

APPROVAL BY BOARD OF EXAMINERS

________________________	________________________
Chairman, school of Electrical and computer Engineering	Signature
Dr. Ashamo Erengo	________________________
Advisor	Signature
K. Saravanan (Ass. Prof)	________________________
Co .Advisor	Signature
________________________	________________________
External Examiner	Signature
________________________	________________________
Internal Examiner	Signature

Declaration

I, the undersigned, declare that this MSc thesis is my original work, has not been presented for fulfillment of a degree in this or any other university, and all sources and materials used for the thesis have been acknowledged.

Alebachew Tenna ________________ ________________

Researcher name Signature Date

The thesis entitled, Transmission line loss minimization and regulation of system voltage using UPFC (FACTS devices) case study of south western region of Ethiopia submitted by Alebachew Tenna to Jimma University in partial fulfillments for the degree of master in Electrical Power Engineering is here by recommended for final evaluation and examination.

Dr. Ashamo Erengo ________________ ________________

Major Advisor name Signature Date

K.Saravanan (Ass. Prof.) ________________ ________________

Co-Advisor

Acknowledgement

First I would like to express my heart gratitude to my major advisor Dr. Ashamo Erengo and Co-Advisor Mr. K. Saravanan (Asst. Prof.) for their guiding and providing constructive ideas in doing this thesis work. Secondly, I wish to express my thanks to Ato Abrham Alem (MSc), Ato Tefera Mekonen (MSc), Ato Henok Ayele (MSc), Ato Melaku Matheos (MSc), and Ato Taye Tolu (MSc) for their unrestricted idea contribution throughout the whole process of this research work. I would also like to thank to Jimma University, Jimma Institute of Technology, school of Electrical and computer engineering for creating such opportunity and facilitating the necessary things for this research work.

Last but not least, I would like to thank all the officers and operators of Ethiopian Electric utility at Addis Ababa main office, load dispatch center office and Jimma district office and substation for their support and treatment during the collection of the required system data.

Table of Contents

List of Figure

List of Tables

List of Abbreviations

AC/DC	Alternating or Direct Current
ATC	Available Transfer Capacity
CCC	Capacitor Commutated Converters
ED	Economic Dispatch
EEU	Ethiopian Electrical Utility
FACTS	Flexible AC Transmission System
GA	Genetic Algorithm
GG	Gilgel Gibe
GTO	Get Turnoff Thyristor
HV	High Voltage
HVAC	High Voltage Alternating Current
HVDC	High Voltage Direct Current
IEEE	Institute of Electrical and Electronics Engineers
IPFC	Interline Power Flow Controller
NTL	Non-Technical Loss
OPF	Optimal Power Flow
PWM	Pulse Width Modulation
SSG	Static Synchronous Generator
SSSC	Static Synchronous Series Compensator
STATCOM	Static Synchronous Compensator
SVC	Static Var Compensator
TCPST	Thyristor-Controlled Phase-Shifting Transformer
TCSC	Thyristor-Controlled Series Capacitor
TCSR	Thyristor-Controlled Series Reactor
TL	Technical Loss
TSC	Thyristor Switched Capacitor
TSR	Thyristor controlled or switched reactor
TSSC	Thyristor-Switched Series Capacitor
TSSR	Thyristor-Switched Series Reactor
UPFC	Universal Power Flow Controller
VSC	Voltage Source Converter

List of Symbols

b	Susceptance
F	Farad
g	Conductance
H	Henry
I	Current
Km	kilometer
KV	kilo Volt
MVA	Mega Volt Ampere
MVar	Mega Volt Ampere Reactive
MW	Mega Watt
P	Real power
P.U	Per Unit
Q	Reactive power
R	Resistance
S	Apparent power
V	Line to line generated voltage
X	Reactance
Y	Admittance
Z	Impedance

Abstract

Now a days, electrical power system is very complex and it requires very careful design of new equipment's which are needed to improve electric power utilization, enhancing power system stability, power loss minimization, power transfer capability and security. The existing power transmission network of Ethiopia consists of 45KV, 66KV, 132KV, 230KV and rarely 400KV lines. This research has been mainly focused on 132KV transmission line of south western region of Ethiopia.

This paper presents the performance analysis, design and incorporation of control device (UPFC) in the existing transmission network of south western region of Ethiopian Electrical Utility by identifying the transmission line losses and voltage regulation problem. The modern power electronics technologies have been used to maintain quality, controllability and power transfer capability of electrical power system. Flexible AC Transmission Systems (FACTS) is one of the modern power electronics technologies which are used in power systems. UPFC is the most powerful and versatile power electronic equipment among the FACTS devices, which has emerged for the control and optimization of power flow in the electrical power transmission system by controlling the impedance, voltage magnitude and phase angle.

For the successfulness of this thesis work primary and secondary data have been collected from the concerned entities. Transmission line data such as generation capacity, transmission line voltage, impedance, transformer data and peak load data have been collected from Ethiopian Electrical Utility. UPFC control strategies have been developed by using mathematical modeling based on the collected data. The design of overall south western region transmission network have been analyzed using MATLAB/Simulink software and comparative analysis of the transmission line with UPFC and without UPFC have been done. This thesis have been showed that the significant improvement of voltage profile, power transfer capability and total power loss minimization have been achieved by incorporating UPFC.

Key words: - Transmission line loss, UPFC, FACTS, Power loss minimization, Voltage regulation.

CHAPTER ONE

INTRODUCTION

1.1. Background

Recent power systems are highly complex and require careful design of new devices, taking into consideration of already existing equipment's, especially for transmission systems in new deregulated electricity markets [1]. This is not an easy task considering that power engineers are severely limited by economic and environmental issues when utilizing the existing transmission network. Due to this, the magnitudes of the power flow in some transmission lines reach closer to their maximum limits, while some other lines may be under loaded compared to their maximum rating. To achieve these new challenges, existing generation or transmission facilities must be utilized more efficiently or new facilities should be added to the existing power system. The development of new generation facility and the new transmission system need more investments and time. Alternatively, load ability of existing systems can be improved by reducing real power loss in the line with the help of Flexible AC Transmission System devices [2].

The two main objectives of FACTS are to increase the transmission capacity and control power flow over designated transmission routes [1]. The improvements in the field of power electronics had a major impact on the development of the concept itself. Since the concept of FACTS was proposed, many various FACTS devices have been utilized to meet a growing demand of the transfer capabilities due to developing transactions in the deregulated environment. Some interesting applications of FACTS devices can be found to economic dispatch(ED), AC/DC optimal power flow (OPF), available transfer capability (ATC), contract path based electricity trading, and transmission congestion management.

UPFC is a versatile FACTS device; has the unique capability to control simultaneously both an active and reactive power flows on the transmission line [1]. So, there has been increasing interest in the analysis of UPFC in power system. The UPFC can provide simultaneous control of all basic power system parameters such as transmission line voltage, impedance and phase angle. The controller can fulfill the functions of shunt compensation, series compensation and phase shifting meeting multiple control objectives.

Currently in Ethiopia the generating units are increasing with no corresponding increase in the transmission network. The existing transmission network has more transmission line losses due to overloading and aging problems. When there is a disturbance in existing 132KV transmission line, bus voltage instability and power loss will be occurred. This leads to system voltage regulation problems. Therefore, it is necessary to design appropriate controlling devices in order to enhance system voltage regulation of the transmission network of Ethiopia.

In Ethiopia, a commonly used transmission line ratings are 45, 66, 132, 230, and rarely 400 KVs; whereas for distribution system either 33 or 15KV transmission lines are used. This thesis has been focused on 132KV transmission network of the south western region of Ethiopia. The losses in this transmission line are more, since this transmission line covers large distances and most of this transmission line is aged.

1.2 Problem Statement

The Ethiopian government currently gives much emphasis to increase more generating units to balance with power demand without corresponding increase in the transmission network. It has to be understood that the result of any increase in the transmission power losses in a network is further loading of the system elements which intends to shorten their life as the losses are dissipated in the form of heat. Higher losses also require a higher rate of the generation sources commitment, which in other words means a higher installed power. Consequently, more transmission line losses will imbalance the energy demand and the power supply.

Therefore, this leads the whole system to be disturbed, hence bus voltages lower. If this is not prevented by use of protective devices such as compensating devices, it can lead to the failure of the transmission network and power interruption. Due to the complexity of the grid and expenditure of protection system, the Ethiopian power transmission system is not well protected. Thus, the state of transmission losses in the existing south western transmission network of EEU should have to be critically analyzed and technology based measures towards loss reduction should have to be implemented. Therefore, in this thesis UPFC was incorporated into the existing system to solve the above stated problems.

1.3 Motivation

Currently, Ethiopia is generating large amounts of power. But the energy demand and the supply energy is not in a balanced situation because of the radial increment of the demand. To meet demand and generation of power it is necessary to reduce the power losses. So my motivation is to minimize the large amount of electrical energy wastage due to transmission line losses and unregulated bus voltage in the south western region of country and the economic effect of it on the country.

1.4 Objectives of the Study

1.4.1. General Objective

The main objective of this research is to minimize transmission line loss and regulate system voltage using UPFC (FACTS devices) with MATLAB/Simulink software for south western region of Ethiopia.

1.4.2. Specific Objectives

The specific objectives of this research are as follows:

- To study performance analysis of the existing transmission network
- To study the load flow, identify the transmission line losses and system voltage profile of the study area
- To model UPFC control strategies for transmission network
- To analyze the impact of UPFC in the transmission line
- To evaluate the performance of the transmission network of south western region of Ethiopia by incorporating UPFC using MATLAB/Simulink software

1.5 Research Questions

At the end of the study the researcher was able to answer the following proposed research questions.

1. How much power is lost using the existing system in the study area?
2. How can the transmission line losses will be minimized?
3. Is it possible to incorporate UPFC in order to reduce the transmission line loss and improve system voltage for the study area?
4. How the transmission line can be used efficiently and economically?
5. What is the performance of the transmission network using the proposed UPFC system?

1.6 Scope of the Study

The scope of this research is to analysis, design, simulate and evaluate the performance of the transmission line without UPFC and with UPFC in order to minimize the transmission line losses and improve bus voltage profile of the selected case study using MATLAB/Simulink software.

1.7 Significance of the Study

The study will be useful for power system planners, load forecasting and decision makers since it presents a concern on how much primary power is lost on the transmission network. As EEU is exporting electrical energy and on the way to increase the export of energy, an additional energy from loss reduction will benefit the corporation to earn more profit. The electrical system losses of EEU should have to be investigated so that appropriate loss mitigation measures can be undertaken. Thus the result of this thesis work will be best input for those study groups and researchers who are working on the implementation of bulk power transmission system loss minimization.

1.8 Limitation of the Study

There are some limitations that have been faced in this study. The first limitation was some offices of EEU are not cooperative to give the recorded data because some data are recorded on hardcopy. The second limitation was because of the budget allowed by Jimma University is not enough for this thesis works it makes difficult to record all hard copy data in to soft copy in order to make it ready for the software. This limitations makes the research difficult to finish on time.

1.9 Thesis Outline

This thesis work consists of six chapters. The first chapter discuses about the introduction i.e. Background, Statement of the problem, Motivation, Objectives, Research Questions, Scope of the study, Significance of the study and limitation of the study. Chapter two looks different review literatures (books, thesis papers, journals and conference researches) and the basic understanding of transmission line losses. Chapter three discusses about the methodology and data analysis of this thesis. In chapter four modeling of UPFC for transmission line loss minimization and system voltage regulation are included. Chapter five discusses about result and discussion of the south western transmission network of the study area without UPFC and with UPFC. Chapter six includes conclusion and recommendation of the study for future work.

CHAPTER TWO

LITERATURE REVIEW AND BASIC UNDERSTANDING OF TRANSMISSION LOSSES

2.1. Literature Review

S.V. Ravi Kumar and A. Siva Nagaraju (2007) [3] have done a paper in the title of loss minimization by incorporating of UPFC in load flow studies. In this paper the mathematical model for UPFC which is referred as UPFC injection model is derived. The UPFC injection model is easily incorporated in newton-Raphson power flow model to study its effect for power flow control and loss minimization in the power system. This paper shows that UPFC has the capability of regulating the power flow and minimizing the power loss simultaneously. In this paper the idea is good but it doesn't use real time analysis.

M. Kowsalya et.al (2009) [4] has used particle swarm optimization technique in order to loss optimization for voltage stability enhancement incorporating UPFC. In this paper voltage stability enhancement with the optimal placement of UPFC using stability index such as nodal analysis, Voltage Phasor method is made and the loss minimization including UPFC is formulated as an optimization problem. This paper proposed particle swarm optimization for the exact real power loss minimization including UPFC and the implementation of loss minimization for the optimal location of UPFC was tested with IEEE-14 and IEEE-57 bus system. But the drawback of this system is it uses the evolutionary optimization techniques and the algorithm is only used to determine the optimal location of the UPFC.

Mark NdubukuNwohu (2010) [5] has discussed on the optimal location of unified power flow controller in Nigerian Grid system. On his research he tried to present an approach to find and choose the optimal location of UPFC based on the sensitivity of the total system active power loss with respect to the control variables of the UPFC. He have developed the control system of the UPFC's injection model to avoid a voltage collapse which are explored by analyzing multi-machine test system. The software MATLAB/Simulink was used in this study to evaluate voltage stability of the system and to determine optimal placement of UPFC in order to provide better damping during transient and dynamic control. Even though the idea is transmission line loss minimization but it chooses the optimal location based on sensitivity of the total active power loss only and not for steady state analysis.

D. BalaGangi Reddy and M. Suryakalavathi (2011) [6], concerns on modeling, analysis and optimal location of UPFC for real power loss minimization. In this paper, an improved UPFC steady-state mathematical model for the implementation of the device in the conventional Newton Raphson (NR) power flow algorithm has been developed from a two-voltage source equivalent of UPFC. An advantage of this model is that the model is capable of taking the losses of UPFC into account. GA is used for optimal placement of UPFC to minimize the total system losses. The proposed approach is tested on IEEE-14 bus test system. For different loadings this researcher tried to show that using optimal placement and optimal settings of UPFC, system line losses are reduced significantly. Its drawback is it doesn’t include optimal power flow and improvement of system voltage.

Thomas John (2011) [7] has done a research on Line loss minimization and voltage regulation using UPFC. This paper presents a method for achieving line loss minimization and voltage regulation in the given power system. In order to achieve these two objectives simultaneously he has used UPFC. In this paper, the injection model of UPFC is used to investigate its effects on bus voltages and loss reduction in a power system.

Sreerama Kumar R. et. al (2014) [8], This paper proposed the application of genetic algorithm for the determination of the optimal placement of unified power flow controller in a power system so as to minimize the system losses and enhance the voltage profile. The method can identify the line in which the UPFC can be located. The genetic algorithm proceeds with an initial randomly generated population. The effectiveness of each of the individuals in the population is evaluated on the basis of a fitness function defined to reflect the effect of the real power losses in the system. Preliminary investigations indicate the effectiveness of this approach in minimizing the transmission line losses and the enhancement of the voltage profile. But still there is a vast deviation of voltage.

A.Anbarasan, M.Y. Sanavullah and S. Ramesh. (2014) [2], this paper presents a method to reduce the transmission line losses in the power system network using FACTS devices. They have tried to propose identification of suitable location of these FACTS devices. The effectiveness of the proposed work is analyzed using IEEE 14-bus test system. The proposed method identifies suitable devices, on suitable lines at suitable location. In this paper the existing transmission line facility are utilized effectively and economically to transfer the power to the consumer but the continuation power flow method is used to identify weakest bus in the system.

Generally it is possible to say in one way or the other the above transmission line loss minimization and voltage regulation includes 1) all the parameters are not controlled 2) The voltage deviation is not at the required level. 3) Uses the evolutionary optimization techniques. The proposed MATLAB/Simulink model for transmission line loss minimization and voltage regulation using UPFC avoids the above discussed issues.

2.2. Electric System Losses

The population Growth and increase of industrialization requires large amount of electrical energy. Unfortunately, electricity is not always used with similar demand in the same location as it has been generated. So, long cables or wires are used to transmit the generated electrical energy either through underground or overhead transmission network, which is referred to as transmission of electrical energy. Along the way, some portion of the generated power is lost due to several reasons. But the main issue is whether this loss is at its lowest possible range of modern energy efficiency or not with this range. Transmission of electrical power and energy must be done at minimum transmission line losses which are referred as technical and non-technical transmission line losses. The losses are commonly classified into two categories: technical losses and non-technical losses [9].

2.2.1. Technical Losses

In the process of supplying electricity to the customer electrical transmission power losses can occur due to technical and non-technical losses. In transmission, sub-transmission and distribution of electrical power the equipment's and conductors can cause technical losses due to dissipation of energy on these devices. There are different loss minimization techniques used in order to reduce technical losses to the optimal level. Depending on the transmission system and stage of power transformation technical losses can be categorized in to transmission line losses (400kV/220kV/132kV/66kV), Sub-transmission line losses (33kV /11kV) and Distribution losses (11kV/0.4kv) [9], [10].

Depending on the origin of loss and due to current flowing in the electrical network technical losses can be classified as copper (resistive) losses, induction and radiation losses, dielectric (leakage) losses and corona losses. Due to the finite resistance of the conductors copper losses are caused by I^2R losses that are produced in all conductors. This type of losses are maximum at peak load condition because this loss depends upon the value of flow of current at that line. The heating effect on the dielectric material between the conductors produces dielectric losses. The effect of electromagnetic field around the conductors creates induction and radiation losses. If the line to line voltage exceeds corona threshold there is a corona loss. Corona can occur within holes of an insulator, at the conductor or at the insulator interface. The corona loss is affected by the type of the surface of the insulator material or conductor such as rough surfaces are more exposed to corona. The breakdown voltage of the insulator material decreases due to the roughness of the surface. Corona is indicated by a visible light in form of dim violet glow, hissing noise and production of ozone gas in an overhead transmission line. The existence of corona on the transmission network degrades the insulation and this reduces the reliability of the transmission network. Without any protection corona effects are continuing, collective and failure of the system can occur. Dusts, water drops, surface irregularities, conductor voltage level, diameter and shape affects the performance and conductor's electrical surface gradients. Therefore, the electrical transmission network corona losses are converted into sound, noise, heat and air components chemical reaction. Generally, corona is a low energy process, over long periods of time, it can significantly degrade insulators, causing a system to fail due to dielectric breakdown [9], [10] and [11].

The other common way of classification of technical losses are load (variable) losses and no-load (fixed) losses.

Load losses depends on the system loads. The system component through which flow of electric current is there would be the cause of load losses. The amount of electricity distributed varies the load losses and this losses are proportional to the square of the current. In the transmission network the losses would be high with small amount of increase in current. On the transmission network the variable losses accounts 2/3 (66.67%) to 3/4 (75%) of technical losses. For the particular load the losses can be reduced by increasing the cross sectional area of transmission lines. Variable losses on the line can be influenced by impedance losses and losses caused by constant resistance [12]. This study mainly focuses on minimizing variable losses by regulating system voltage in order to reduce transmission line active and reactive power losses.

Fixed losses do not vary with respect to current. These losses take the form of heat and noise, occur as long as a transformer is energized. The fixed losses accounted between 1/4 (25%) and 1/3 (33.33%) of technical losses on transmission network. Fixed losses on a network can be influenced in the ways of corona losses, leakage current losses, dielectric losses, open-circuit losses, losses caused by continuous load of measuring elements and losses caused by continuous load of control elements [12].

The computing and controlling of technical losses are possible by using different loss minimization techniques. As it have been discussed above there are different causes of technical losses. Some of the causes are losses due to overloading of the line and poor system voltage profile, long single phase lines, harmonics distortion, improper earthing at consumer end, unbalanced loading and losses due to poor standard of equipment's [11].

2.2.2. Non-Technical Losses

Non-Technical losses (NTL) are man induced losses which are produced due to the effect of external actions to the power system and in which the computation of technical losses fail. Measuring non-technical losses is the difficult thing. This type of losses are unexplained for by the system operators and there is no recorded information. NTL occur as a result of electricity theft, arranging false readings by bribing meter readers, tapping (hooking) on LT lines, metering inaccuracies, inadequate accounting and record keeping, delay in meter reading and unmetered energy. Theft of electrical power is energy which is delivered to demand but not measured by the energy meter. Meter tampering, illegal connection to the grid or bypassing the meter causes theft of electrical power. Losses due to metering inaccuracies are the difference between the amount of energy actually delivered through the meters and the amount of energy registered by the meters. The effects of non-technical losses are that those customers who are accurately billed and regularly paying their bills are funding those users who do not pay for electricity consumption [9], [11] and [13].

2.3. Factors Influencing System Losses

The factors that influence system losses are circulating current, phase balancing, power factor and voltage regulation. Flow of circulating current is the failure to maintain a flat voltage profile across modern highly interconnected networks. Therefore to minimize losses it is important to maintain voltage limits to its specified value for a transmission network. Heavily loaded lines can be balanced with other phase by using phase balancing system, the maximum deviation from the average value is below 10% [9]. At unity power factor there will be minimum current flow but any reactive component will cause the current to increase as a result real power losses also increases. When the current increases in the transmission system the voltage drop due to line resistance is high and the transmission network voltage reduces at receiving end side when comparing to unity power factor. It is necessary to reduce energy losses in transmission lines by maintaining the system voltage profile [9].

2.4. Analysis of Technical Losses in Power System

Electrical system losses can be determined by using different techniques. The losses incurred in resistive materials can be reduced by means of reducing the current, reducing the resistance and the reactance of the line and regulating system voltages [14].

Electrical power system losses can be computed using several formulae/techniques by including the arrangement of generation station and loads, [14] by means of any of the following methods:

i. Computing transmission losses as I^2R

ii. Differential power loss method

iii. Computing line flows and line losses.

iv. Analyzing system parameters

v. Using loss coefficient formula B_{ij}

vi. Load flow simulation

2.4.1. Computing Transmission Losses as I^2R

Consider a simple three-phase radial transmission line between two points of generating and receiving ends as illustrated in one line diagram of figure2.1 below, including the generated power P_G, line resistance R, line reactance jx and load [14].

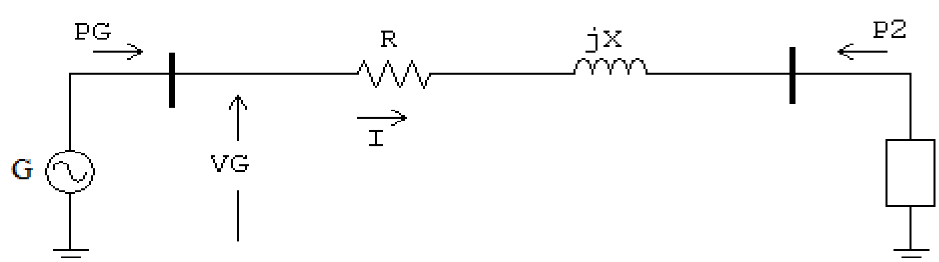

Figure 2.1: One line diagram with one generation and one load (source: [14])

Transmission line real power loss is calculated as,

$$P_{Loss} = 3I^2R \qquad (2.1)$$

Then the current which is flowing throughout the line can be determined as,

$$|I| = \frac{P_G}{\sqrt{3}V_{G}\cos\phi_G} \qquad (2.2)$$

Where,

I is the current

R is the resistance of the line in ohms per phase.

P_G is the power generated

V_G is the magnitude of the line to line generated voltage

$\cos\Phi_G$ is the generator power factor

Substituting equation 2.2 into equation 2.1, we can get:

$$P_{Loss} = \frac{R}{V_G^2\,(\cos\phi_G)^2} P_G^2 \qquad (2.3)$$

Assuming constant generator voltage and power factor, we can write the losses as

$$P_{Loss} = BP_G^2 \qquad (2.4)$$

Where,

$$B = \frac{R}{V_G^2\,(\cos\phi_G)^2} \qquad (2.5)$$

2.4.2. Using Loss Coefficient B_{ij}

Losses can be expresses as second order function of generated power by using B-coefficient method. If there are two generating power plants present to supply the load as shown in figure2.2, then transmission losses can be expressed as a function of the two plant loadings [14].

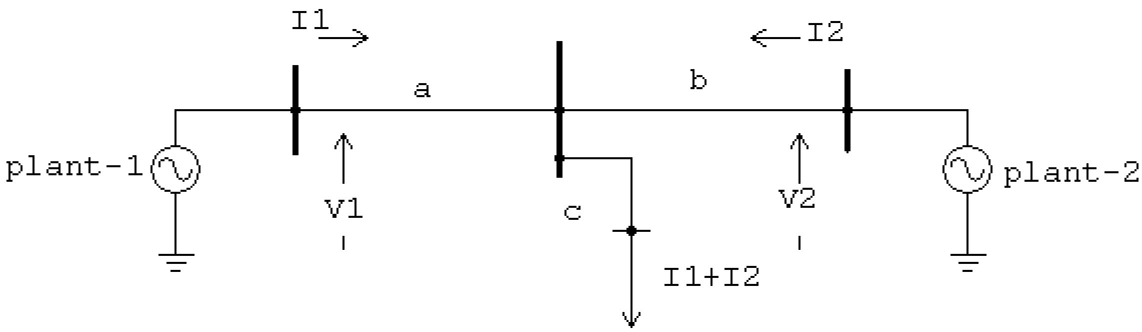

Figure 2.2: Simple radial systems with two generation plant and one load bus (source: [14])

The above transmission system real power loss in terms of resistance and current flow is given by:

$$P_{Loss} = 3|I_1|^2R_a + 3|I_2|^2R_b + 3[|I_1| + |I_2|]^2R_c \qquad (2.6)$$

But the currents I_1 and I_2 are given by,

$$I_1 = \frac{P_1}{\sqrt{3}V_{1}\cos\phi_1} \qquad (2.7)$$

$$I_2 = \frac{P_2}{\sqrt{3}V_{2}\cos\phi_2} \qquad (2.8)$$

Substituting equation 2.7 and 2.8 into equation 2.6 equation we can get,

$$P_{Loss} = \frac{P_1^2(R_a+R_c)}{|V_1|^2\ (\cos\phi_1)^2} + \frac{P_2^2(R_b+R_c)}{|V_2|^2\ (\cos\phi_2)^2} + \frac{2R_c(P_1+P_2)}{|V_1|\,|V_2|\cos\phi_1\ \cos\phi_2} \qquad (2.9)$$

In the equation 2.9 above the coefficients of generated power are functions of line resistance, voltage and power factor; and known to be B-coefficient. Therefore, each B-coefficients are given by:

$$B_{11} = \frac{(R_a+R_c)}{|V_1|^2\ (\cos\phi_1)^2} \qquad (2.10)$$

$$B_{22} = \frac{(R_b+R_c)}{|V_2|^2\ (\cos\phi_2)^2} \qquad (2.11)$$

$$B_{12} = \frac{R_c}{|V_1|\ |V_2|\cos\phi_1\ \cos\phi_2} \qquad (2.12)$$

Then, the active power loss P_{Loss} can be expressed in terms of B-coefficient and power generation as [14]:

$$P_{Loss} = B_{11}P_1^2 + B_{22}P_2^2 + 2B_{12}P_1P_2 \qquad (2.13)$$

From B-coefficient method we can easily understand that increasing the system voltage level or power factor or reducing line resistance will minimize the transmission line real power loss.

For the interconnected transmission network which have more than two generation plant, the transmission line real power loss using B-coefficient equation is given by:

$$P_{Loss} = \sum_{k=1}^{n}\sum_{m=1}^{n} P_k\ P_m B_{km} \qquad (2.14)$$

Where,

- P_k and P_m are the generated powers from all generator plants, n is the total number of generators.
- B_{km} are commonly referred as the loss coefficients and are functions of line resistance, line voltage and power factor.

2.4.3. Differential Power Loss Method

Real power loss in the transmission network can be expressed as the difference between the transmitted power and received power [14] [15].

$$P_{loss} = P_{Sent} – P_{Received} \qquad (2.15)$$

As expressed in equation 2.15 the transmission line losses can be easily determined by subtracting the receiving end power from the sending end power. But this method is used only if both sending end power and receiving power are known only. This method may not be applicable for the large interconnected system because the system will be complex.

If we have buses i and k, then the complex power leaving bus-i is given by [15],

$$S_i = P_i + jQ_i = V_i i_i^* \tag{2.16}$$

The complex power which is entering bus-k is also given by [15],

$$S_k = P_k + jQ_k = V_k i_k^* \tag{2.17}$$

Therefore, from equation 2.16 and 2.17 the real power loss due to I^2R on the transmission line between bus-i and bus-k is determined as [15],

$$P_{loss,\, i\text{-}k} = P_i - P_k \tag{2.18}$$

Similarly, the reactive power loss due to I^2X on the transmission line between bus-i and bus-k is determined as [15],

$$Q_{drop,\, i\text{-}k} = Q_i - Q_k \tag{2.19}$$

2.4.4. Computations of Load (line) Flows

Computation of transmission line losses for the given network as shown in the figure2.3 that shows a line connecting i^{th} and k^{th} buses [14], [16].

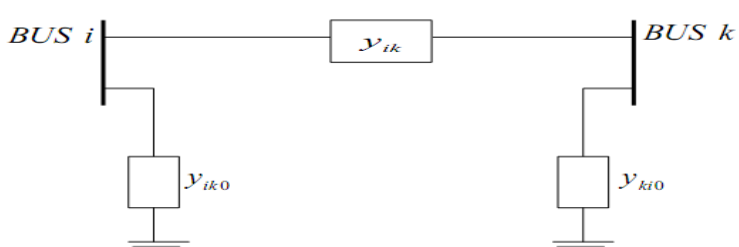

Figure 2. 3: Transmission line between two buses (source: [14], [16])

The current flowing from bus-i towards bus-k is given by,

$$I_{ik} = (V_i - V_k)Y_{ik} + V_iY_{iko} \tag{2.20}$$

Where V_i and V_k are the bus voltages at the buses i and k respectively.

The power flow in the line i-k at bus-i is given by [14] [16]:

$$S_{ik} = P_{ik} + Q_{ik} = V_iI_{ik}^* \tag{2.21}$$

Substituting equation 2.20 into equation 2.21 we can get,

$$S_{ik} = V_i\,(V_i^* - V_k^*)\ Y_{ik}^* + V_iV_i^*Y_{iko}^* \tag{2.22}$$

Similarly, the power flow in the line i-k at bus k is given by,

$$S_{ki} = V_kI_{ki}^* \tag{2.23}$$

$$S_{ki} = V_k\,(V_k^* - V_k^*)\ Y_{ik}^* + V_kV_k^*Y_{kio}^* \tag{2.24}$$

Where,

S_{ik} = apparent power injection from bus i to the line between bus i & bus k

S_{ki} = apparent power injection from bus k to the line between bus i & bus k

I_{ik}^*= complex conjugate of current I_{ik}

I_{ki}^* = complex conjugate of current I_{ki}

Then apparent power flow over all the lines can be computed by using the above equations 2.22 and 2.24. The apparent power losses of $(i\text{-}k)^{th}$ line is given by the sum of the power flows determined from above equations which is expressed as,

$$S_{Lik} = S_{ik} + S_{ki} \tag{2.25}$$

Where, S_{Lik} = apparent power loss in a single line between bus-i and bus-k

Therefore, the total apparent power loss in all lines can be calculated as the sum of losses in all lines.

$$S_{loss} = \sum S_{Lik} \qquad (2.26)$$

Where, S_{loss} is the total apparent power loss of all the transmission lines.

2.4.5. Dopezo Transmission Loss Formula

Dopezo et al. have derived an exact formula for calculating transmission losses by making use of the bus powers and the system parameters. Let S_i be the total injected bus apparent power at bus i and is equal to the generated power minus the load at bus i. The summation of all such powers over all the buses gives the total losses of the system [14].

$$S_{Loss} = P_L + jQ_L = \sum_{i=1}^{n} S_i = \sum_{i=1}^{n} V_i I_i^* = V_{bus}^T I_i^* \qquad (2.27)$$

$$V_{bus} = Z_{bus} I_{bus} \qquad (2.28)$$

Where,

P_L and Q_L are the real and reactive power loss of the system.

V_{bus} and I_{bus} are the column vectors of voltages and currents of all the buses respectively.

Z_{bus} is the bus impedance matrix of the transmission network

The impedance matrix is given by:

$$Z_{bus} = R + jX = \begin{bmatrix} r_{11} & \cdots & r_{1n} \\ \vdots & \ddots & \vdots \\ r_{n1} & \cdots & r_{nn} \end{bmatrix} + j \begin{bmatrix} x_{11} & \cdots & x_{1n} \\ \vdots & \ddots & \vdots \\ x_{n1} & \cdots & x_{nn} \end{bmatrix} \qquad (2.29)$$

Since Z_{bus} is symmetrical matrix then $Z_{bus}^T = Z_{bus}$

The bus current vector I_{bus} can also be written as the sum of a real and reactive component of current vectors as,

$$I_{bus} = I_p + jI_q = \begin{bmatrix} I_{p1} \\ I_{p2} \\ \vdots \\ I_{pn} \end{bmatrix} + j \begin{bmatrix} I_{q1} \\ I_{q2} \\ \vdots \\ I_{qn} \end{bmatrix} \quad (2.30)$$

From the above equation we can simplify as,

$$P_L + jQ_L = I_{bus}{}^T Z_{bus}{}^T I_{bus}{}^*$$

$$= (I_p + jI_q)^T (R + jX) (I_p - jI_q) \quad (2.31)$$

Separating the real and reactive power we can get the following equation,

$$P_L = I_p{}^T R\, I_p + I_p{}^T X\, I_q + I_q{}^T RI_q - I_q{}^T XI_p \quad (2.32)$$

Since X is symmetrical matrix,

$$I_p{}^T X\, I_q = I_q{}^T XI_p \quad (2.33)$$

Then,

$$P_L = I_p{}^T R\, I_p + I_q{}^T RI_q \quad (2.34)$$

Generally the real power loss can be expressed as,

$$P_L = \sum_{i,k=1}^{n} r_{ik}(I_{pi}I_{pk} + I_{qi}\, I_{qk}) \quad (2.35)$$

From equation 2.35 above the transmission loss has been expressed in terms of bus currents. The generated power, the power at the buses and the bus voltage profile are known by the system operators. Therefore, it is more practical to express real power in terms of these quantities.

The bus power at bus-i is expressed as,

$$P_i + jQ_i = V_i I_i^* = V_i(I_{pi} - jI_{qi}) = |V_i|(\cos\delta_i + j\sin\delta_i)\,(I_{pi} - jI_{qi}) \quad (2.36)$$

Where δ_i is the phase angle of voltage V_i with respect to the reference voltage (slack bus voltage) [14].

Then separating the real and imaginary parts of the bus power from equation 2.36, we have:

$$P_i = |V_i|\, I_{pi} \cos\delta_i + |V_i|\, I_{qi} \sin\delta_i \quad (2.37)$$

$$Q_i = |V_i|\, I_{pi} \sin\delta_i - |V_i|\, I_{qi} \cos\delta_i \quad (2.38)$$

Solving equations 2.37 and 2.38 simultaneously we can determine I_{pi} and I_{qi} as,

$$I_{pi} = \frac{1}{|V_i|}(P_i \cos\delta_i + Q_i \sin\delta_i) \quad (2.39)$$

$$I_{qi} = \frac{1}{|V_i|}(P_i \sin\delta_i - Q_i \cos\delta_i) \quad (2.40)$$

2.5. Loss Minimization Techniques

Transmission line loss consists of two major loss components: real and reactive. Real part cost money, millions of dollars per year and reactive part costs voltage stability. Both of them need to be assessed properly for power system security and stability. Line flow Method, B-coefficient method, dopezo method, differential power loss method, transmission loss expressions are used to calculate transmission line loss [14]. Out of these loss calculation methods, differential power loss calculation method is the simplest one for few bus transmission network. On the other hand computing line flow method is the most popular and powerful, since it gives all power flows, line losses and voltage level of all buses in a system.

The capacity of Power generated, transmitted and distributed increases to overcome the demand, so do the requirements for a high quality, secured and reliable supply. Therefore, the control of active power, reactive power and system voltage in an electrical power system is important for proper utilization of electrical equipment in order to reduce transmission line losses and to increase the ability of the electrical transmission network to withstand and reduce voltage drop on the line [17].

Reducing transmission line losses requires either reduction the resistance of the line or in the current flowing through the line. In other words regulating system voltage reduces transmission line losses.

There are many transmission line loss reduction strategies which is useful to implement in electrical power industry. The main problem is how to utilize the existing resources effectively at optimum level. So it is necessary to understand different loss minimization techniques which are implemented in power industry from different literatures and how they are applicable in electrical transmission system. Present day transmission line loss reduction and voltage regulation techniques used in utility companies are described below.

2.5.1. Raising Transmission Line Nominal Voltage

The generated electrical power is transmitted through transmission lines in order to deliver the power to the demand side. Whenever power is transmitted through out the line there will be loss due to the resistive effect of the conductors. Even if the overall transmitted power, the conductor type and the conductor size is the same low voltage high current transmission would have much losses than high voltage low current transmission lines. The voltage drops occur on the transmission line when power is transmitted from the sending end to receiving end. This voltage drop along the AC line is directly proportional to line resistance, reactance and reactive power flow [18].

Therefore, it is necessary to increase the nominal voltage of transmission line to minimize the losses. This type of transmission line loss minimization technique requires construction of new transmission lines, new substations or upgrading the exciting substations. This technique requires high investment (initial) cost and it takes long time planning.

2.5.2. Bundling Conductors

One of the transmission line loss minimization method is bundling conductors together. The existing single conductor per phase can be combined together with a new conductor stringing in parallel to existing conductor. When we bundle conductors the electrical characteristics such as resistance and inductance of the transmission line reduces. The reduction of electrical characteristics (resistance and inductance) reduces transmission line losses because line losses are directly proportional to resistance and inductance of the line.

Bundling the existing conductor with other new conductor of the same conductor type, the same length, same diameter reduces resistance of the line by 50%. This will reduce the transmission line loss by half. When we compare with raising transmission line nominal voltage bundling of conductors can reduce investment cost. Removing and replacing the existing conductor with the installation of single conductor of twice the diameter of existing conductor will reduce loss but it need high initial cost. The drawback of bundling the existing conductor with other new conductor will increase the conductor weight on the existing structure.

2.5.3. HVDC Transmission

The development of power electronics based semiconductor devices leads to HVDC transmission system. The essential process that occurs in an HVDC transmission network is the conversion of electrical current from AC to DC at the sending end, and from DC to AC at the receiving end [19].

There are three ways of achieving conversion of electrical current in HVDC transmission network. These are natural Commutated Converters, capacitor Commutated Converters and forced Commutated Converters [19].

Natural commutated converters are most used in the HVDC Transmission systems. Thyristor plays the main role in the conversion process, which is a controllable semiconductor device that can carry very high current and is capable to block very high voltages. Thyristor valve can be created by connecting thyristors in series, capable to operate at very high voltages. The thyristor valve is operated at normal frequency of 50/60Hz and the DC voltage level of the bridge can be changed by means of a control angle. Therefore, the ability of these devices makes it to control the transmitted power efficiently and rapidly [19].

The Capacitor Commutated Converters (CCC) uses capacitor commutation inserted in series between converter transformer and thyristor valves. The capacitor commutation improves the failure of converters commutation performance [19].

Forced Commutated Converters has a lot of advantages such as feed of passive networks, independent control of active and reactive power and power quality. The valves of these converters have the ability to turn-on and to turn-off. They are known as voltage source converters (VSC) commutating at high frequencies. The converters operation can be achieved by Pulse Width Modulation technique (PWM). PWM can provide to control both active and reactive power independently. Due to this PWM voltage source converter considered as ideal component in the transmission network [19].

The overall investment costs for HVDC transmission network is higher when we compare to high voltage AC transmission network. But the costs of overhead transmission lines, land acquisition, operation and maintenance are lower in the HVDC transmission network. The loss levels at the starting stage are higher in HVDC transmission network but they do not vary with increasing the distance. In contrast, loss levels are minimum at initial stage but increase with distance in HVAC transmission network. Figure 2.4 shows the comparison of cost between HVDC and HVAC transmission [19].

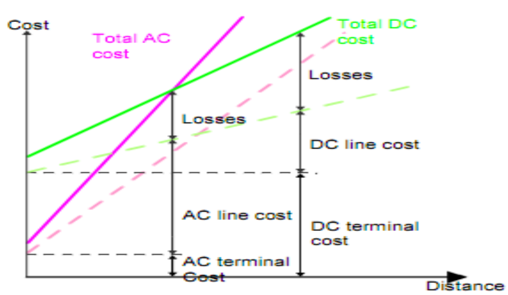

Figure 2.4: Comparison of HVDC and AC transmission line cost with respect to distance of transmission line (source: [19])

Line loss comparison between HVDC and HVAC can be made assuming the same power P, phase resistance R and peak voltage V.

For HVDC bipole,

$$P = 2VI_{DC} \tag{2.41}$$

And for 3-phase AC transmission line,

$$P = 3V_{Rms}I_{Rms} = 3\frac{V}{\sqrt{2}}I_{Rms} \tag{2.42}$$

Equating the above two equations,

$$2VI_{DC} = 3\frac{V}{\sqrt{2}}I_{Rms}$$

$$I_{Rms} = 2\frac{\sqrt{2}}{3}I_{DC} = 0.943I_{DC} \tag{2.43}$$

Then, the losses are given by,

$$\text{Real power } AC_{loss} = 3I^2_{Rms}R = 3(0.943IDC)^2R = 2.668I^2_{DC}R \tag{2.44}$$

$$\text{DC power losses} = 2I^2_{DC}R \tag{2.45}$$

$$\frac{\text{AC loss}}{\text{DC power losses}} = \frac{2.668I^2_{DC}\text{R}}{2I^2_{DC}\text{R}} = 1.333 \tag{2.46}$$

Therefore, the Dc transmission power loss is 75% of that of AC transmission losses.

HVDC lines have some of the advantages in efficiency over AC transmission lines. The absence of reactive current flow and skin effect are the two phenomena for boosting the efficiency of HVDC transmission. According to an ABB study, HVDC lines provide 25 percent lower transmission line losses, two to five times the capacity of AC lines at similar voltages and there is ability of power flow control [12]. The main drawback of this type of loss minimization technique is it requires high investment cost in order to change the existing AC transmission lines to HVDC.

2.5.4. Changing Conductors

Transmission line losses can be reduced by replacing the existing conductor with one of larger diameter or modern conductors having lower resistance for the same diameter. However, larger conductors significantly increase strain-structure tension loads and increase transverse wind/ice conductor loads on suspension structures. The use of modern conductors with the same diameter rather than replacing with large conductors has the primary advantage of minimizing structure modifications of the transmission system but it may not reduce transmission line losses as the same as large conductors.

2.5.5. Series Compensation

The overall series line impedance of the transmission line can be controlled by series compensation. Series reactive impedance of the transmission line limits the transmitted electrical power. A series compensator reduces series line impedance by adding a voltage to transmission line in opposition to transmission line voltage drop.

2.5.6. Shunt Compensation

Shunt compensation used in transmission network in order to regulate the voltage magnitude, improve quality of voltage and enhance stability of the transmission system. The line over voltage can be reduced using shunt connected reactors by consuming reactive power and shunt connected capacitors are used to maintain system voltage by compensating reactive power.

2.5.7. FACTS Devices

Due to economic and environmental constraints, it is forcing the power utilities to meet the future demand by fully utilizing the existing resource. This increases the transmission facilities without constructing new transmission lines. Steady state power flow or dynamic stability control is achieved by using flexible alternating current transmission system providing new facilities. FACTS devices are used to control the phase angle, voltage and impedance of high voltage AC lines. By using FACTS devices maximum benefits of transmission system can be attained i.e.

utilization of existing transmission assets; increased transmission system availability and enabling environmental benefits. The placement of FACTS on transmission line can help to reduce flows in heavily loaded lines, reduce power system loss and improve the system voltage profile [17], [20]-[23].

There are different types of FACTS devices. According to their connection to the transmission line they are classified into four main categories. These are shunt connected FACTS devices, series connected FACTS devices, combined series-series connected FACTS devices and combined series-shunt connected FACTS devices [17] [20], [23].

2.5.7.1 Series Connected FACTS Devices

Series FACTS devices could be variable impedances such as capacitor, reactor or power electronics based variable sources of different frequencies. These devices inject voltage in series with the transmission line. The series controller absorbs or produces reactive power when the line voltage is in phase quadrature with the line current otherwise the controllers absorbs or produces real and reactive power. Types of this devices include Static Synchronous Series Compensator, Thyristor-Switched Series Capacitor, Thyristor-Controlled Series Capacitor, Thyristor-Switched Series Reactor and Thyristor-Controlled Series Reactor. The flow of power and current in the system can be controlled and system oscillation can be damped using such devices [17], [22], [23].

2.5.7.2. Shunt Connected FACTS Devices

Shunt connected FACTS devices are variable impedance, variable source, or a combination of these [23]. Current is injected by shunt controller into the system at the point where they are connected to the system. There is a variable current flow to system because of injected current to the system due to shunt connected variable impedance to transmission line. If the current injected is in phase quadrature with the line voltage the controller modifies reactive power and otherwise the controller modifies real power. The families of such Devices are Static Synchronous Generator, Static Var Compensator and Static Synchronous Compensator. Injecting active or reactive current to the system can be used to control the voltage in and around the point of connection [17], [22], [23].

2.5.7.3. Combined Series-series Connected FACTS Devices

Combined series-series FACTS device is a combination of two different series FACTS devices with coordinated manner. A combined series-series controller has two circuits. One consists of series controllers operating in a coordinated manner in a multiline transmission network and the other provides independent reactive power control for each line of a multiline transmission network and, at the same time facilitates real power transfer through the power link. The family of such devices is Interline Power Flow Controller (IPFC) that balances real and reactive power flows on the transmission lines [17], [23].

2.5.7.4. Combined Series-Shunt Connected FACTS Devices

Combined series-shunt FACTS devices is a combination of one shunt and one series devices, which are controlled in a coordinated manner [23]. A combined series-shunt controller may have two different configurations. These are two separate series and shunt controllers that operate in a coordinated manner and interconnected series and shunt components. In each configuration, the shunt component injects a current into the system while the series component injects a series voltage. When these two elements are combined together, a real power can be exchanged between them through the power link. The families of such devices are unified power flow controller and thyristor-controlled phase-shifting transformer. These devices are more advantageous due to both series and shunt controllers facilitate effective and independent power flow i.e current flow and line voltage control.

Brief review of the main types of FACTS devices which are used for power flow control are described below:

2.5.7.5. Static Synchronous Series Compensator (SSSC)

SSSC can increase or decrease the overall reactive voltage drop across the transmission line and thereby controlling the transmitted electric power [22]. SSSC is series-connected synchronous-voltage source that can vary the effective impedance of a transmission line by injecting a voltage containing an appropriate phase angle in relation to the line current [22]. Transmission line inductance is compensated by series capacitor presenting a lagging quadrature voltage with respect to the transmission-line current. This voltage acts in opposition to the leading quadrature voltage appearing across the transmission-line inductance, which has a net effect of reducing the line inductance [22]. It can inject a voltage with controllable magnitude and phase angle at the line frequency and found to be more capable of handling power flow control, improvement of transient stability margin and improve damping of transient [20].

2.5.7.6. Static Var Compensators (SVC)

SVC is shunt connected type FACTS device that exchanges capacitive or inductive power by adjusting its output and is used to control reactive power in the transmission network. The SVC consist thyristor controlled or switched reactor (TSR) and thyristor switched capacitor (TSC). The reactive power is absorbed by TSR and supplied by TSC under abnormal conditions of transmission network. The accuracy, availability and fast response enable Static Var Compensators to provide high performance steady state and transient voltage control compared with shunt compensation. Static Var Compensators are also used to improve the transient stability, damp power swings and reduce system losses by using reactive power control [20], [24].

2.5.7.7. Static Synchronous Compensator (STATCOM)

STATCOM's are GTO based SVC's. They do not require large inductive and capacitive components to provide inductive or capacitive reactive power to high voltage transmission systems as required in SVC [20]. VSCs use pulse width modulation (PWM) technology, which makes it capable of providing high quality ac output voltage to the grid or even to a passive load. STATCOM utilizes a voltage source converter rather shunt capacitors and reactors. The basic principle of operation of a STATCOM is the generation of a controllable AC voltage source behind a transformer leakage reactance by a voltage source converter connected to a DC capacitor. The voltage difference across the reactance produces active and reactive power exchanges between the STATCOM and the power system [24].

2.5.7.8. Thyristor Controlled Series Capacitor (TCSC)

TCSC is an extension of conventional series capacitors by adding thyristor-controlled reactor with in it. If the reactance is connected in parallel to the series capacitor it provides continuous and rapidly variable series compensation system. The main advantages of TCSC's are damping power oscillation and sub-synchronous resonances damping, real power increasing power transfer capability and power flow line control [20], [21].

2.5.7.9. Unified Power Flow Controller (UPFC)

UPFC is a versatile FACTS device; has the unique capability to control simultaneously both an active and reactive power flows on the transmission system [1]. UPFC can be used in power systems for a lot of applications such as shunt compensation, series compensation, phase shifting, voltage profile improvement and power flow control [25]. The UPFC can provide simultaneous control of all basic power system parameters (transmission voltage, impedance and phase angle) [1]. This study uses UPFC based transmission line loss minimization and system voltage regulation since this device simultaneously do the application of SSSC and STATCOM.

CHAPTER THREE

METHODOLOGY AND DATA ANALYSIS

3.1. Literature Review

Literature reviewing was the first step in performing this thesis work. A review on the terms, definitions, causes and effects of losses in transmission system, types of losses, transmission line loss minimization techniques for bulk power transmission had been given a wide coverage.

3.2. Data Collection

For this thesis work primary data and secondary data's was collected from EEU. The collected data includes line impedance, line reactance, line length, Bus connected ID (From Bus to Bus), bus description, bus nominal voltage, reactive and active power flow, transformers data, actual voltage level of the line and peak load data of the transmission network of case study.

3.3. Load Flow Analysis

Load flow analysis forms the core of power system analysis. Load flow analysis used to determine the voltage, current, real power, reactive power, losses and power factor in a power system. Load flow analysis should be used to confirm adequate voltage profiles during different operating conditions, such as heavily loaded and lightly loaded system conditions.

Planning the operation of power system under existing conditions, its improvement and also future expansion requires the load flow studies. However the load flow studies is very important for planning, control and operations of existing systems as well as planning its future expansion as satisfactory operation of the system depends upon knowing the effect of interconnection, new load, new generation stations or new line transmission, change of network configuration etc, before they are installed. Load flow studies also help to select power electronics based devices and locate them at optimal location in order to minimize the losses.

Generally, load flow analysis solves for any unknown bus voltage and unspecified generation and finally form complex power flow in the network components for a given power system network, with known loads and some set of specifications or restrictions on power generation and voltages. A load flow analysis can be utilized to determine total transmission loss in a system as well as losses in individual components. It provides real and reactive powers at different buses. Total transmission loss can be calculated from the algebraic sum of powers injected at all buses.

All necessary data's like generators' rated active power and output active power, minimum and maximum reactive power limits of generators, peak active and reactive loads of HV substations, transformer data, transmission line parameters such as line resistance per kilometer, reactance of line per kilometer and line length and available data were collected from EEU concerned offices and analyzed in this section as required by the MATLAB/Simulink software and power world simulation software.

In this study load flow analysis was used to determine the bus voltages profiles, active power flows, reactive power flows and transmission line losses on all lines and transformers of the south western region of EEU's high voltage transmission network. The software used in carrying out this analysis was MATLAB/Simulink.

3.4. One-line (single line) Diagram

The first step of any power system problem is the development of a single-line diagram of the interconnected power system, from which computer solutions can be obtained. The one line diagram of the case study network, south western region of Ethiopian Transmission line, was thus drawn on the power world simulator 16 for this study. All the organized data were then fed to the one-line diagram. The one-line diagram is given below in both edit and run modes of power world simulator.

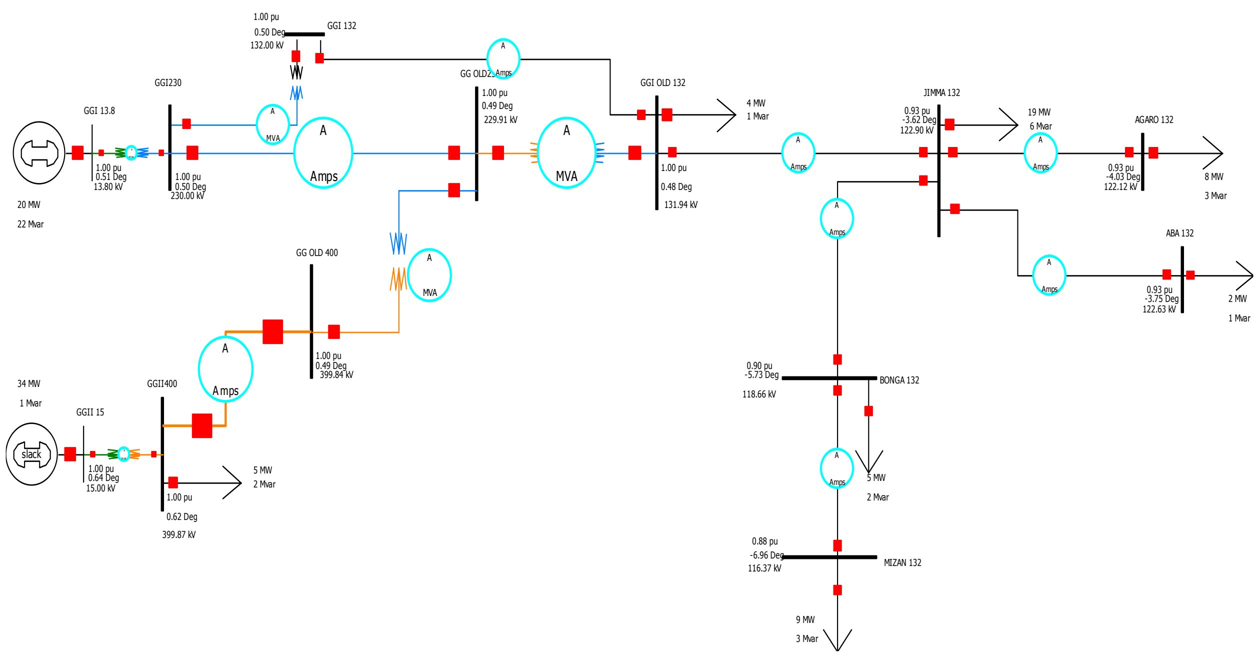

Figure 3.1: Edit mode one-line diagram of EEU south western region transmission network

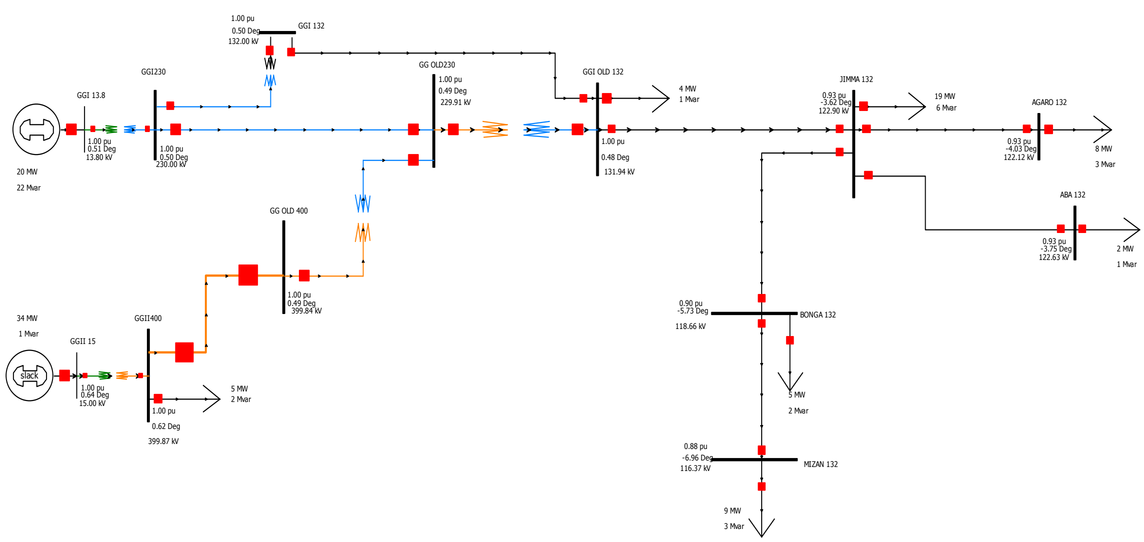

Figure 3.2: Run-mode one-line diagram of EEU south western region transmission network

The study encompassed lines of the existing voltage levels; namely 66, 132, 230 and 400 kV and transformers which extend from generation to main high voltage distribution substation transformers. The line parameters of the model circuits were taken from the existing parameters of EEU transmission lines which helped to match the condition variations with the real network.

After completing the one-line diagram with the necessary data, load flow simulation was run. As a result, the peak active power losses for each line and transformer as well as the total loss have been determined. The load flow simulation report also delivered the voltage profiles of each bus in the network.

Candidate lines to be controlled for loss reduction were then identified. The identification of the candidate lines depended on the type of technique proposed for loss reduction. In this study UPFC based transmission line loss minimization and improving bus voltage profile technique was undertaken to minimize the power loss of EEU south western region transmission network from its existing state.

3.5. UPFC Modeling and Overall System Design

The UPFC modelling includes the basic circuit arrangement of UPFC, operating principle of UPFC, active and Reactive Power Control by UPFC, Series Connected Voltage Source Converter Model, Shunt converter model and UPFC injection model for power flow studies.

The overall system design of the transmission network and UPFC modeling is done depending on the collected data, analyzed data and single line diagram in order to reduce the transmission line losses and regulate system voltage of the south western region of Ethiopian transmission network. On this research conventional controller method is used and modeling using MATLAB/Simulink is done to analyses the performance of transmission line of the case study.

3.6. EEU's High Voltage System Data

All necessary data of EEU south western region of Ethiopia high voltage transmission network were collected from the concerned offices of EEU and analyzed in this section to make it ready for the software.

3.6.1. Generator Data

On this study two hydropower plants are considered as generating sources. The generator rated power, number of generating units, generating unit type, voltage level, power output, minimum and maximum reactive power are the necessary data required by power world simulator and MATLAB/Simulink software are given in the following table. The power output recorded was based on the current condition of generators output. Gilgel-Gibe-II power plant, which currently delivers the maximum power output from the two was used as a slack generator for this study.

Table 3.1: Generator data

No.	Power station	Units	Voltage level (KV)	P_{rated} (MW)	P_{max} (MW)	Q_{min} (MVar)	Q_{max} (Mvar)
1	Gilgel Gibe-I	3	13.8	183	210	-63	+63
2	Gilgel Gibe-II	4	15	380	420	-200	+200

3.6.2. Transmission Line Data

The study area existing EEU transmission network consists around 8 transmission lines. From these the 132 kV network constitute 6 lines, the 66 kV network constitutes1 line and the 400 kV network constitutes 1 line. EEU transmission line data is shown in Appendix A.

The collected EEU data consists of transmission line length (km), resistance of a line (ohm/km), reactance of a line (ohm/km) and shunt capacitance (nF/km). The flexibility of MATLAB/Simulink software and power world simulator allowed us to feed most of the data such as line length (km), resistance of a line (ohm/km), capacitance of the line (F/km) for MATLAB/Simulink and reactance of a line (ohm/km) for power world directly. But in the case of MATLAB/Simulink software it is necessary to convert reactance of the line into inductance of the line and in the case of power world software converting capacitance of the line into shunt admittance of the line.

The shunt capacitance (nF/km) was converted to shunt admittance (mho/km) which is required by the power world software in the following manner.

$$y = g + jb \tag{3.1}$$

Where; y, g and b are shunt admittance (mho/km), shunt conductance (mho/km) and shunt susceptance (mho/km) respectively. Since shunt conductance is ignored in such cases, the admittance was equated to the susceptance.

$$y = b = 2\pi fc \tag{3.2}$$

Where,

f is the power frequency (50 Hz) and

C is the shunt capacitance (F/km).

The reactance of the line (ohm/km) is converted to line inductance (H/km) which is required by MATLAB/Simulink software in the following manner.

$$L = \frac{x}{2\pi f} \tag{3.3}$$

Where,

f is the power frequency (50 Hz)

L is line inductance (H/km) and

X is line reactance (ohm/km)

The shunt admittance (mho/km) and line inductance (H/km) is thus included in the following table3.2.

Table 3.2: Transmission line Data

From Bus	To Bus	Line (Km)	R_1(Ω /km)	X_1(Ω /km)	R_0(Ω /km)	X_0(Ω /km)	C(nF /km)	C_0(nF /km)	y(℧/km)	L(H/k m)	L_0(H/ km
GG-I 132	GG Old 132	2.61	0.1835	0.4486	0.3619	1.2773	8.2	5.4	0.00000 25761	0.0014 28	0.004 066
GGII 400	GG Old 400	28	0.0375	0.4259	0.286	1.0839	8.7	6.8	0.00000 27	0.0013 56	0.003 45
GG OLD 132	Jimma 132	71.32	0.1905	0.4373	0.4155	1.2481	8.4	6.5	2.6389E -06	0.0013 92	0.003 973
Jimma 132	Agaro 132	34.82	0.1905	0.4373	0.4155	1.2481	8.4	6.5	2.6389E -06	0.0013 92	0.003 973
Jimma 132	Aba 132	53	0.1834	0.4229	0.3267	1.3894	8.8	5.9	2.7646E -06	0.0013 46	0.004 423
Jimma 132	Bonga 132	102.2 7	0.1834	0.4229	0.3267	1.3894	8.8	5.9	2.7646E -06	0.0013 46	0.004 423
Bonga 132	Mizan 132	88.3	0.1834	0.4229	0.3267	1.3894	8.8	5.9	2.7646E -06	0.0013 46	0.004 423
Mizan 66	Teppi 66	30.15	0.4262	0.4131	0.612	1.4464	8.8	5.1	2.7646E -06	0.0013 15	0.004 604

3.6.3. Transformer Data

EEU south western region transmission network considered in this study consists 15 two winding and 5 three winding transformers.

Three-phase three-winding transformers are widely used in power systems. When the VA rating of the third winding is appreciably lower than the primary or secondary winding ratings, the third winding is called a tertiary winding. The most common reason for the additional third set of windings to a three-phase transformer is to provide path for the third harmonics; to provide connection for reactive compensation plant such as shunt rectors, shunt capacitors, static variable compensators or synchronous compensators or synchronous condensers and to supply auxiliary load in substations and to generators.

3.6.3.1. Two Winding Transformer Data

Primary and secondary voltages, MVA rating and nameplate percentage impedance $\%Z_{np}$ are the necessary data to be fed in modeling two winding transformers. The collected EEU's two winding transformer data provided at Appendix B-1 consists of nameplate percentage reactance %X and nameplate percentage resistance %R instead of X/R ratio. This value was easily determined as shown below and included in the data:

$$\frac{X}{R} = \frac{\%X_{np}}{\%R_{np}} \tag{3.4}$$

Since the nameplate values are generally given taking the nameplate MVA rating of transformers as base MVA, it is necessary to convert the nameplate values in to the system base of 100 MVA by using the following formula.

$$\left.\begin{aligned} \%R_{100MVA} &= \%R_{np} \text{ x } \frac{100MVA}{S_{np}} \\ \%X_{100MVA} &= \%X_{np} \text{ x } \frac{100MVA}{S_{np}} \end{aligned}\right\} \tag{3.5}$$

$$\left.\begin{aligned} R_{p.u.} &= \frac{\%R}{100\%} \\ X_{p.u.} &= \frac{\%X}{100\%} \end{aligned}\right\} \quad (3.6)$$

$$L_{p.u.} = \frac{X_{p.u}}{2\pi f} \quad (3.7)$$

Where,

- $\%R_{100\,MVA}$ is percentage resistance value with 100MVA base system
- $\%X_{100\,MVA}$ is percentage reactance values with 100MVA base system
- $R_{p.u}$ is per unit resistance value of the transformer with 100MVA base system
- $X_{p.u}$ is per unit reactance value of the transformer with 100MVA base system
- $L_{p.u}$ is the per unit inductance values of the transformer with 100MVA base system
- $\%R_{np}$ is percentage resistance nameplate value
- $\%X_{np}$ is percentage reactance nameplate value
- S_{np} is the nameplate MVA rating of a transformer

The following table provides X/R ratio, per unit resistance, reactance and inductance and %R and %X when converted to 100 MVA system base.

Table 3.3: Two winding transformer data

From Bus	To bus	S_{np}	X/R	%R	%X	100 MVA base				
						%R	%X	$R_{p.u.}$	$X_{p.u.}$	$L_{p.u}$
ABA 132	ABA 33	9.6	11.92	0.62	7.40	6.458	77.08	0.06458	0.7708	0.0024
AGARO132	AGARO 15	6.3	9.53	0.85	8.08	13.45	128.2	0.1345	1.282	0.0040
GG I 230	GG I 13.8	51.0	41.44	0.21	8.76	0.41	17.2	0.0041	0.172	0.0005
GG I 230	GG I 13.8	51.0	41.44	0.21	8.76	0.41	17.2	0.0041	0.172	0.0005
GG I 230	GG I 13.8	51.0	41.44	0.21	8.76	0.41	17.2	0.0041	0.172	0.0005
GG I 230	GG I 132	30.0	45.53	0.20	8.97	0.66	29.9	0.0066	0.299	0.0009
GGOLD 132	GGOLD 15	6.3	9.53	0.85	8.10	13.48	128.5	0.1348	1.285	0.0041
GG II 400PP	GG II 15PP	125	25.12	0.41	10.30	0.33	8.2	0.0033	0.082	0.00026
GG II 400PP	GG II 15PP	125	25.12	0.41	10.30	0.33	8.2	0.0033	0.082	0.00026
GG II 400PP	GG II 15PP	125	25.12	0.41	10.30	0.33	8.2	0.0033	0.082	0.00026
GG II 400PP	GG II 15PP	125	25.12	0.41	10.30	0.33	8.2	0.0033	0.082	0.00026
GGOLD 400	GGOLD230	250	25.12	0.41	10.30	0.16	4.1	0.0016	0.041	0.00013

GGOLD 230	GGOLD132	30	45.53	0.20	8.97	0.66	29.9	0.0066	0.299	0.00095
JIMMA 132	JIMMA 15	16	22.33	0.36	7.94	2.22	49.6	0.0222	0.496	0.0016
MIZAN 66	MIZAN 15	6.3	17.17	0.53	9.04	8.36	143.6	0.0836	1.436	0.00457

3.6.3.2. Three Winding Transformer Data

For a three winding transformer, voltage and MVA ratings of each winding, per unit resistance and reactance of each winding are the necessary data required by MATLAB/Simulink to model it. The three winding data collected from EEU shown at Appendix B-2 provides voltage and MVA ratings, nameplate short circuit test resistances between windings ($\%R_{ps}$, $\%R_{pt}$, $\%R_{st}$) and short circuit test reactance ($\%X_{ps}$, $\%X_{pt}$, $\%X_{st}$) where p, s, and t stand for primary, secondary and tertiary windings. When these resistance and reactance values were converted to per unit resistance and per unit reactance, the following simple formulas were used. Each transformer will have three per unit resistance and three per unit reactance.

$$\left.\begin{aligned}\%R_{ps\ 100MVA} &= \%R_{ps} \times \frac{100MVA}{S_{ps}}\\ \%R_{st\ 100MVA} &= \%R_{st} \times \frac{100MVA}{S_{st}}\\ \%R_{pt\ 100MVA} &= \%R_{pt} \times \frac{100MVA}{S_{pt}}\end{aligned}\right\} \quad (3.8)$$

$$\left.\begin{aligned}\%X_{ps\ 100MVA} &= \%X_{ps} \times \frac{100MVA}{S_{ps}}\\ \%X_{st\ 100MVA} &= \%X_{st} \times \frac{100MVA}{S_{st}}\\ \%X_{pt\ 100MVA} &= \%X_{pt} \times \frac{100MVA}{S_{pt}}\end{aligned}\right\} \quad (3.9)$$

$$\left.\begin{aligned} \frac{X_{ps}}{R_{ps}} &= \frac{\%X_{ps}}{\%R_{ps}} \\ \frac{X_{st}}{R_{st}} &= \frac{\%X_{st}}{\%R_{st}} \\ \frac{X_{pt}}{R_{pt}} &= \frac{\%X_{pt}}{\%R_{pt}} \end{aligned}\right\} \quad (3.10)$$

$$\left.\begin{aligned} R_{ps\ p.u.} &= \frac{\%R_{ps}}{100\%} \\ R_{st\ p.u.} &= \frac{\%R_{st}}{100\%} \\ R_{pt\ p.u.} &= \frac{\%R_{pt}}{100\%} \\ X_{ps\ p.u.} &= \frac{\%X_{ps}}{100\%} \\ X_{st\ p.u.} &= \frac{\%X_{st}}{100\%} \\ X_{pt\ p.u.} &= \frac{\%X_{pt}}{100\%} \end{aligned}\right\} \quad (3.11)$$

Where,

- $\%R_{ps\ 100MVA}$, $\%R_{st\ 100MVA}$, $\%R_{pt\ 100MVA}$, $\%X_{ps\ 100MVA}$, $\%X_{st\ 100MVA}$ and $\%X_{pt\ 100MVA}$ are percentage resistance and reactance values with 100MVA system base
- $R_{ps\ p.u.}$, $R_{st\ p.u.}$, $R_{pt\ p.u}$, $X_{ps\ p.u}$, $X_{st\ p.u}$ and $X_{pt\ p.u}$ are the per unit resistance and reactance values of the transformer with 100MVA base system
- $\%R_{ps}$, $\%R_{st}$, $\%R_{pt}$, $\%X_{ps}$, $\%X_{st}$ and $\%X_{pt}$ are percentage resistance and reactance nameplate values
- S_{ps}, S_{st} and S_{pt} is the nameplate MVA rating of a transformer

The following table provides per unit resistance and per unit reactance and $\%R_{ps}$, $\%R_{st}$, $\%R_{pt}$ and $\%X_{ps}$, $\%X_{st}$, $\%X_{pt}$ when converted to 100 MVA system base.

Table 3.4: Three winding transformer data

Node 1	Node 2	Node 3	S_{np}	%R for 100MVA			%X for 100MVA			$R_{p.u}$			$X_{p.u}$		
				$\%R_{ps}$	$\%R_{st}$	$\%R_{pt}$	$\%X_{ps}$	$\%X_{st}$	$\%X_{pt}$	R_{ps} p.u	R_{st} p.u	R_{pt} p.u	X_{ps} p.u	X_{st} p.u	X_{pt} p.u
BONGA 132	BONGA 33	BONGA 15	20/9.6/9.6	1.915	2.05	2.71	42.95	53.23	158.23	0.01915	0.0205	0.0271	0.4295	0.5323	1.58
MIZAN 132	MIZAN 66	MIZAN 33	20/9.6/9.6	3.174	3.03	4.19	43.16	26.0	75.68	0.03174	0.0303	0.0419	0.4316	0.26	0.7568
TEPI 66	TEPI 33	TEPI 15	9.6/5.04/5.04	4.03	4.21	5.32	76.46	80.75	249.40	0.0403	0.0421	0.0532	0.7646	0.8075	2.494
Jimma132	Jimma33	Jimma15	16/16/8	2.448	1.49	2.35	52.5	42.63	27.00	0.02448	0.0149	0.0235	0.525	0.4263	0.27
Agaro132	Agaro33	Agaro15	16/16/8	2.448	1.49	2.35	52.5	42.63	27.00	0.02448	0.0149	0.0235	0.525	0.4263	0.27

Therefore it is necessary to determine the per unit resistance, reactance and inductance values of each winding of the transformer in order to provide to MATLAB/Simulink software i.e. primary winding resistance, secondary winding resistance, tertiary winding resistance, primary winding reactance, secondary winding reactance, tertiary winding reactance, primary winding inductance, secondary winding inductance and tertiary winding inductance. These values are determined converting the per unit R_{ps}, R_{st}, R_{pt}, X_{ps}, X_{st} and X_{pt} into R_p, R_s, R_t, X_p, X_s, X_t, L_p, L_s, L_t by using the following formula.

$$\left.\begin{aligned} R_p\ \text{p.u} &= \tfrac{1}{2}\left(R_{ps,\ p.u} + R_{pt,\ p.u} - R_{st,\ p.u}\right) \\ R_s\ \text{p.u} &= \tfrac{1}{2}\left(R_{ps,\ p.u} + R_{st,\ p.u} - R_{pt,\ p.u}\right) \\ R_t\ \text{p.u} &= \tfrac{1}{2}\left(R_{pt,\ p.u} + R_{st,\ p.u} - R_{ps,\ p.u}\right) \end{aligned}\right\} \quad (3.12)$$

$$\left.\begin{aligned} X_p\ p.u &= \tfrac{1}{2}\,(X_{ps,\ p.u} + X_{pt,\ p.u} - X_{st,\ p.u}) \\ X_s\ p.u &= \tfrac{1}{2}\,(X_{ps,\ p.u} + X_{st,\ p.u} - X_{pt,\ p.u}) \\ X_t\ p.u &= \tfrac{1}{2}\,(X_{pt,\ p.u} + X_{st,\ p.u} - X_{ps\ p.u}) \end{aligned}\right\} \tag{3.13}$$

$$\left.\begin{aligned} L_{p,\ p.u} &= X_{p,p.u}/(2\pi f) \\ L_{s,\ p.u} &= X_{s,p.u}/(2\pi f) \\ L_{t,\ p.u} &= X_{t,p.u}/(2\pi f) \end{aligned}\right\} \tag{3.14}$$

Where, f is the power frequency (50 Hz), L_p, L_s and L_t are per unit inductance and X_p, X_s and X_t are per unit reactance of primary winding, secondary winding and tertiary winding respectively.

The following table provides per unit resistance, per unit reactance and per unit inductance of each windings of three phase three winding transformer when converted to 100 MVA system base.

Table 3.5: Per unit resistance and reactance of each winding for 3-winding transformer

Node 1	Node2	Node 3	S_{np}	$R_{p.u}$			$X_{p.u}$			$L_{P.u}$		
				R_p p.u	R_s p.u	$R_{t\ p.u}$	X_p p.u	X_s p.u	X_t p.u	$L_{p,\ p.u}$	$L_{s,\ p.u}$	$L_{t.\ p.u}$
BONGA 132	BONGA 33	BONGA 15	20/9.6/9.6	0.012875	0.006275	0.014225	0.7386	0.3091	0.8414	0.002351037	0.000983896	0.002678259
MIZAN 132	MIZAN 66	MIZAN 33	20/9.6/9.6	0.02167	0.01007	0.02023	0.4642	0.0326	0.2926	0.001477594	0.000103769	0.000931375
TEPI 66	TEPI 33	TEPI 15	9.6/5.04/5.04	0.0257	0.0146	0.0275	1.22555	0.46095	1.26845	0.003901047	0.001467249	0.004037602
Jimma 132	Jimma 33	Jimma 15	16/16/8	0.01654	0.00794	0.00696	0.18435	0.34065	0.08565	0.000586804	0.001084323	0.000272632
Agaro 132	Agaro 33	Agaro 15	16/16/8	0.01654	0.00794	0.00696	0.18435	0.34065	0.08565	0.000586804	0.001084323	0.000272632

3.6.4. Peak Load Data

The peak load data of each substation buses is summarized as shown in the following table.

Table 3.6: peak load data

No.	Load Node	Network Level (KV)	P_{load} (MW)	P.f.	Q_{load} (MVar)	S_{load} (MVA)
1.	ABA33	33	1.80	0.95	0.592	1.895
2.	AGARO15	15	6.40	0.95	2.104	6.737
3.	AGARO33	33	1.80	0.95	0.592	1.895
4.	BONGA15	15	2.92	0.95	0.9598	3.074
5.	BONGA33	33	1.82	0.95	0.598	1.916
6.	GILGEL GIBE OLD15	15	3.60	0.95	1.183	3.789
7.	JIMMA15	15	14.4	0.95	4.733	15.158
8.	JIMMA33	33	5.0	0.95	1.643	5.263
9.	MIZAN15	15	2.69	0.95	0.8842	2.832
10.	MIZAN33	33	1.80	0.95	0.592	1.895
11.	TEPI15	15	3.0	0.95	0.986	3.158
12.	TEPI33	33	1.80	0.95	0.592	1.895

CHAPTER FOUR

UPFC MODELING

4.1. Basic Structure of UPFC

UPFC is designed by the combination of SSSC and STATCOM coupled with a common DC capacitor. UPFC has the ability to control all the transmission parameters such as voltage, impedance and phase angle of power systems simultaneously. It consists of two voltage source converters one connected in series with the transmission line through a series inserted transformer and the other one connected in shunt with the transmission line through a shunt transformer. These converters are operated from a common DC link provided by a DC storage capacitor as shown in figure 4.1below [7] [25] - [32].

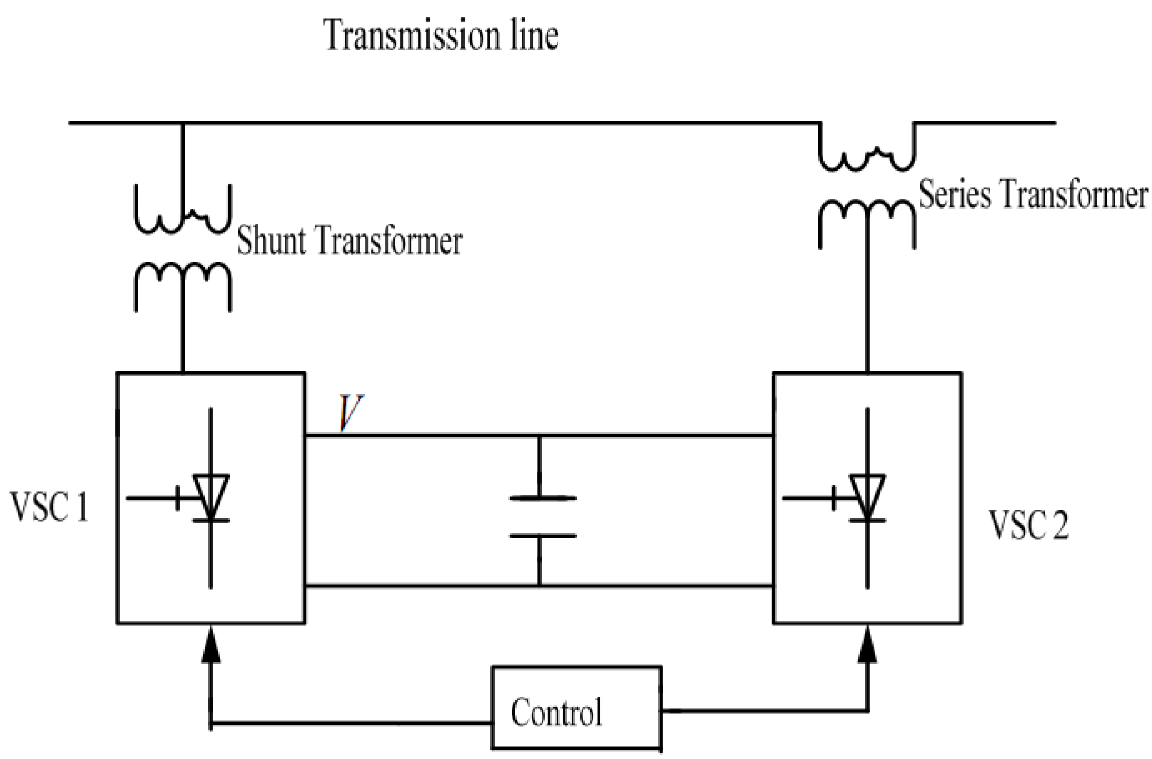

Figure 4.1: Structure of UPFC (source: [26])

4.2. Operating Principle of UPFC

The voltage source Converter 2 (VSC 2) provides the main function of the UPFC by injecting an AC voltage with controllable magnitude and phase angle in series with the transmission line via a series transformer. The basic function of voltage source converter 1 (VSC 1) is to supply or absorb the real power demand by converter 2 at the common dc link. It can also generate or absorb controllable reactive power and provide independent shunt reactive compensation for the line. Converter 2 supplies or absorbs locally the required reactive power and exchanges the active power as a result of the series injection voltage [7] [25] - 32].

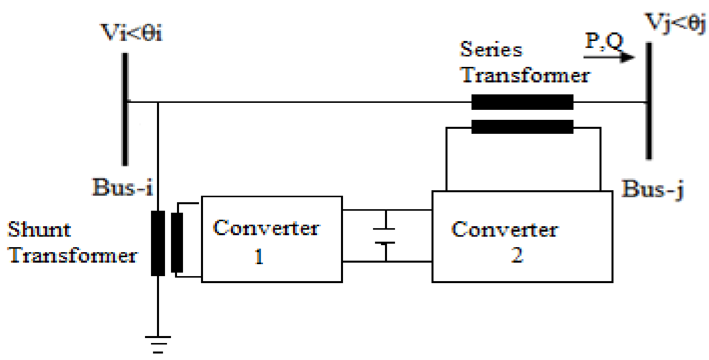

Figure 4.2: Basic circuit arrangement of UPFC (source: [7] [27])

4.3. UPFC Injection Model

In this thesis, at steady state power system operation the UPFC injection model is derived. In steady state condition UPFC can be represented by two voltage sources representing fundamental components of output voltage waveforms of the two converters and impedances being leakage reactance of the two coupling transformers. The impact of UPFC on transmission network at steady state condition is understandable by using this model. Furthermore, the UPFC injection model can be easily incorporated in the steady state power flow model [25] [29] [30] [32]. Figure 4.3 shows that the two voltage-source model of UPFC.

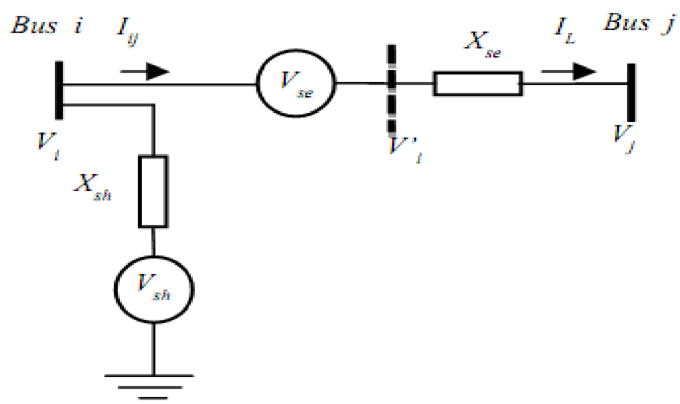

Figure 4.3: Voltage-source model of UPFC (source: [25], [30])

Bus-i voltage is taken as reference $V_i = |V|<0^0$. All other bus voltage angles are taken with respect to this bus angle. The voltage sources, V_{se} and V_{sh} are controllable in both magnitude and phase angles.

Therefore, the voltage up to UPFC is given by,

$$V_i' = V_i + V_{se} \tag{4.1}$$

Then Series voltage source converter voltage, V_{se} is defined in terms of reference bus voltage as,

$$V_{se} = rV_i e^{j\gamma} \tag{4.2}$$

The values of series voltage source coefficient r and series voltage source angle γ are defined within the limits of $0 \le r \le r_{max}$ and $0 \le \gamma \le 2\pi$. Where r is per unit value of output voltage of series branch of UPFC and γ is phase angle difference between V_i and V_{se}

In UPFC injection model there are two voltage source converter models. These are series connected voltage source converter model and shunt connected voltage source converter model. Using superposition theorem it is easy to determine the power fed by the UPFC. Since the series connected voltage source converter does the main function of the UPFC, it is appropriate to discuss the modeling of a series connected voltage source converter first and then the shunt connected voltage source converter model.

4.3.1. Series connected voltage source converter model

Consider that a series connected voltage source is located between bus-i and bus-j in a power system. The series voltage source converter can be modeled with an ideal series voltage V_{se} in series with a reactance X_{se} as shown in figure-4.4. The voltage Vi' represents the voltage behind the series reactance.

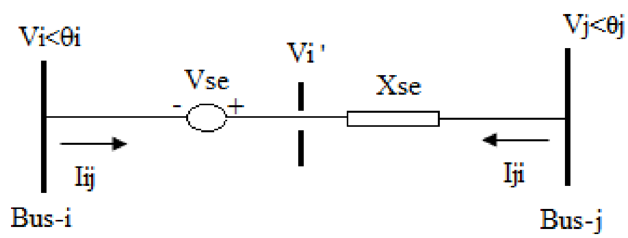

Figure 4.4: Representation of series connected VSC (source [7] [30])

Using duality principle the series voltage source V_{se} represented by a current source to develop the steady-state UPFC mathematical model. Figure 4.5 shows that current source which is connected in parallel with the transmission line. [29] [30].

$$I_{se} = -jb_{se}V_{se} \qquad (4.3)$$

Where, $b_{se}=1/X_{se}$

The negative sign in equation 4.3 indicates that the current is leaving bus-i, since the current which is leaving the node is represented by negative and the current which is entering the node is represented by positive by using convention of current flow.

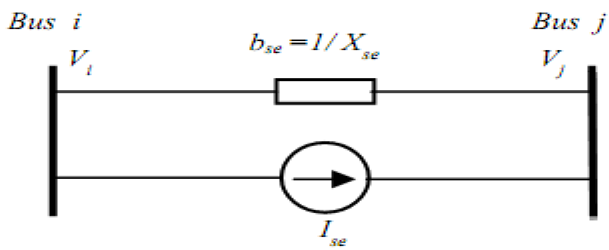

Figure 4.5: Replacement of series voltage source by current source (source [29] [30])

The current source I_{se} can be modeled by injection powers S_{ise} and S_{jse} at the two buses which are expressed by,

$$S_{ise} = V_i(-I_{se})^* \qquad (4.4)$$

$$S_{jse} = V_j(I_{se})^* \qquad (4.5)$$

Substituting equations 4.2 and 4.3 into equation 4.4 injected power S_{ise} can be simplified as,

$$S_{ise} = V_i(jb_{se}rV_ie^{j\gamma})^* \qquad (4.6)$$

$$S_{ise} = V_i(e^{-(\gamma+90)}b_{se}rV_i^*) \qquad (4.7)$$

By using Euler Identity, i.e. $e^{j\gamma} = \cos\gamma + j\sin\gamma$, equation 4.7 is simplified as,

$$S_{ise} = V_i^2b_{se}r(\cos(-\gamma-90) + j\sin(-\gamma-90)) \qquad (4.8)$$

By using trigonometric identities equation 4.8 can be simplified as,

$$S_{ise} = -rb_{se}V_i^2\sin\gamma - jrb_{se}V_i^2\cos\gamma \qquad (4.9)$$

Since $S_{ise} = P_{ise} + jQ_{ise}$, then separating the real and imaginary part we can get,

$$P_{ise} = -rb_{se}V_i^2\sin\gamma \qquad (4.10)$$

$$Q_{ise} = -rb_{se}V_i^2\cos\gamma \qquad (4.11)$$

Similarly, substituting equation 4.2 and 4.3 into equation 4.5 the injected power S_{jse} can be modified as,

$$S_{jse} = V_j(-jb_{se}rV_ie^{j\gamma})^* \qquad (4.12)$$

$$S_{jse} = b_{se}rV_iV_j\sin(\theta_i - \theta_j + \gamma) + j\, b_{se}rV_iV_j\cos(\theta_i - \theta_j + \gamma) \qquad (4.13)$$

But, $\theta_{ij} = \theta_i - \theta_j$ substituting this value into equation 4.13 then the final equation can be written as,

$$S_{jse} = b_{se}rV_iV_j\sin(\theta_{ij} + \gamma) + j\, b_{se}rV_iV_j\cos(\theta_{ij} + \gamma) \qquad (4.14)$$

Since $S_{jse} = P_{jse} + jQ_{jse}$, then separating the real and imaginary part we can get,

$$P_{jse} = b_{se}rV_iV_j\sin(\theta_{ij} + \gamma) \qquad (4.15)$$

$$Q_{jse} = b_{se}rV_iV_j\cos(\theta_{ij} + \gamma) \qquad (4.16)$$

The above equations 4.10, 4.11, 4.15, and 4.16 shows that power injection model of the series connected voltage source can be seen as two dependent loads at buses i and j as shown in figure 4.6.

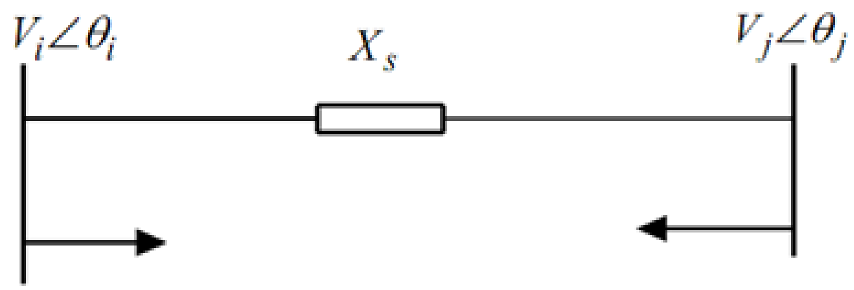

$P_{ise} = -rb_{se}V_i^2\sin\gamma$ $\qquad$ $P_{jse} = b_{se}rV_iV_j\sin(\theta_{ij} + \gamma)$

$Q_{ise} = -\, rb_{se}V_i^2\cos\gamma$ $\qquad$ $Q_{jse} = b_{se}rV_iV_j\cos(\theta_{ij} + \gamma)$

Figure 4. 6: Power injection model for a series connected VSC (source [27])

4.3.2. Shunt connected voltage source converter model

The shunt connected converter of UPFC is used mainly in order to provide both the active power demand of the series connected voltage source converter, which is injected to the system, and the total losses within the UPFC. The total switching losses of the two converters is estimated to be about 2% [30] of the power transferred for converters.

If we consider the losses in the active power injection of the shunt connected voltage source converter at bus-i, Pconv1 is equal to 1.02 times the injected series active power Pconv2 through the series connected voltage source converter to the system.

$$P_{conv1} = 1.02P_{conv2} \quad (4.17)$$

The apparent power supplied by the series converter is given by,

$$S_{conv2} = V_{se}I_{ij}^{*} \quad (4.18)$$

$$I_{ij} = \frac{V_i' - V_j}{jX_{se}} \quad (4.19)$$

Substituting equations 4.2 and 4.19 into equation 4.18 it is modified as,

$$S_{conv2} = rV_i e^{j\gamma}\left(\frac{V_i' - V_j}{jX_{se}}\right)^{*} \quad (4.20)$$

Again substituting equations 4.1 and 4.2 into equation 4.20 it is simplified as,

$$S_{conv2} = re^{j\gamma}V_i((re^{j\gamma}V_i + V_i - V_j) / jX_{se})^{*} \quad (4.21)$$

$$S_{conv2} = \frac{rV_i\, e^{j(\theta_i+\gamma)}(rV_i\, e^{-j(\theta_i+\gamma)} + V_i\, e^{-j\theta_i} - V_j\, e^{-j\theta_i})}{-jX_{se}} \quad (4.22)$$

Substituting $b_{se}=1/X_{se}$ in the above equation 4.22 it gives,

$$S_{conv2} = \frac{rb_{se}V_i\, e^{j(\theta_i+\gamma)}(rV_i\, e^{-j(\theta_i+\gamma)} + V_i\, e^{-j\theta_i} - V_j\, e^{-j\theta_i})}{-j} \quad (4.23)$$

Multiplying the numerator and denominator of equation 4.23 by conjugate of –j we can get,

$$S_{conv2} = jrb_{se}V_i\, e^{j(\theta_i+\gamma)}(rV_i\, e^{-j(\theta_i+\gamma)} + V_i\, e^{-j\theta_i} - V_j\, e^{-j\theta_i}) \quad (4.24)$$

Then simplifying the above equation we can get,

$$S_{conv2} = jr^2b_{se}V_i^2 + jrb_{se}V_i^2e^{j\gamma} - jrb_{se}V_iV_je^{j(\theta_i - \theta_j+\gamma)} \quad (4.25)$$

By using Euler Identity, i.e. $e^{j\gamma} = \cos\gamma + j\sin\gamma$ and $e^{j(\theta_i - \theta_j + \gamma)} = \cos(\theta_i - \theta_j + \gamma) + j\sin(\theta_i - \theta_j + \gamma)$, equation 4.25 is simplified as,

$$S_{conv2} = jr^2 b_{se} V_i^2 + jrb_{se}V_i^2(\cos\gamma + j\sin\gamma) - jrb_{se}V_iV_j(\cos(\theta_i - \theta_j + \gamma) + j\sin(\theta_i - \theta_j + \gamma))$$

$$S_{conv2} = jr^2 b_{se} V_i^2 + jrb_{se}V_i^2\cos\gamma - rb_{se}V_i^2\sin\gamma - jrb_{se}V_iV_j(\cos(\theta_i - \theta_j + \gamma)$$

$$+ rb_{se}V_iV_j(\sin(\theta_i - \theta_j + \gamma) \quad (4.26)$$

Therefore, separating the real and imaginary part we can get active power and reactive power at converter-2 as follows,

$$P_{conv2} = rb_{se}V_iV_j(\sin(\theta_i - \theta_j + \gamma) - rb_{se}V_i^2\sin\gamma \quad (4.27)$$

$$Q_{conv2} = -rb_{se}V_iV_j(\cos(\theta_i - \theta_j + \gamma) + rb_{se}V_i^2\cos\gamma + r^2 b_{se}V_i^2 \quad (4.28)$$

Then the active power injected at converter-1 is determined by substituting equation 4.27 into equation 4.17 as,

$$P_{conv1} = 1.02rb_{se}V_iV_j(\sin(\theta_i - \theta_j + \gamma) - 1.02rb_{se}V_i^2\sin\gamma \quad (4.29)$$

The reactive power delivered or absorbed by voltage source converter 1 is independently controllable by UPFC and can be modeled as a separate controllable shunt reactive source. In the view of above, it is assumed that the reactive power of converter-1 is equal to zero. The UPFC injection model is constructed from the series connected voltage source converter model with the addition of a power equivalent to P_{conv1} + j0 to bus-i [25] [27] [29] [30].

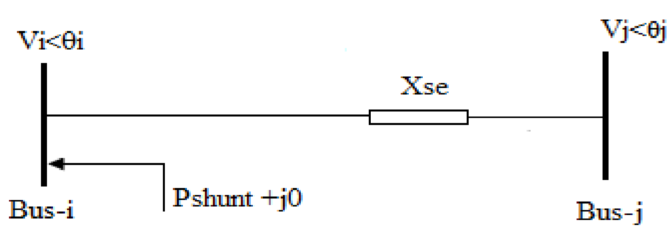

Figure4.7: Power injection model of shunt connected voltage source converter (source: [25] [27])

Therefore, the steady-state UPFC mathematical modeling can be constructed by combining the series power injection and shunt power injection at bus-i and bus-j.

The element of power injection model of UPFC can be expressed as follows,

$$P_{i,UPFC} = b_{se}rV_iV_j\sin(\theta_{ij} + \gamma) + 1.02rb_{se}V_iV_j(\sin(\theta_i - \theta_j + \gamma) - 1.02rb_{se}V_i^2\sin\gamma$$

$$P_{i,UPFC} = 0.02b_{se}rV_iV_j\sin(\theta_{ij} + \gamma) + 1.02rb_{se}V_iV_j(\sin(\theta_i - \theta_j + \gamma) \quad (4.30)$$

$$Q_{i,UPFC} = -rb_{se}V_i^2\cos\gamma \quad (4.31)$$

$$P_{j,UPFC} = b_{se}rV_iV_j\sin(\theta_{ij} + \gamma) \quad (4.32)$$

$$Q_{j,UPFC} = b_{se}rV_iV_j\cos(\theta_{ij} + \gamma) \quad (4.33)$$

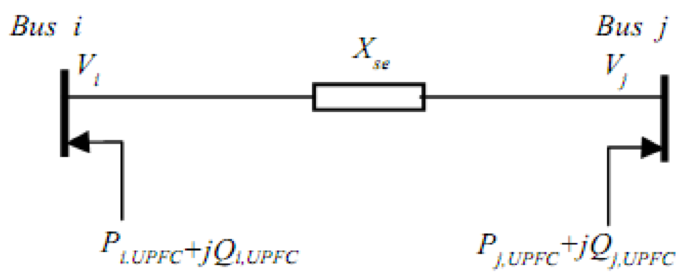

Figure 4.8: The overall steady state UPFC mathematical model (source [27] [30])

CHAPTER FIVE

RESULT AND DISCUSSION

5.1. Analysis of the Existing Transmission Network of the South western Region

In this section, the active power flow, reactive power flow, power loss and system bus voltage of each buses for south western region of EEU network were analyzed. Figure 5.1 and figure 5.2 shows that the overall existing interconnected transmission network of south western Region of EEU without incorporating UPFC.

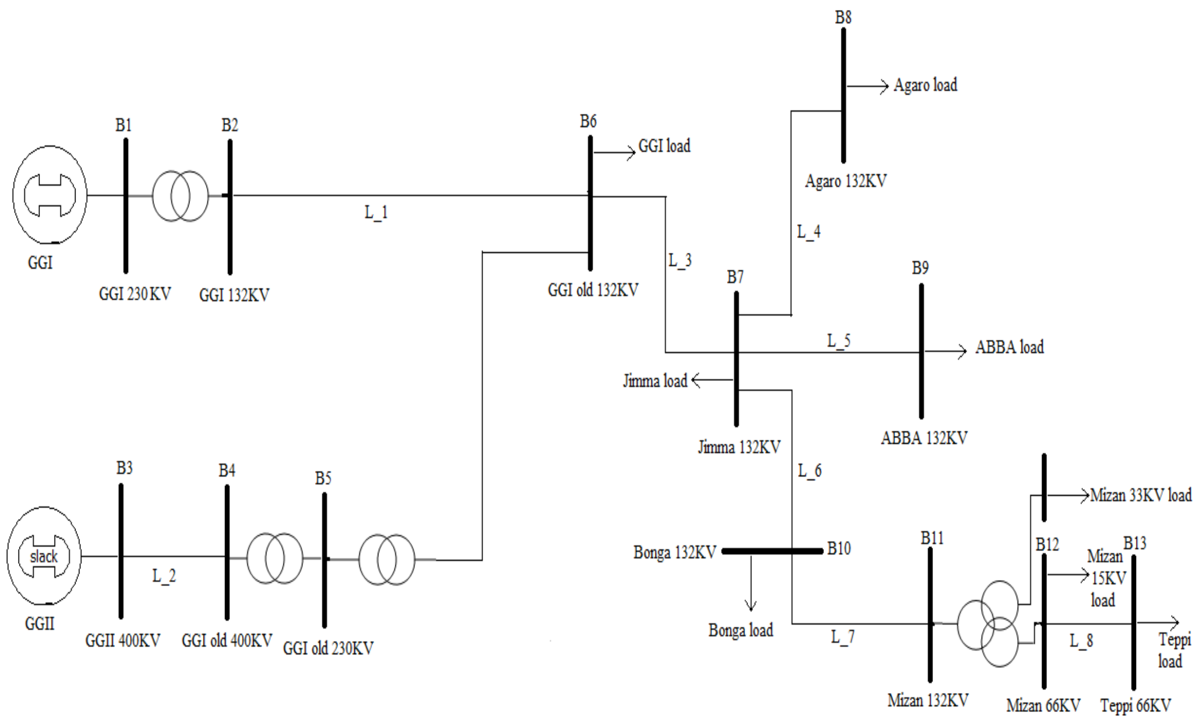

Figure 5.1: One-line diagram of south western EEU transmission network

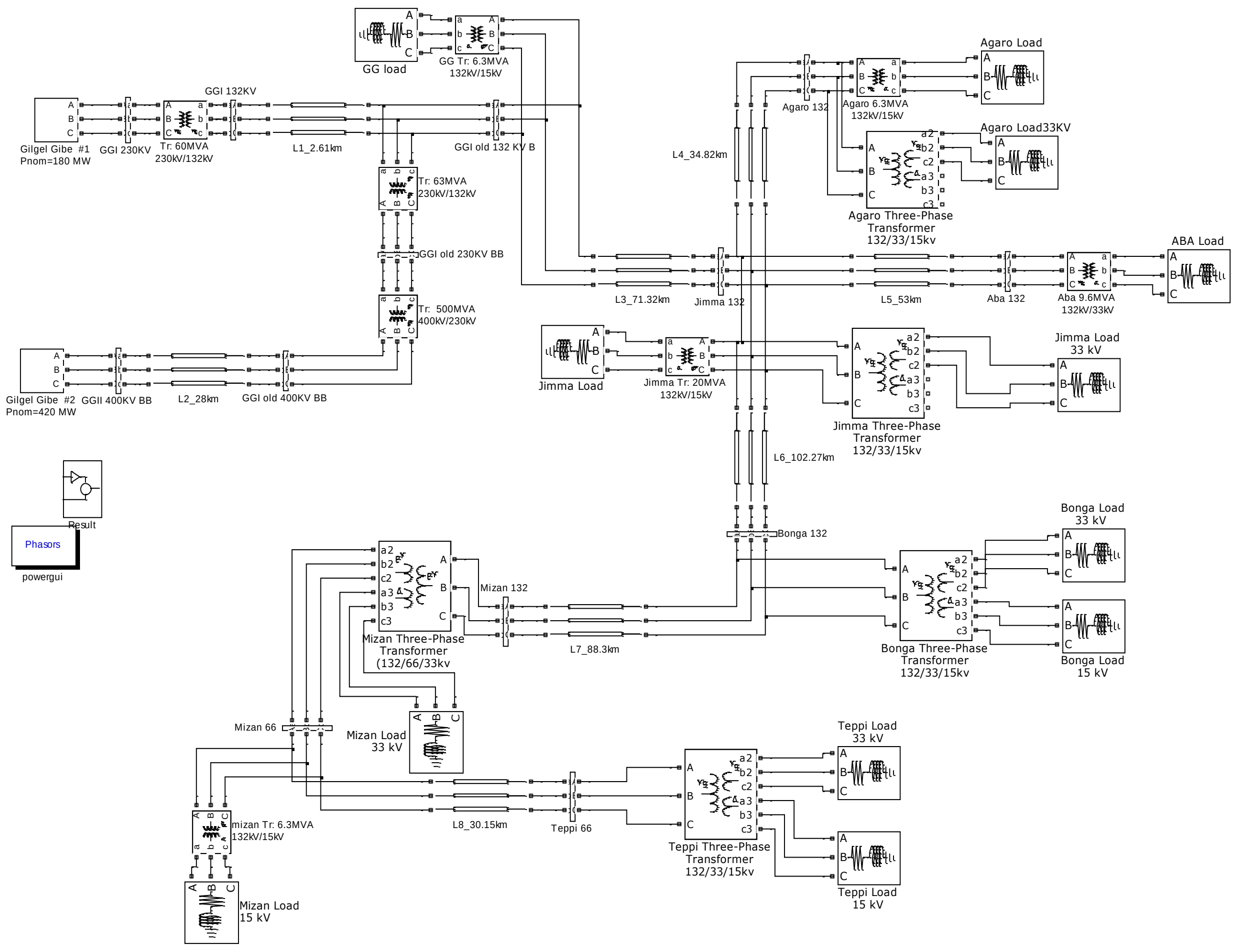

Figure 5.2: Overall existing transmission network of south western region of EEU

After filling all the necessary data in to the transmission network diagram of the existing south western region of EEU network starting from generating stations to the main HV/15kV distribution transformers in to MATLAB/Simulink software, the load flow simulation was run for the peak load condition. From the load flow result, active and reactive power at the buses, total transmission active and reactive power losses and bus voltages were identified. Table 5.1 shows that the overall MATLAB/Simulink result of the existing transmission network of south western region of EEU.

Table 5.1: Ethiopian south western Region Transmission network bus voltage and power without UPFC

Bus No.	Bus/Node Name	Bus Voltage (p.u)	Bus Voltage in KV	Real power (MW)	Reactive power (Mvar)	Bus Voltage (%nominal KV)
1	GGI-230	0.9996	229.908	-12.02	-4.328	99.96
2	GGI-132	0.9983	131.7756	11.89	4.205	99.83
3	GGII-400	1	400	-30.27	14.89	100
4	GGI old-400	1	400	-30.25	-2.708	100
5	GGI old-230	1	230	29.25	-3.709	100
6	GGI old-132	0.9974	131.6568	40.91	0.4636	99.74
7	Jimma-132	0.9392	123.9744	35.34	-0.029	93.92
8	Agaro-132	0.9326	123.1032	6.552	1.965	93.26
9	ABBA-132	0.9381	123.8292	1.583	0.5259	93.81
10	Bonga-132	0.9225	121.77	-9.938	0.5012	92.25
11	Mizan-132	0.9109	120.2388	-5.81	-1.638	91.09
12	Mizan-66	0.9014	59.4924	4.25	1.12	9.86
13	Teppi-66	0.8736	57.6576	3.609	1.183	87.36

From table 5.1 the bus voltages profiles of GGI-230, GGI-132, GGII-400, GGI old-400, GGI old-230 and GGI old 132 was between 99% and 100%. But the voltage profile of Jimma-132, Agaro-132, ABBA-132, Bonga-132, Mizan-132, Mizan-66 and Teppi-66 are less than 95%. This indicated that there is more real and reactive power losses on the transmission line and the voltage profile of the buses is unregulated. Due to this the power delivered to the load side is not as required level i.e. the power transmitted does not meet the demand power at each substation because of unregulated voltage attained at the buses. The simulation result shown in figure5.3 quantifies that the bus voltages are not regulated.

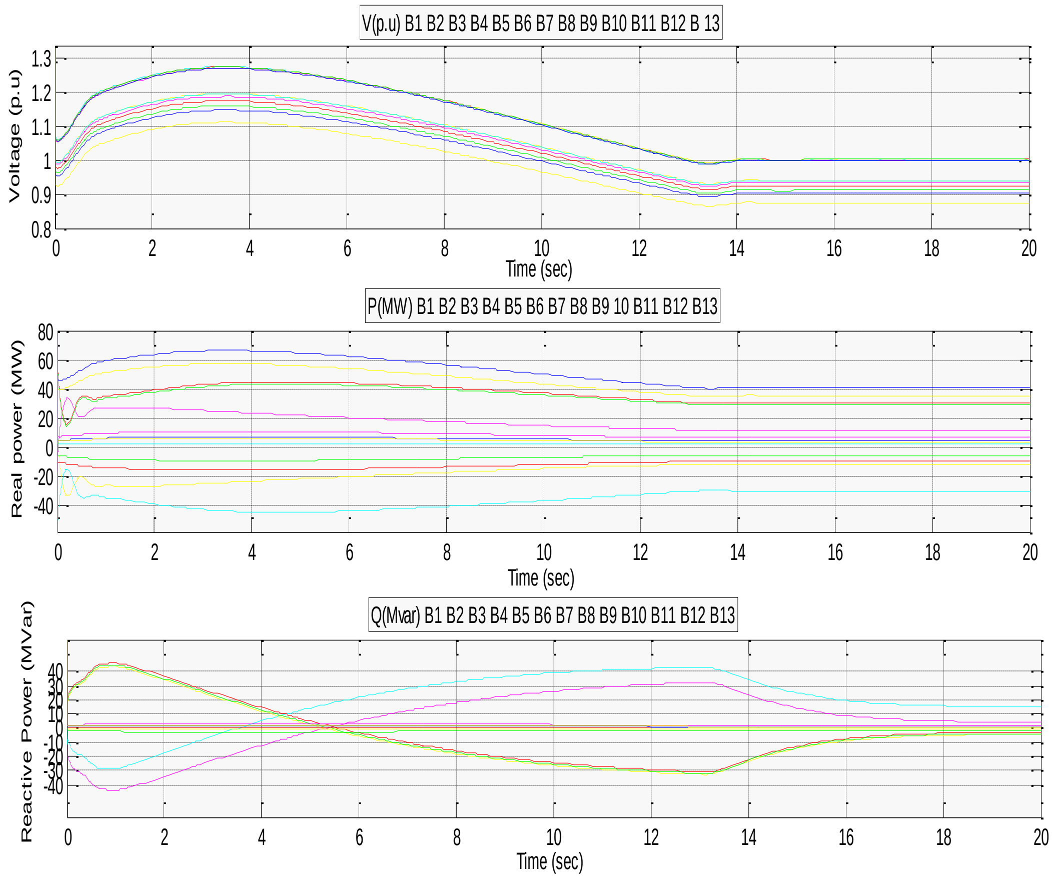

Figure 5.3: Bus-voltages, Real power and Reactive power of the interconnected system

Figure 5.3 indicated that the overall graphical result for bus voltages, real and reactive power injected at each buses.

The real power demand of total south western region of Ethiopia is 47.03MW at peak load condition but the total power delivered to load side is 36.61MW which is only 77.85% of the peak load will get the power. The total transformer real power loss is 2.31MW and total transmission line loss is 3.3667MW real power loss and 24.099Mvar reactive power loss as shown on table 5.2. Therefore, UPFC is incorporated between two buses of south western region transmission network in order to improve bus voltage, minimize the transmission line loss and optimize the power which is delivered to the load.

Table 5.2: Real power and reactive power losses of each transmission line without UPFC

Line number	From Bus	To Bus	Real power loss (MW)	Reactive power loss (MVar)
1	GGI-132	GGI old-132	0.04	0.0956
2	GGII-400	GGI old-400	0.02	14.78
3	GGI old-132	Jimma132	2.695	0.7287
4	Jimma-132	Agaro-132	0.048	1.6568
5	Jimma-132	ABBA-132	0.005	1.4564
6	Jimma-132	Bonga-132	0.33	4.8375
7	Bonga-132	Mizan-132	0.096	0.26
8	Mizan-66	Teppi-66	0.1327	0.2844
Total loss			3.3667	24.099

5.2. Incorporating UPFC into Transmission Network of South Western Region of EEU

The UPFC is incorporated into different places of EEU southwestern 132KV transmission network to regulate the bus voltage which increases the load-ability of the transmission line and get the optimal location of the UPFC. In this case there are five alternatives at which the UPFC were placed i.e. between GG-I old132-bus and Jimma-bus, Jimma-bus and Agaro-bus, Jimma-bus and ABBA-bus, Jimma-bus and Bonga-bus, Bonga-bus and Mizan-bus. The result obtained when UPFC is placed in different places is discussed below. The maximum UPFC injected voltage is 0.1p.u in all cases. The MVA rating of the UPFC is considered as 100MVA.

There are two modes of operation for shunt connected converter. These are voltage regulation mode and Var control mode. In the case of Var control mode the UPFC maintain the transmission line voltage at its reference value by absorbing from or providing reactive power to the transmission line. In case of voltage regulation mode UPFC shunt connected converter is used to keep the voltage level of the DC link capacitor at its reference value by drawing real power from the line.

5.2.1. Incorporating UPFC between GG-I old 132-bus and Jimma-bus

The UPFC is incorporated between GGI old-bus and Jimma-bus in transmission network of south western region of Ethiopia as shown in the figure 5.4 below.

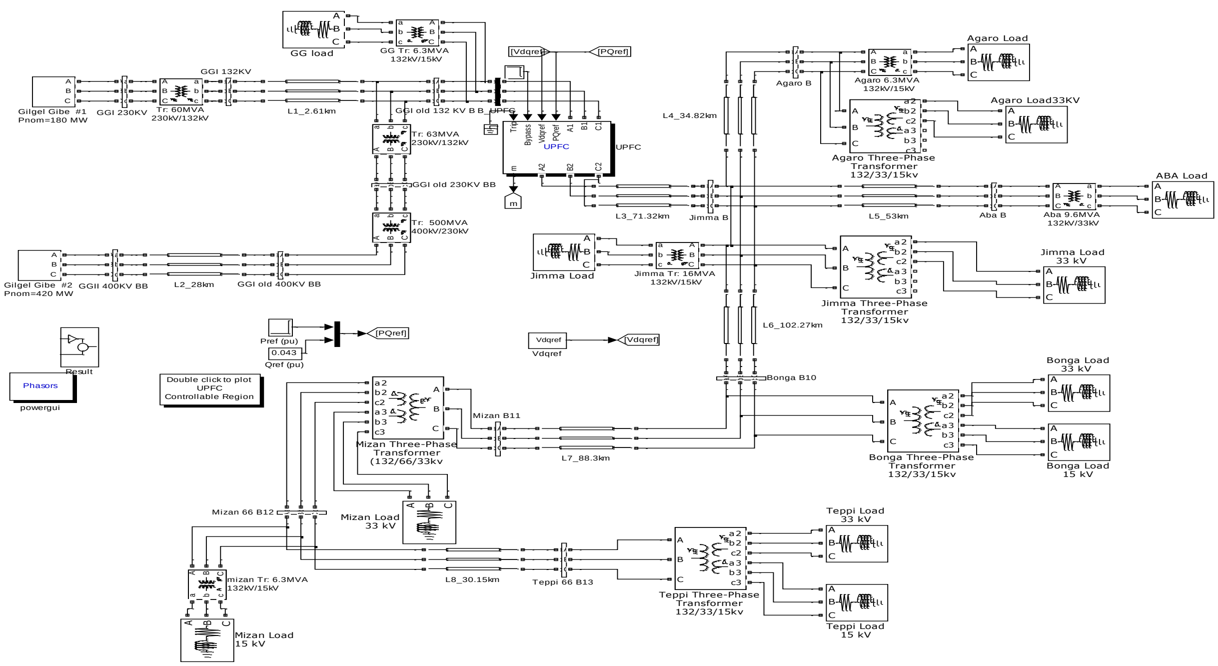

Figure 5.4: Transmission network of south western region of EEU with UPFC between GGI old-bus and jimma-bus

The addition of UPFC between GGI old132-bus and jimma bus improved the real power delivered to all substations to 41.8532 which is 88.99% of the peak load demand of the substations. When it is compared to the result without UPFC it has the difference of 11.14%. This indicated that the power transfer capability of the transmission line increases by 11.14% when UPFC is incorporated between GGI old132 bus and jimma bus of south western region transmission network. Table 5.3 shows the detailed MATLAB/Simulink result of the regulated bus voltage profile, real power and reactive power delivered to buses when UPFC is added in to the system.

Table 5.3: Ethiopian south western Region Transmission network bus voltage and power with UPFC incorporated between GGI old132-bus and jimma-bus

Bus No.	Bus/Node Name	Shunt converter is Voltage regulation mode			When Shunt converter is Var control mode		
		Bus Voltage (p.u)	Real power (MW)	Reactive power (Mvar)	Bus Voltage (p.u)	Real power (MW)	Reactive power (Mvar)
1	GGI-230	0.9993	-13.7	0.4328	0.9993	-13.68	-3.817
2	GGI-132	0.9979	13.56	-0.5553	0.9978	13.54	3.695
3	GGII-400	0.9999	-34.52	22.07	1	-34.49	17.1
4	GGI old-400	1.001	34.5	-9.92	1	34.47	-4.95
5	GGI old-230	1.001	33.5	-10.92	1	33.47	-5.951
6	GGI old-132	0.9972	46.8	-11.52	0.9968	46.75	-2.296
7	Jimma-132	1.01	40.87	-0.03354	1.009	40.84	-0.03351
8	Agaro-132	1.003	7.576	2.273	1.002	7.569	2.271
9	ABBA-132	1.009	1.831	0.6081	1.008	1.829	0.6076
10	Bonga-132	0.992	-11.49	0.5796	0.9916	-11.48	0.579
11	Mizan-132	0.9795	-6.719	-1.894	0.9791	-6.713	-1.893
12	Mizan-66	0.9694	4.915	1.295	0.9689	4.91	1.294
13	Teppi-66	0.9395	4.174	1.367	0.9391	4.17	1.366

The table 5.3 above quantifies that the bus voltages of all the buses are regulated to maximum level, the real power delivered also increased and the reactive power is compensated. The figures 5.5 and 5.6 demonstrated the graphical result of the overall south western region transmission network of EEU with UPFC when shunt converter is voltage regulation mode and Var control mode respectively.

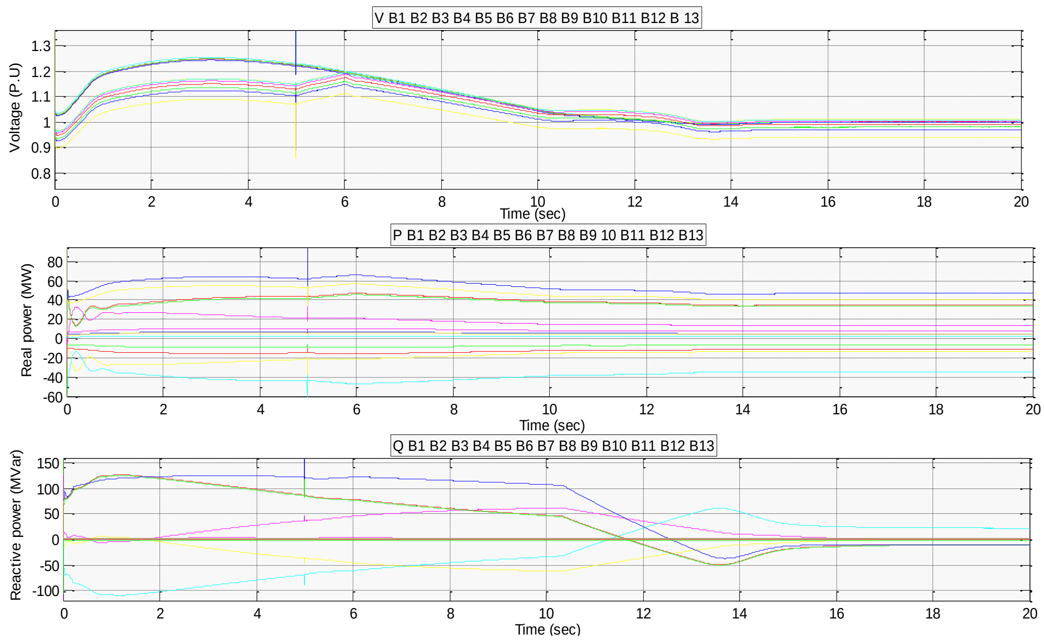

Figure 5.5: Bus-voltages, Real power and Reactive power with UPFC between GGI old-132 bus and jimma bus when shunt connected converter is voltage regulation mode

From figure 5.5 it is clear that the bus voltages are unregulated, real power delivered is not controllable manner and reactive power is not compensated up 5seconds until UPFC comes into the action. After the time is 5second the UPFC became into the system and starts injecting voltage of 0.1p.u in series with the line current. At this condition the bus voltage profiles start going to its regulated value, the real power delivered improved and reactive power starts compensating. Then when the UPFC injected voltage reached its maximum value the bus voltages are regulated, real power delivered to the buses is increased and the reactive power is compensated to its maximum level.

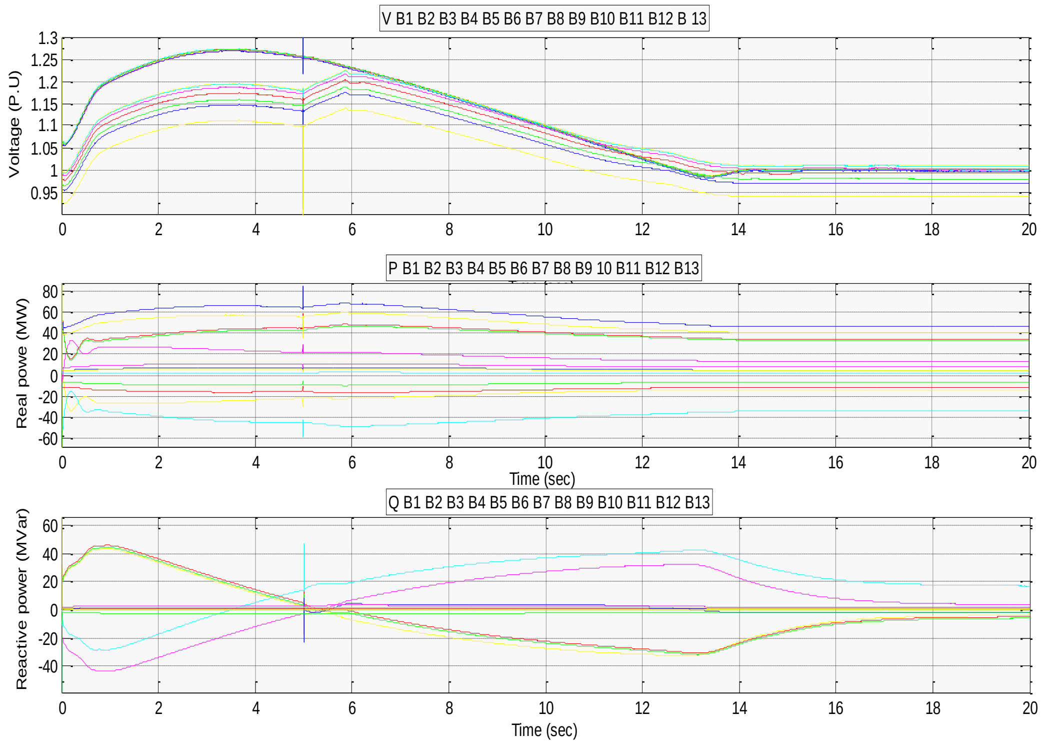

Figure 5.6: Bus-voltages, Real power and Reactive power with UPFC between GGI old-132 bus and jimma bus when shunt connected converter is Var control mode

The figure 5.6 above showed that the bus voltage profile and real power delivered to the buses in the case of shunt converter Var control mode is the same as that of shunt converter voltage regulation mode. But the reactive power delivered to the buses is more compensated because of the shunt compensator is used as Var controller as shown in the table 5.3 above. The UPFC series control real power, reactive power and converter voltage are shown in the appendix C.

The total active power loss is 3.156MW and reactive power loss is 21.2872Mvar when shunt connected converter is used as voltage regulation. When the shunt converter is operated as Var control mode, the total active power loss is 3.156MW and total reactive power is 21.287Mvar. Comparing this result with the total loss without UPFC 0.2107MW active power loss and 2.8118Mvar reactive power loss was minimized. The detailed result of transmission line loss with UPFC between GGI old132-bus and jimma-bus for the case study was summarized in the table5.4.

Table 5.4: Real power and reactive power losses of transmission line with UPFC between GGI old132-bus and Jimma-bus

Line number	From Bus	To Bus	UPFC b/n GGI-old & Jimma			
			Real power loss (MW)		Reactive power loss (MVar)	
			voltage Regulation mode	Var control mode	voltage Regulation mode	Var control mode
1	GGI-132	GGI old-132	0	0.01	0.1	0.1
2	GGII-400	GGI old-400	0.02	0.02	12.148	12.14
3	GGI old-132	Jimma132	2.55	2.55	0.99	1.03
4	Jimma-132	Agaro-132	0.045	0.045	1.5705	1.56
5	Jimma-132	ABBA-132	0.005	0.005	1.3809	1.37
6	Jimma-132	Bonga-132	0.32	0.32	4.5854	4.581
7	Bonga-132	Mizan-132	0.09	0.09	0.247	0.246
8	Mizan-66	Teppi-66	0.126	0.126	0.2654	0.26
Total loss			3.156	3.166	21.2872	21.287

5.2.2. Incorporating UPFC between Jimma-bus and Agaro-bus

Figure 5.7 showed that When the UPFC was incorporated between Jimma-bus and Agaro-bus in transmission network of south western region of Ethiopia.

When UPFC is located between Jimma-bus and Agaro-bus the real power delivered to all substations was improved to 41.3642 which is 87.95% of the peak load demand of the substations. When it is compared to the result without UPFC it has the difference of 10.10% and when compared to UPFC between GGI old132-bus and jimma-bus the transfer of power decreases by

1.04%. This indicated that the transfer capability of the transmission line increases by 10.10% when UPFC is incorporated between Jimma-bus and Agaro-bus of south western region transmission network.

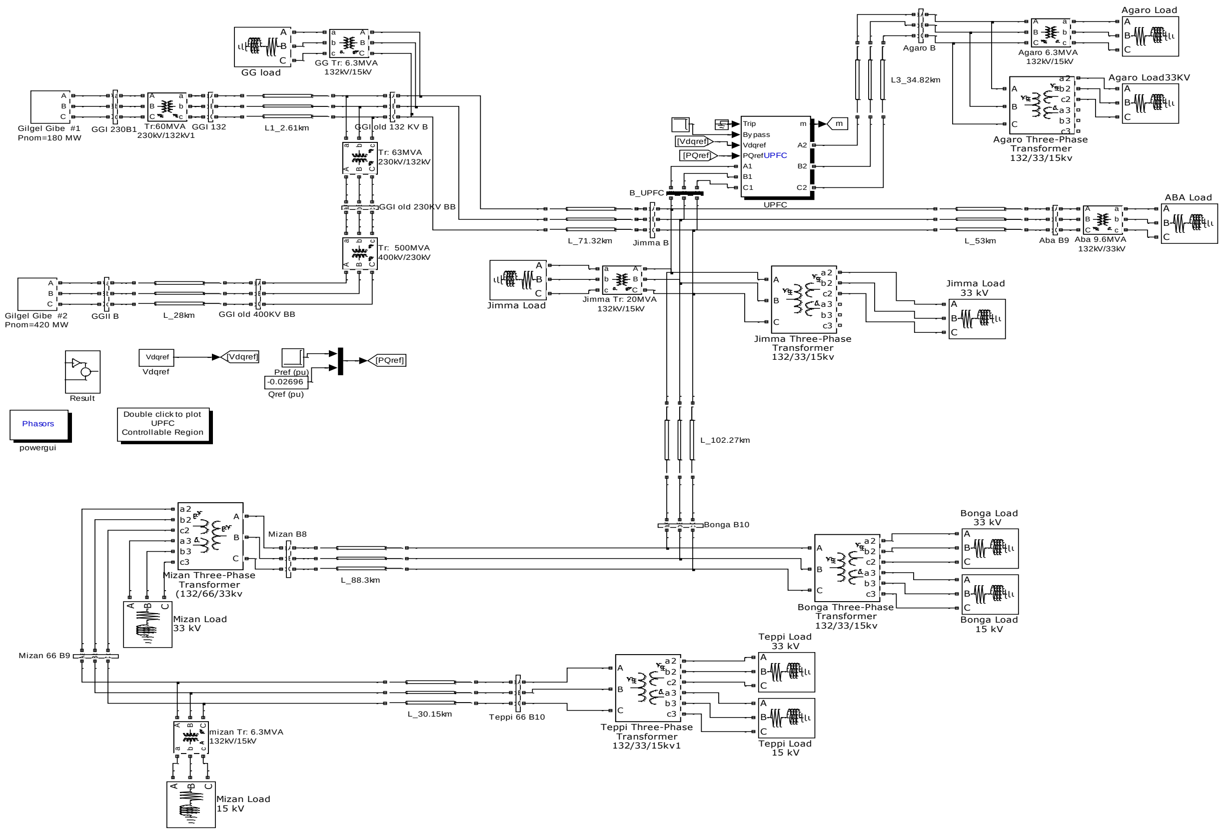

Figure 5.7: Transmission network of south western region of EEU with UPFC between Jimma-bus and Agaro-bus.

Table 5.5 showed the detailed MATLAB/Simulink result of the regulated bus voltage profile and real and reactive power delivered to buses when UPFC was incorporated between Jimma-bus and Agaro-bus. The bus voltage profile improved but it is not as better as when the UPFC is located between GGI old132-bus and Jimma-bus. And also the real power which is delivered to Agaro-bus was increased and on the other buses it is reduced in comparison to the first one.

Table 5.5: Ethiopian south western Region Transmission network bus voltage and power with UPFC incorporated between Jimma-bus and Agaro-bus

Bus No.	Bus/Node Name	Shunt converter is Voltage regulation mode			When Shunt converter is Var control mode		
		Bus Voltage (p.u)	Real power (MW)	Reactive power (Mvar)	Bus Voltage (p.u)	Real power (MW)	Reactive power (Mvar)
1	GGI-230	0.9996	-14.18	8.852	0.9998	-12.35	-4.3359
2	GGI-132	0.9983	14.03	-8.976	0.9985	12.22	4.237
3	GGII-400	1	-35.77	32.73	1	-31.11	15.22
4	GGI old-400	1.002	35.75	-20.61	1.001	31.1	-3.034
5	GGI old-230	1.001	34.75	-21.62	1.001	30.09	-4.035
6	GGI old-132	0.9981	48.45	-30.64	0.9976	42.08	0.1672
7	Jimma-132	0.9899	40.51	-33.71	0.9383	36.37	-0.4857
8	Agaro-132	1.058	8.429	2.528	1.006	7.626	2.288
9	ABBA-132	0.9888	1.759	0.5843	0.9372	1.58	0.5249
10	Bonga-132	0.9724	-11.04	0.5569	0.9216	-9.92	0.5002
11	Mizan-132	0.9601	-6.456	-1.82	0.91	-5.799	-1.635
12	Mizan-66	0.9502	4.722	1.245	0.9006	4.242	1.118
13	Teppi-66	0.9209	4.01	1.314	0.8728	3.603	1.18

The graphical result of the bus voltage, real and reactive power transfer is shown in the figure 5.8 when the UPFC shunt connected converter was operated as voltage regulation mode.

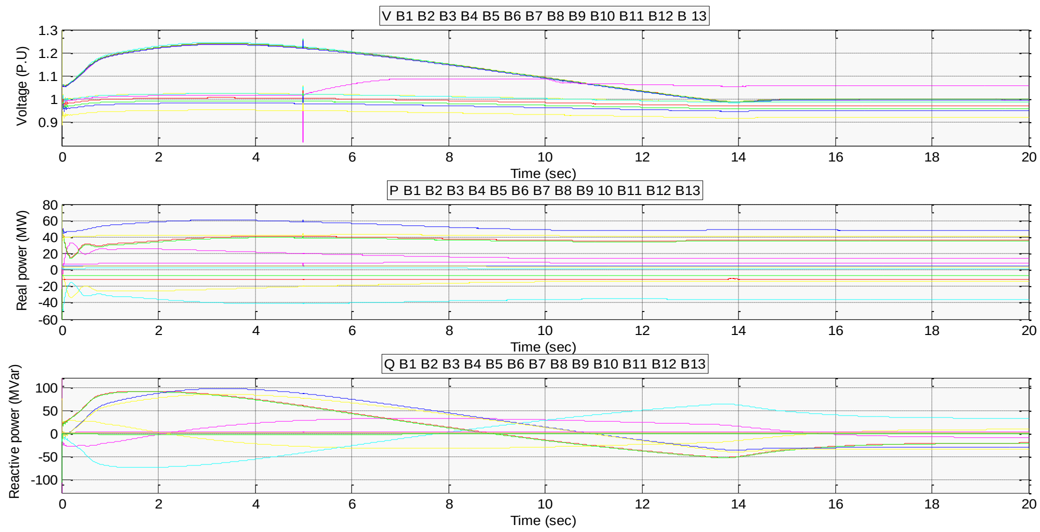

Figure 5.8: Bus-voltages, Real power and Reactive power with UPFC between Jimma-bus and Agaro-bus when shunt connected converter is voltage regulation mode

The graphical result of all bus voltage profile, real power and reactive power transferred to each buses when the UPFC shunt connected converter is operated as Var control mode is shown in the figure 5.9.

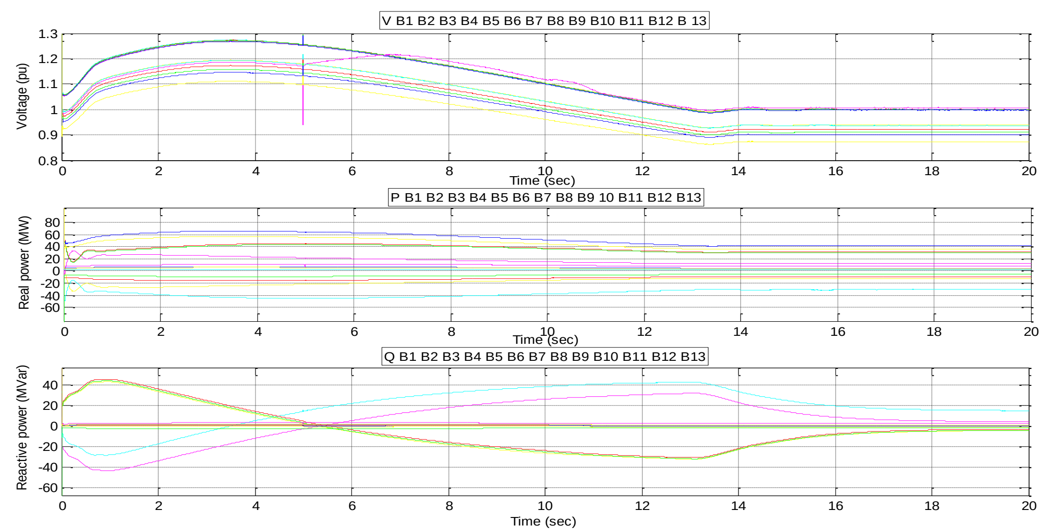

Figure 5.9: Bus-voltages, Real power and Reactive power with UPFC between Jimma-bus and Agaro-bus when shunt connected converter is Var control mode

The total active power loss is 5.2606MW and reactive power loss is 22.869Mvar when shunt connected converter is used as voltage regulation. This result showed that the real power loss increases by 1.8939MW, the reactive power loss is reduced by 1.23Mvar and the power transfer capability increased.

When the shunt converter is operated as Var control mode the total active power loss is 2.8816MW and total reactive power loss is 21.3158Mvar. This indicated that when shunt connected converter is functioned as Var control mode the real power loss reduced by 0.4851MW and reactive power by 2.784Mvar. The detailed result of transmission line loss with UPFC between Jimma-bus and Agaro-bus for the case study was summarized in the table 5.6.

Table 5.6: Real power and reactive power losses of transmission line with UPFC between Jimma-bus and Agaro-bus

Line number	From Bus	To Bus	Real power loss (MW)		Reactive power loss (MVar)	
			voltage Regulation mode	Var control mode	voltage Regulation mode	Var control mode
1	GGI-132	GGI old-132	0.02	0.01	0.106	0.1055
2	GGII-400	GGI old-400	0.02	0.01	12.12	12.186
3	GGI old-132	Jimma132	4.579	2.352	2.036	1.3505
4	Jimma-132	Agaro-132	0.128	0.047	2.3784	2.0784
5	Jimma-132	ABBA-132	0.005	0.005	1.3267	1.1921
6	Jimma-132	Bonga-132	0.3	0.27	4.4061	3.9578
7	Bonga-132	Mizan-132	0.087	0.079	0.237	0.213
8	Mizan-66	Teppi-66	0.1216	0.1086	0.2588	0.2325
Total loss			5.2606	2.8816	22.869	21.3158

5.2.3. Incorporating UPFC between Jimma-bus and ABBA-bus

The overall simulation diagram of the south western region transmission network of EEU with UPFC is placed between Jimma-bus and ABBA-bus is shown in the figure 5.10 below. In this section the power flow of the case study transmission network of 13–bus system is tested on MATLAB/Simulink.

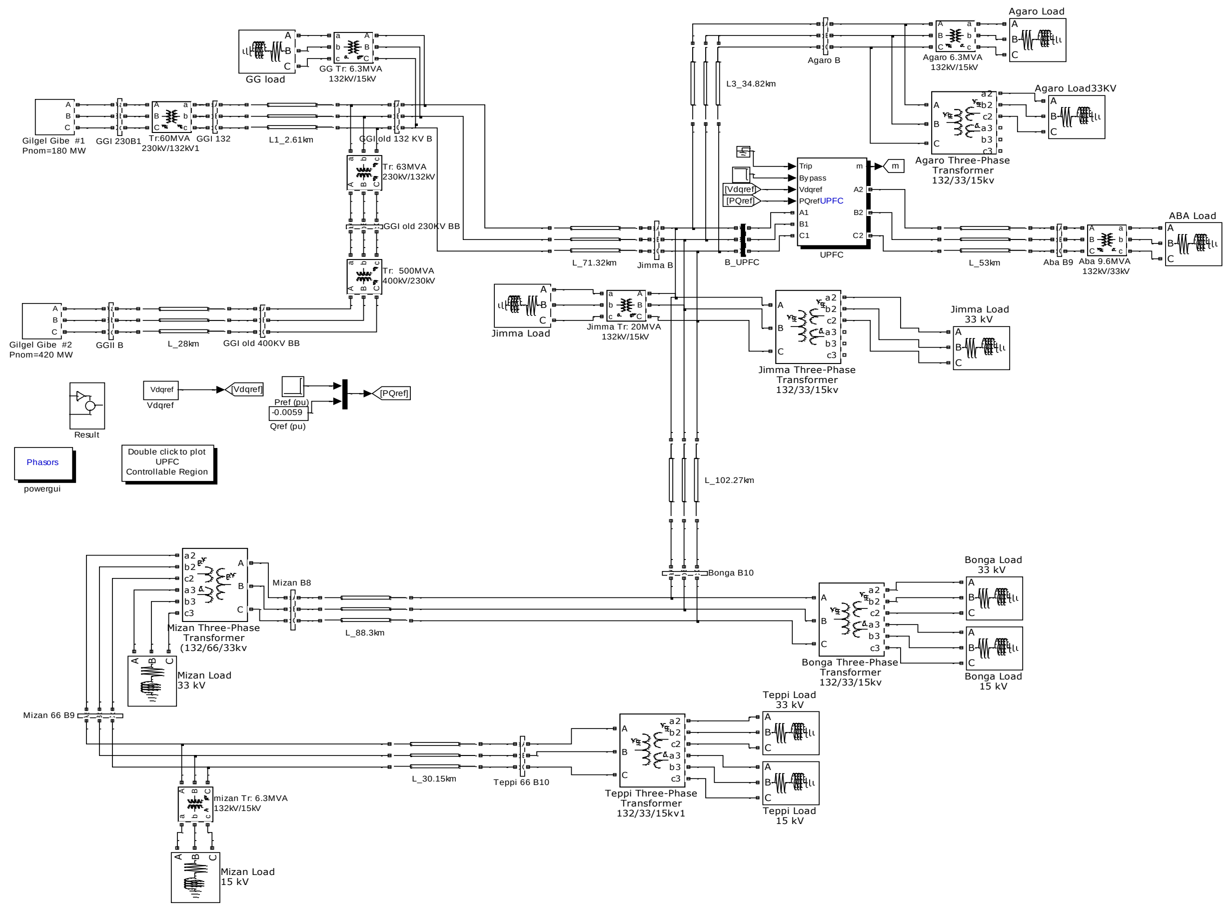

Figure 5.10: Transmission network of south western region of EEU with UPFC between Jimma-bus and ABBA-bus.

We can clearly see that on table 5.7 the voltage profile of the buses and the power flow was improved by relieving the lines in the area where by introducing UPFC between jimma bus and ABBA-bus. The improved bus voltage profile is as good as UPFC between Jimma bus and Agaro bus but not as better as when the UPFC is introduced between GGI old132-bus and Jimma-bus. And also the real power which is delivered to ABBA-bus was increased and on the other buses it is reduced in comparison to the UPFC between GGI old132-bus and jimma bus.

Table 5.7: Ethiopian south western Region Transmission network bus voltage profile and power with UPFC introduced between Jimma-bus and ABBA-bus

Bus No.	Bus/Node Name	Shunt converter is Voltage regulation mode			When Shunt converter is Var control mode		
		Bus Voltage (p.u)	Real power (MW)	Reactive power (Mvar)	Bus Voltage (p.u)	Real power (MW)	Reactive power (Mvar)
1	GGI-230	0.9996	-13.88	8.697	0.9996	-12.11	-4.271
2	GGI-132	0.9984	13.73	-8.821	0.9983	11.97	4.149
3	GGII-400	1	-34.99	32.23	1	-30.48	15.05
4	GGI old-400	1.002	34.96	-20.1	1	30.47	-2.868
5	GGI old-230	1.001	33.95	-21.11	1	29.46	-3.87
6	GGI old-132	0.9982	47.38	-29.98	0.9974	41.21	0.2464
7	Jimma-132	0.9902	39.64	-32.8	0.9392	35.61	-0.2858
8	Agaro-132	0.9833	7.282	2.184	0.9326	6.552	1.965
9	ABBA-132	1.064	2.038	0.6768	1.013	1.848	0.6136
10	Bonga-132	0.9726	-11.05	0.5571	0.9225	-9.938	0.5012
11	Mizan-132	0.9603	-6.458	-1.821	0.9109	-5.81	-1.638
12	Mizan-66	0.9504	4.724	1.245	0.9014	4.25	1.12
13	Teppi-66	0.9211	4.012	1.314	0.8736	3.609	1.183

When UPFC is located between Jimma-bus and ABBA-bus the real power delivered to all substations was improved to 40.6264 which is 86.38% of the peak load demand of the substations. When it is compared to the result without UPFC it has the difference of 8.53%. This indicated that the transfer capability of the transmission line increases by 8.53% when UPFC is incorporated between Jimma-bus and ABBA-bus of south western region transmission network. But it can be seen that the transfer capability of power by introducing UPFC between Jimma-bus and ABBA-bus is the least compared to UPFC between GGI old132 and Jimma or Jimma and Agaro.

The graphical MATLAB/Simulink result that shows active power flow, reactive power flow and the bus voltage profile when UPFC shunt converter is functioned as voltage regulation mode are shown in the figure 5.11.

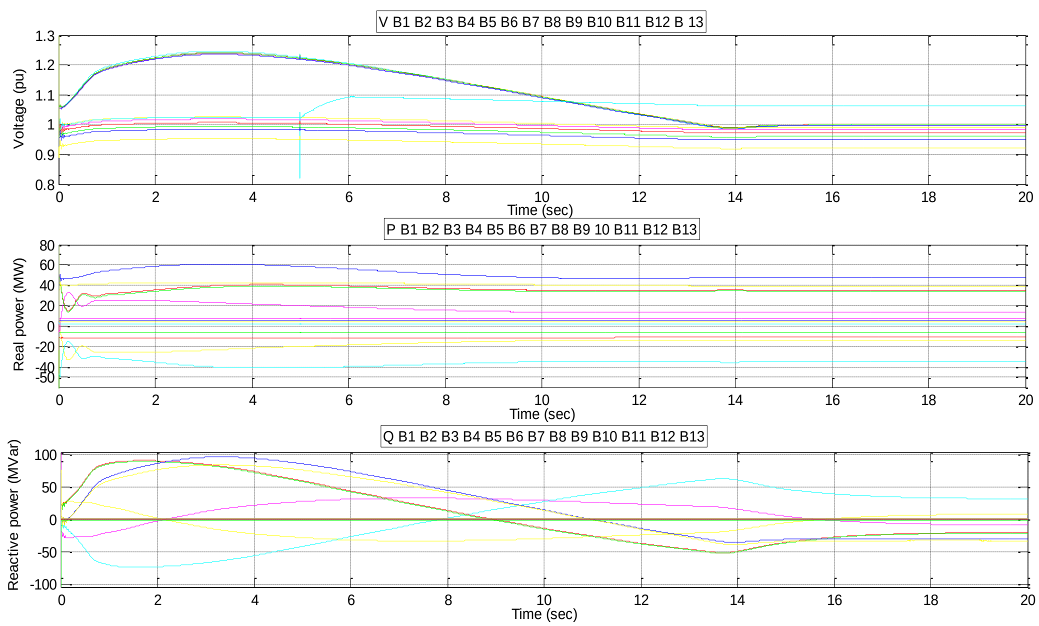

Figure 5.11: Bus-voltages, Real power and Reactive power with UPFC between Jimma-bus and ABBA-bus when shunt connected converter is voltage regulation mode

Similarly, for shunt converter var control mode the graphical MATLAB/Simulink result that shows active power flow, reactive power flow and the bus voltage profile are shown in the figure 5.12.

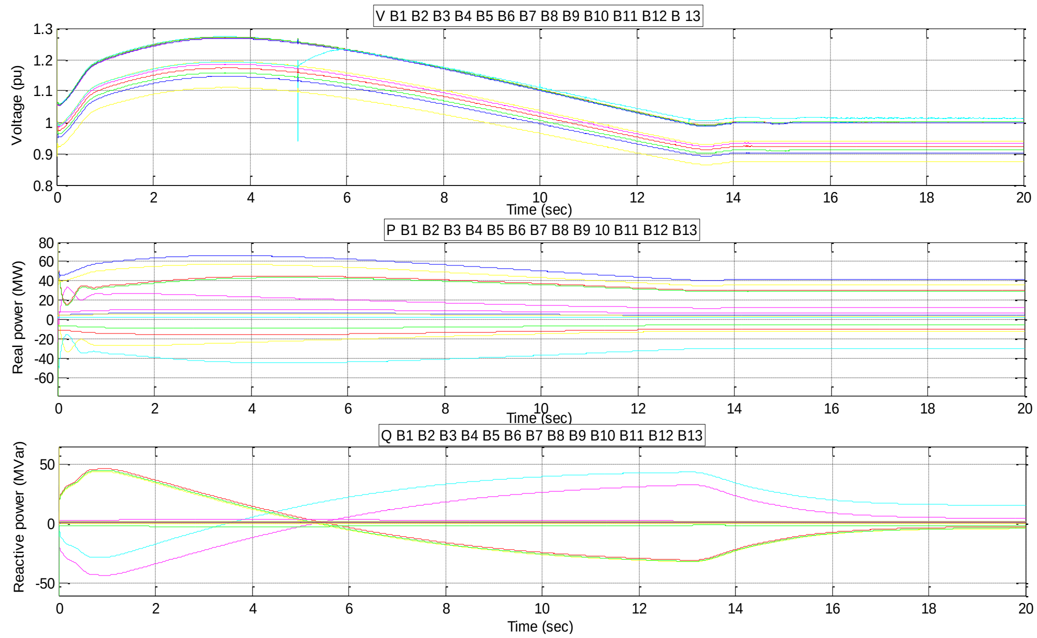

Figure 5.12: Bus-voltages, Real power and Reactive power with UPFC between Jimma-bus and ABBA-bus when shunt connected converter is Var control mode

Therefore, total active power loss is 5.0523MW which accounts 10.33% of total generated power and reactive power loss is 21.7997Mvar when shunt connected converter is used as voltage regulation. This result showed that the real power loss increases by 1.6856MW since the transfer capacity increases and the reactive power loss is reduced by 2.2993Mvar.

When the shunt converter is operated as Var control mode the total active power loss is 2.7566MW which accounts 6.47% of total generated power and total reactive power loss is 20.4933Mvar. This indicated that when shunt connected converter is functioned as Var control mode the real power loss reduced by 0.6101MW and reactive power by 3.6057Mvar. The detailed result of transmission line loss with UPFC between Jimma-bus and ABBA-bus for the case study was summarized in the table 5.8.

Table 5.8: Real power and reactive power losses of transmission line with UPFC between Jimma-bus and ABBA-bus

Line number	From Bus	To Bus	UPFC b/n Jimma & ABBA			
			Real power loss (MW)		Reactive power loss (MVar)	
			voltage Regulation mode	Var control mode	voltage Regulation mode	Var control mode
1	GGI-132	GGI old-132	0.01	0	0.101	0.1064
2	GGII-400	GGI old-400	0.03	0.01	12.2	12.182
3	GGI old-132	Jimma132	4.378	2.244	1.786	1.0714
4	Jimma-132	Agaro-132	0.044	0.039	1.5088	1.3575
5	Jimma-132	ABBA-132	0.081	0.003	1.3002	1.3634
6	Jimma-132	Bonga-132	0.3	0.272	4.4079	3.9648
7	Bonga-132	Mizan-132	0.088	0.079	0.237	0.214
8	Mizan-66	Teppi-66	0.1213	0.1096	0.2588	0.2338
Total loss			5.0523	2.7566	21.7997	20.4933

5.2.4. Incorporating UPFC between Jimma-bus and Bonga-bus

At this condition the UPFC is introduced between Jimma-bus and Bonga-bus of south western region transmission network as shown in the figure 5.13 in order to improve the bus voltage, transmission line transfer capacity and loss minimization.

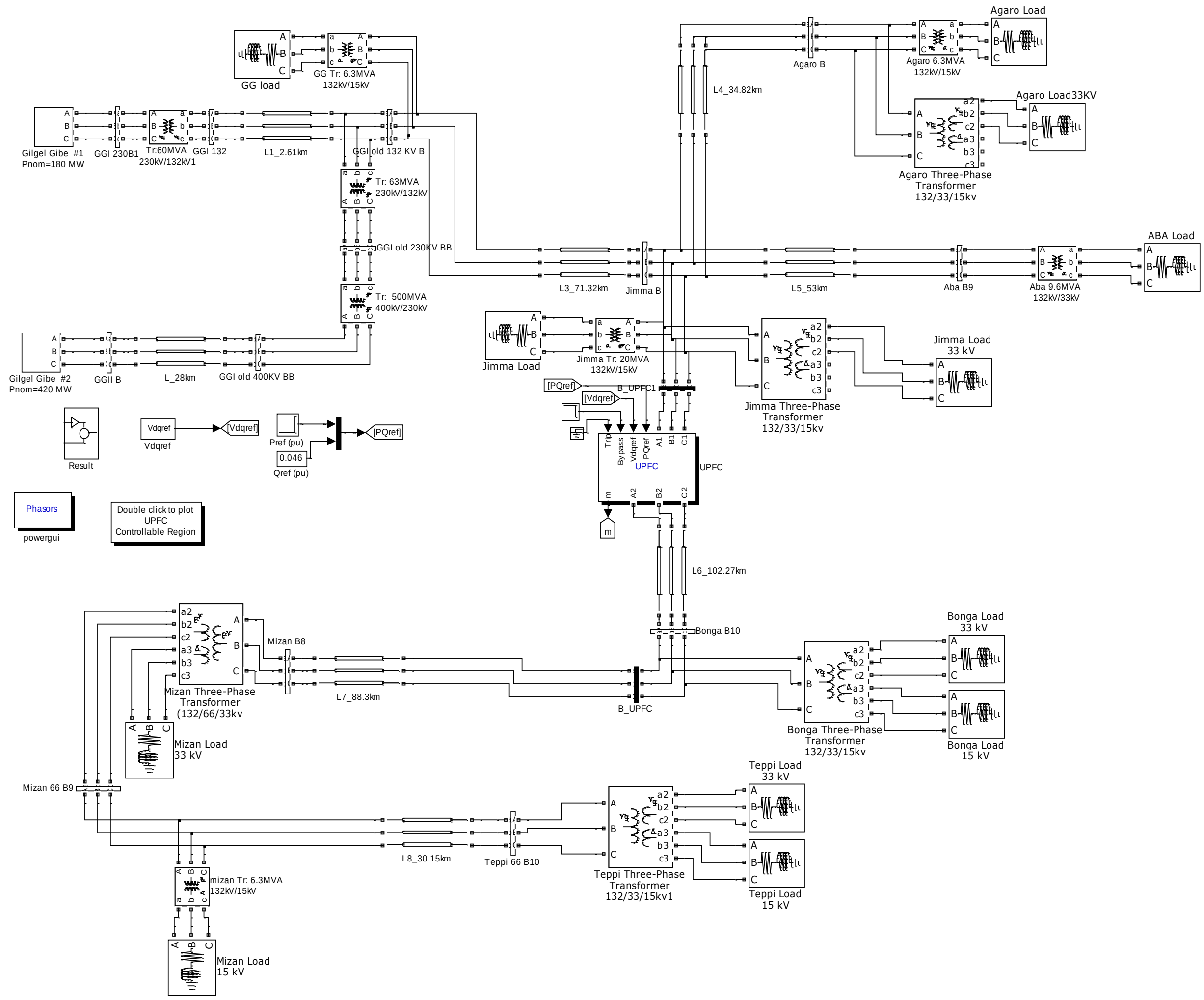

Figure 5.13: Transmission network of south western region of EEU with UPFC between Jimma-bus and Bonga-bus.

The simulation result clearly shows that the power transfer capability of the transmission line and bus profile voltage is improved well. But the bus voltage of Agaro-bus and ABBA-bus is not better when compared to UPFC located to other places. The table 5.9 shows that the detailed improved bus voltage profile and power flow of all buses.

Table 5.9: Ethiopian south western Region Transmission network bus voltage profile and power flow with UPFC introduced between Jimma-bus and Bonga-bus

Bus No.	Bus/Node Name	Shunt converter is Voltage regulation mode			When Shunt converter is Var control mode		
		Bus Voltage (p.u)	Real power (MW)	Reactive power (Mvar)	Bus Voltage (p.u)	Real power (MW)	Reactive power (Mvar)
1	GGI-230	0.9996	-14.41	9.002	0.9996	-12.55	-4.198
2	GGI-132	0.9983	14.27	-9.126	0.9983	12.41	4.075
3	GGII-400	1	-36.37	33.13	1	-31.6	15.63
4	GGI old-400	1.002	36.34	-21.02	1.001	31.59	-3.452
5	GGI old-230	1.001	35.33	-22.02	1	30.58	-4.453
6	GGI old-132	0.9981	49.27	-31.2	0.9973	42.76	-0.413
7	Jimma-132	0.99	41.16	-34.46	0.9381	36.97	-1.163
8	Agaro-132	0.9831	7.279	2.184	0.9316	6.537	1.961
9	ABBA-132	0.9888	1.759	0.5843	0.9371	1.58	0.5247
10	Bonga-132	1.046	-12.79	0.6449	0.9956	-11.58	0.5838
11	Mizan-132	1.033	-7.476	-2.108	0.9831	-6.768	-1.908
12	Mizan-66	1.023	5.469	1.441	0.9729	4.95	1.305
13	Teppi-66	0.991	4.644	1.522	0.9429	4.204	1.377

When UPFC is located between Jimma-bus and Bonga-bus the real power delivered to all substations was improved to 42.0025MW which is 89.31% of the peak load demand of the substations. When it is compared to the result without UPFC it has the difference of 11.46%. This indicated that the transfer capability of the transmission line increases by 11.46% when UPFC is incorporated between Jimma-bus and Bonga-bus of south western region transmission network. It can be seen that the transfer capability of power by introducing UPFC between Jimma-bus and Bonga-bus is the best compared to UPFC between other buses.

The graphical MATLAB/Simulink result that shows active power flow, reactive power flow and the bus voltage profile when UPFC shunt converter is functioned as voltage regulation mode are shown in the figure 5.14.

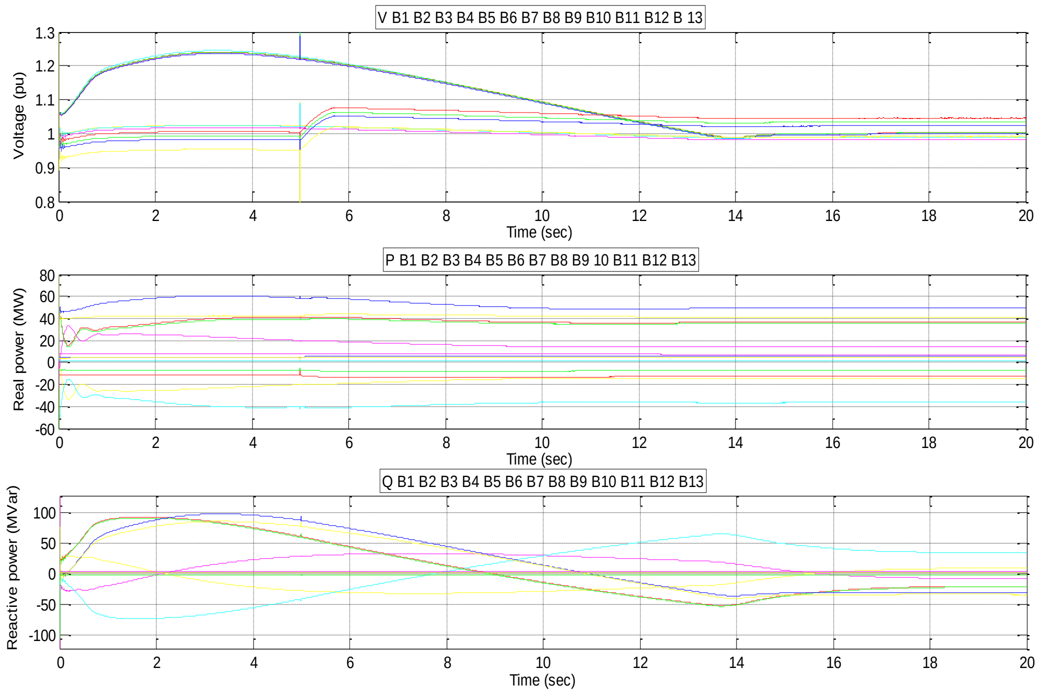

Figure 5.14: Bus-voltages, Real power and Reactive power with UPFC between Jimma-bus and Bonga-bus when shunt connected converter is voltage regulation mode

Similarly, for shunt converter Var control mode the graphical MATLAB/Simulink result that shows active power flow, reactive power flow and the bus voltage profile are shown in the figure5.15.

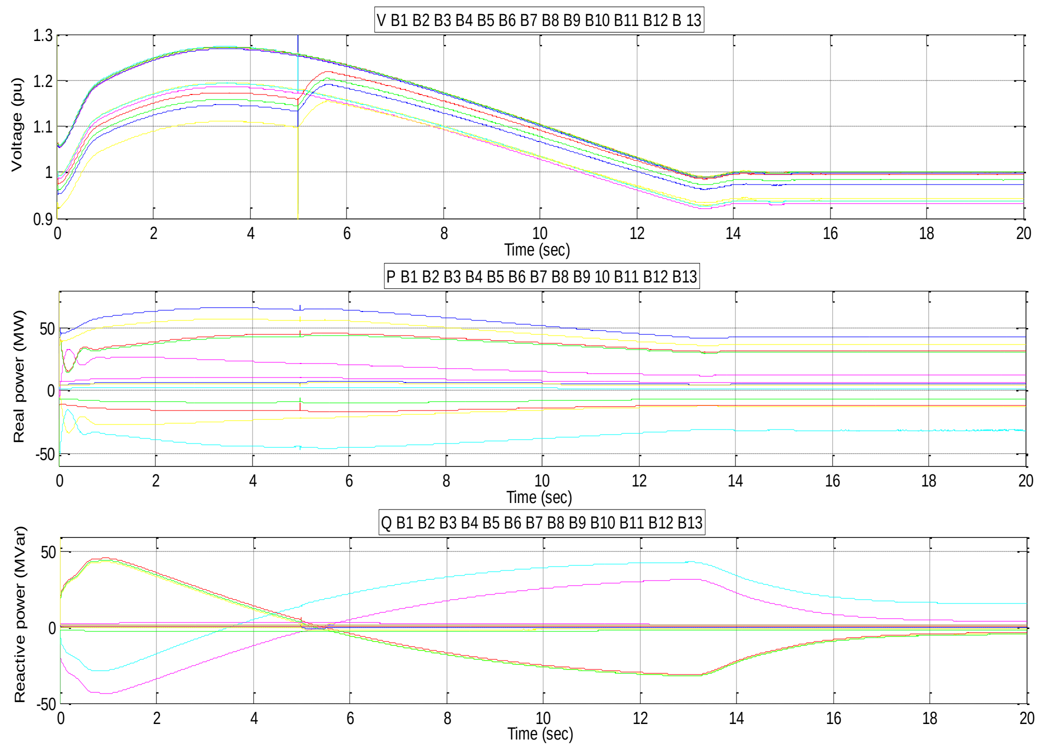

Figure 5.15: Bus-voltages, Real power and Reactive power with UPFC between Jimma-bus and Bonga-bus when shunt connected converter is Var control mode

It is identified that when UPFC shunt converter is functioned as voltage regulation mode total active power loss is 5.5313MW which accounts 10.89% of total generated power and reactive power loss is 22.7906Mvar. This result showed that the real power loss increases by 2.1648MW since the transfer capacity increases and the reactive power loss is reduced by 1.3084Mvar.

When the shunt converter is operated as Var control mode the total active power loss is 3.026MW which accounts 6.85% of total generated power and total reactive power loss is 22.1393Mvar. This indicated that when shunt connected converter is functioned as Var control mode the real power loss reduced by 0.3405MW and reactive power by 1.9597Mvar. The detailed result of transmission line loss with UPFC between Jimma-bus and Bonga-bus for the case study was summarized in the table 5.10.

Table 5.10: Real power and reactive power losses of transmission line with UPFC between Jimma-bus and Bonga-bus

Line number	From Bus	To Bus	UPFC b/n Jimma & Bonga			
			Real power loss (MW)		Reactive power loss (MVar)	
			voltage Regulation mode	Var control mode	voltage Regulation mode	Var control mode
1	GGI-132	GGI old-132	0.02	0.01	0.096	0.106
2	GGII-400	GGI old-400	0.03	0.01	12.11	12.178
3	GGI old-132	Jimma132	4.749	2.434	2.227	1.782
4	Jimma-132	Agaro-132	0.044	0.039	1.509	1.3549
5	Jimma-132	ABBA-132	0.005	0.004	1.3267	1.1913
6	Jimma-132	Bonga-132	0.44	0.31	4.9461	5.0072
7	Bonga-132	Mizan-132	0.102	0.092	0.275	0.249
8	Mizan-66	Teppi-66	0.1413	0.127	0.3008	0.2709
Total loss			5.5313	3.026	22.7906	22.1393

5.2.5. Incorporating UPFC between Bonga-bus and Mizan-bus

The UPFC is introduced between Bonga-bus and Mizan-bus of south western region transmission network as shown in the figure 5.16 in order to improve the bus voltage, transmission line transfer capacity and loss minimization.

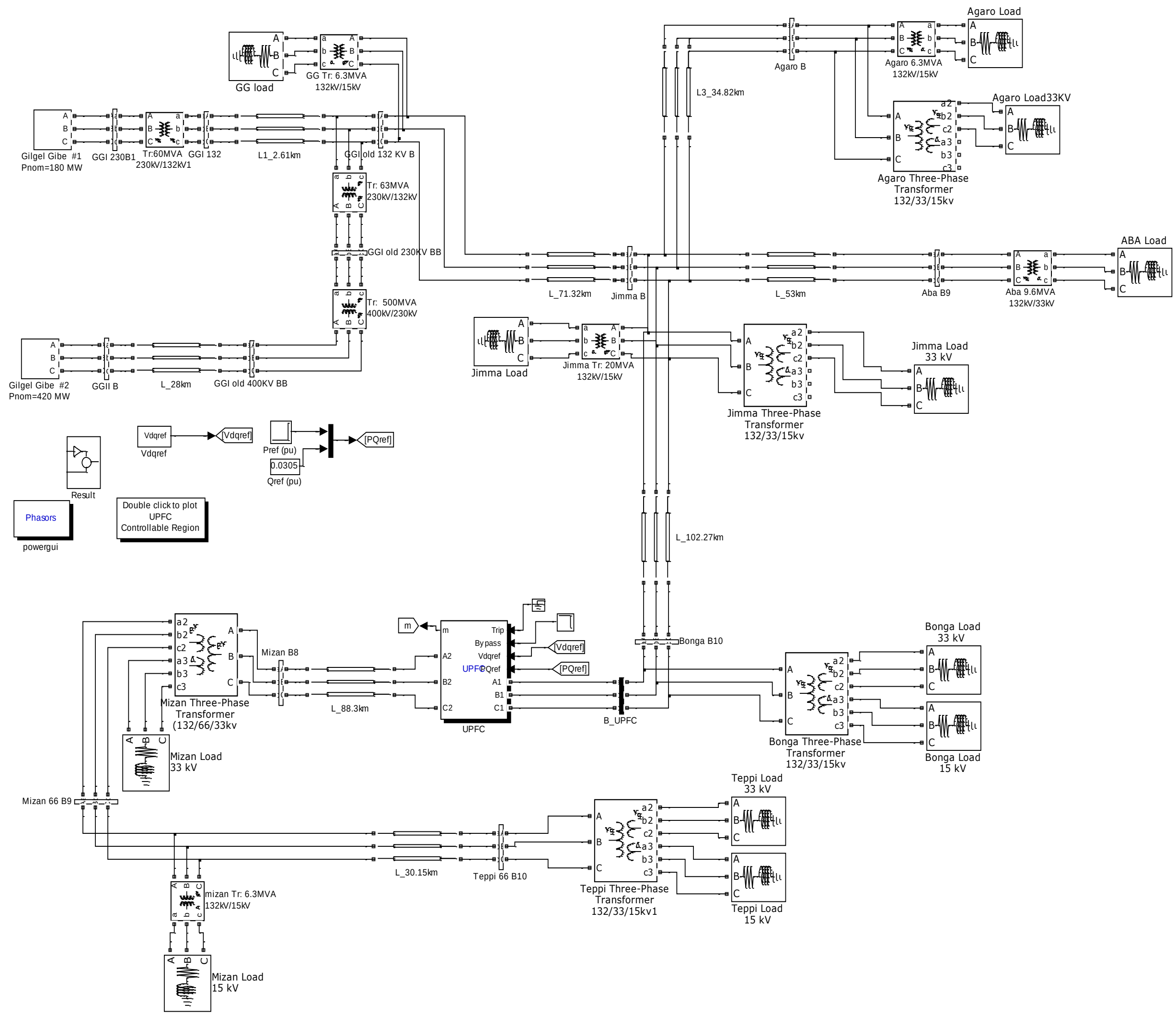

Figure 5.16: Transmission network of south western region of EEU with UPFC between Bonga-bus and Mizan-bus.

The simulation result clearly shows that the power transfer capability of the transmission line and bus voltage profile is improved. But the bus voltages of jimma-bus, Agaro-bus, ABBA-bus, Bonga-bus, and Teppi-bus is not as the required level of voltage profile. The table 5.11 shows that the detailed simulation result of bus voltage profile and power flow of all buses.

Table 5.11: Ethiopian south western Region Transmission network bus voltage profile and power flow with UPFC introduced between Bonga-bus and Mizan-bus

Bus No.	Bus/Node Name	Shunt converter is Voltage regulation mode			When Shunt converter is Var control mode		
		Bus Voltage (p.u)	Real power (MW)	Reactive power (Mvar)	Bus Voltage (p.u)	Real power (MW)	Reactive power (Mvar)
1	GGI-230	1.029	-22.32	14.91	0.9999	-12.34	-4.321
2	GGI-132	1.027	22.13	-15.04	0.9986	12.21	4.199
3	GGII-400	1.028	-53.88	57.01	1.001	-31.09	15.26
4	GGI old-400	1.031	53.81	-44.41	1.001	31.07	-3.073
5	GGI old-230	1.031	52.74	-45.48	1.001	30.07	-4.074
6	GGI old-132	1.026	74.21	-60.65	0.9976	42.04	0.09023
7	Jimma-132	1.046	57.96	-72.82	0.9385	36.34	-0.5563
8	Agaro-132	1.039	8.128	2.438	0.932	6.543	1.963
9	ABBA-132	1.045	1.965	0.6524	0.9375	1.581	0.5252
10	Bonga-132	1.191	-14.17	86.72	0.921	-10.91	1.102
11	Mizan-132	1.257	-11.06	-3.118	0.9838	-6.777	-1.911
12	Mizan-66	1.244	8.089	2.132	0.9736	4.957	1.307
13	Teppi-66	1.205	6.87	2.251	0.9436	4.21	1.379

The graphical MATLAB/Simulink result that shows active power flow, reactive power flow and the bus voltage profile when UPFC shunt converter is functioned as voltage regulation mode are shown in the figure 5.17. This quantified that the power transferred to each buses is not at stable condition and the voltage instability occurs because the UPFC is introduced in the transmission network at far away position of the generation plant.

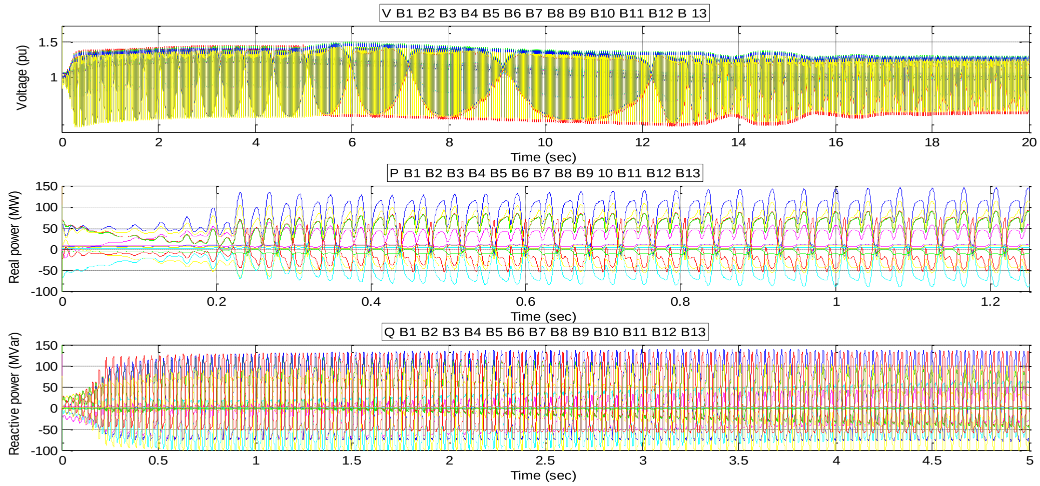

Figure 5.17: Bus-voltages, Real power and Reactive power with UPFC between Bonga-bus and Mizan-bus when shunt connected converter is voltage regulation mode

Similarly, for shunt converter var control mode the graphical MATLAB/Simulink result that shows active power flow, reactive power flow and the bus voltage profile are shown in the figure 5.18.

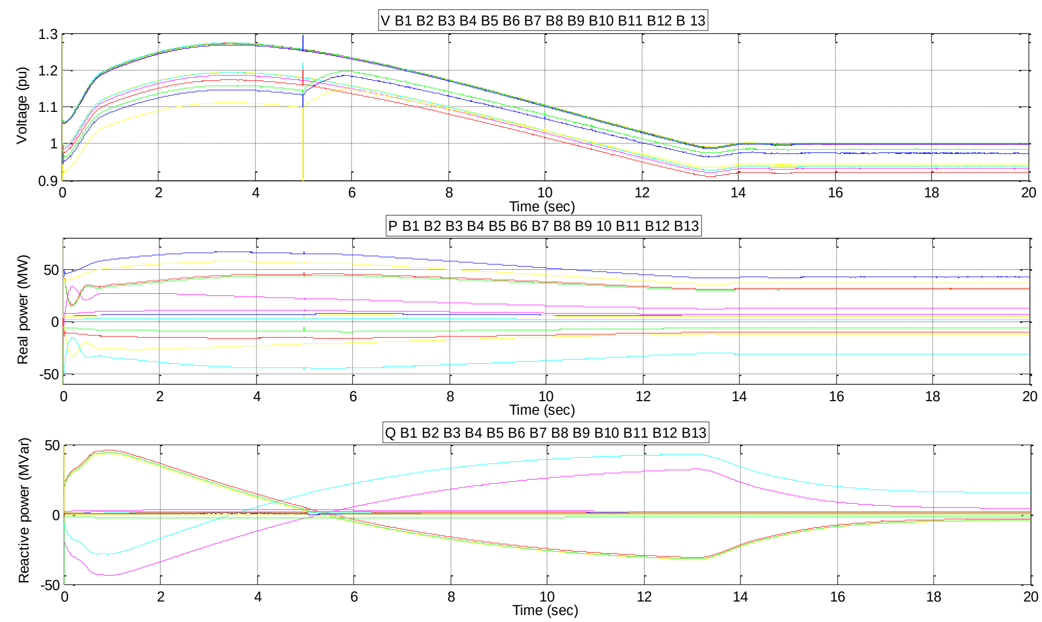

Figure 5.18: Bus-voltages, Real power and Reactive power with UPFC between Jimma-bus and Bonga-bus when shunt converter is Var control mode

We can clearly understand that when UPFC is located between Bonga-bus and Mizan-bus and shunt converter is functioned as voltage regulation mode total active power loss is 3.981MW which accounts 5.22% of total generated power and reactive power loss is 26.5587Mva. When the shunt converter is operated as Var control mode the total active power loss is 2.9682MW which accounts 3.89% of total generated power and total reactive power loss is 21.03437Mvar. This indicated that when shunt connected converter is functioned as Var control mode the real power loss reduced by 0.3405MW and reactive power by 1.9597Mvar. The detailed result of transmission line loss with UPFC between Jimma-bus and Bonga-bus for the case study was summarized in the table 5.12.

Table 5.12: Real power and reactive power losses of transmission line with UPFC between Bonga-bus and Mizan-bus

Line number	From Bus	To Bus	Real power loss (MW)		Reactive power loss (MVar)	
			voltage Regulation mode	Var control mode	voltage Regulation mode	Var control mode
1	GGI-132	GGI old-132	0.05	0.01	0.07	0.105
2	GGII-400	GGI old-400	0.07	0.02	12.6	12.187
3	GGI old-132	Jimma132	2.695	2.342	1.107	1.49907
4	Jimma-132	Agaro-132	0.049	0.039	1.6843	1.3563
5	Jimma-132	ABBA-132	0.005	0.005	1.4816	1.1928
6	Jimma-132	Bonga-132	0.61	0.33	8.4	3.886
7	Bonga-132	Mizan-132	0.36	0.095	0.7717	0.537
8	Mizan-66	Teppi-66	0.142	0.1272	0.4441	0.2712
Total loss			3.981	2.9682	26.5587	21.03437

As we have seen various MATLAB/Simulink simulation test results, this paper presents the optimal location of UPFC based on improving bus voltage profile, minimizing the system power losses and improving the power flow in the south western region transmission network of EEU. In order to determine the optimal location of UPFC let as to compare all bus voltage profiles, power flow and power loss when UPFC is located in different places.

Figure 5.19 and figure 5.20 shows that the bus voltage values in p.u. when UPFC is located at different locations. These figures quantified that the best voltage profile was obtained when the UPFC is connected to line 3, between GGI old 132-bus and Jimma-bus.

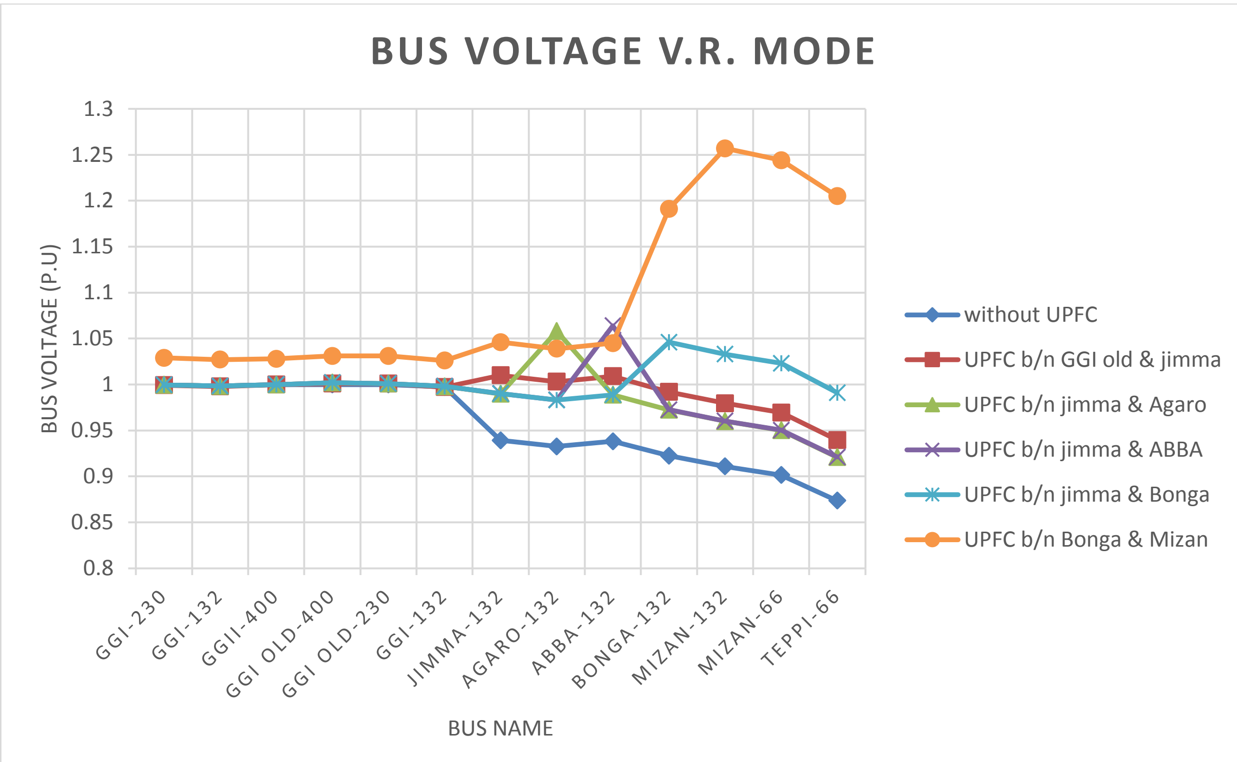

Figure 5.19: bus voltage profile without UPFC and With UPFC at different position with shunt converter V.R. mode

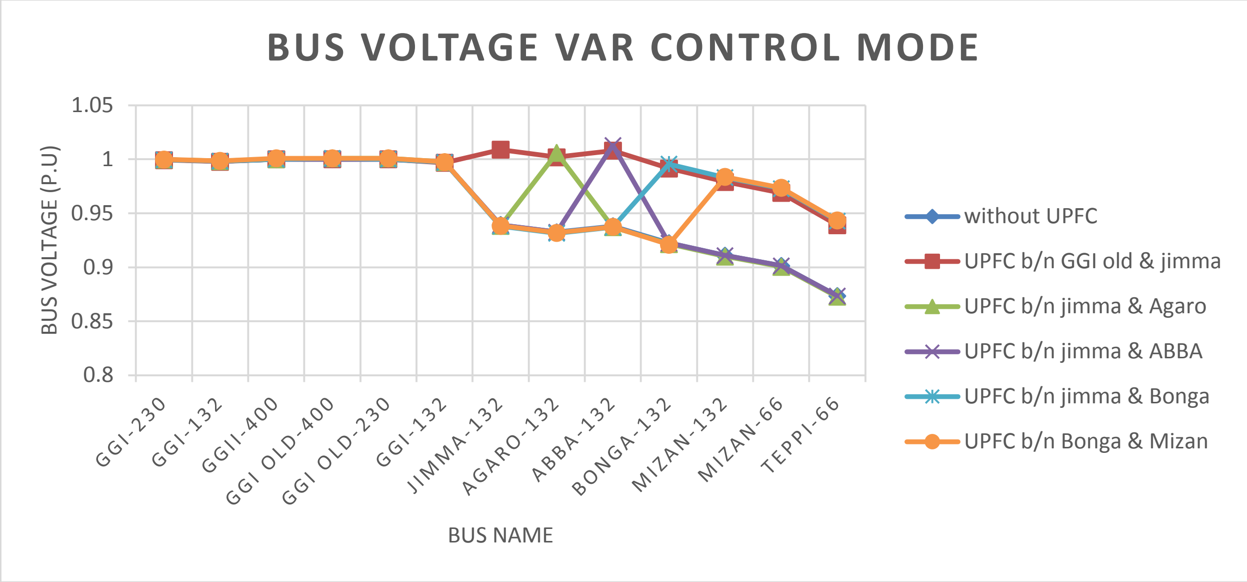

Figure 5.20: bus voltage profile without UPFC and With UPFC at different position with shunt converter Var control mode

The real power flow comparison of all buses without UPFC and when UPFC is located at different location was shown in the figure 5.21 and figure 5.22 for UPFC shunt converter voltage regulation mode and Var control mode respectively.

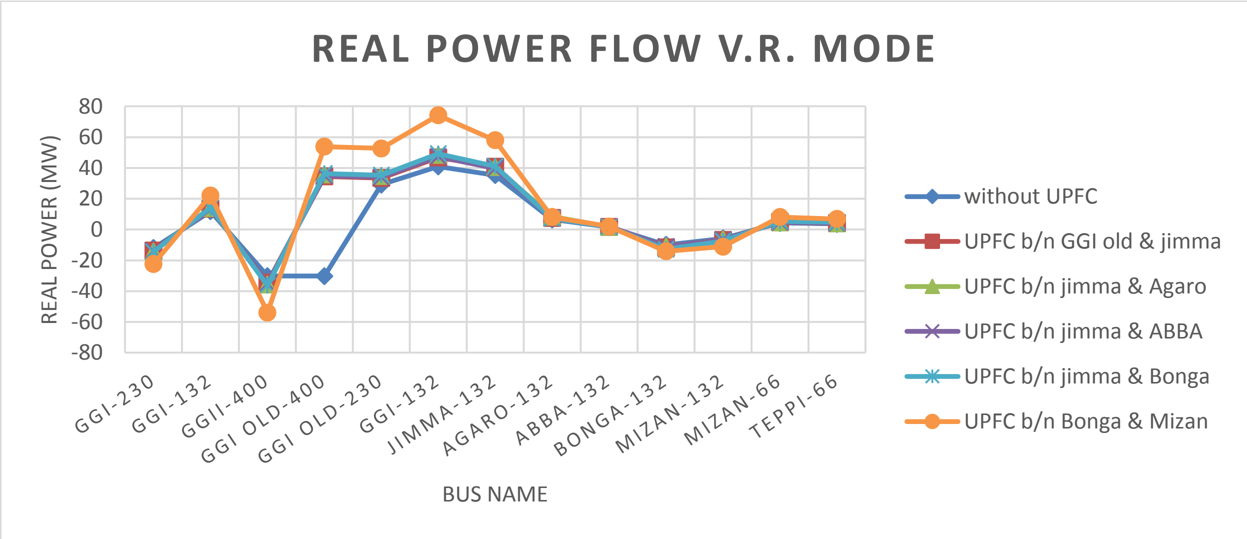

Figure 5.21: Real power flow without UPFC and With UPFC at different location when shunt converter is V.R. mode

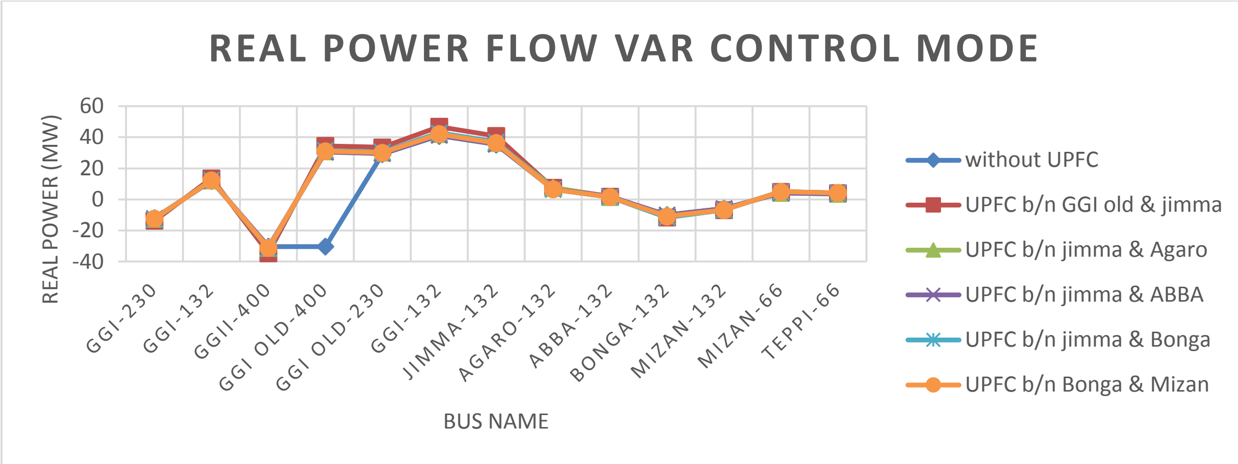

Figure 5.22: Real power flow without UPFC and With UPFC at different location when shunt converter is Var control mode

From figures 5.21 and 5.22 it can be observed that the active power flow in lines changes by incorporating the UPFC. The best real power flow of all the lines was obtained when UPFC is located in the line 3, between GGI old 132-bus and Jimma-bus.

The reactive power flow comparison of all buses without UPFC and with UPFC located at different location was shown in the figure 5.23 and figure 5.24 for UPFC shunt converter voltage regulation mode and Var control mode respectively.

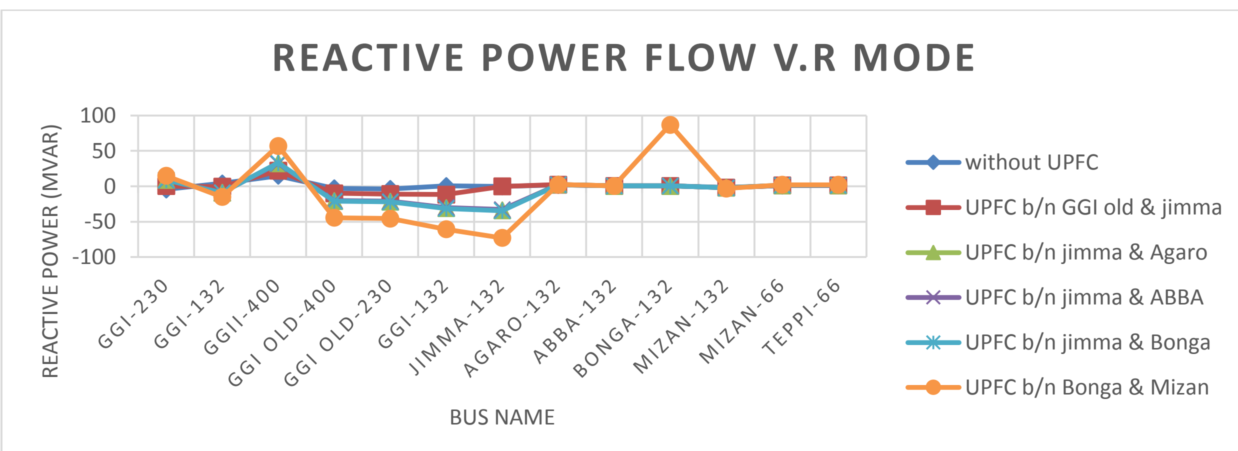

Figure 5.23: Reactive power flow without UPFC and With UPFC at different location when shunt converter is V.R. mode

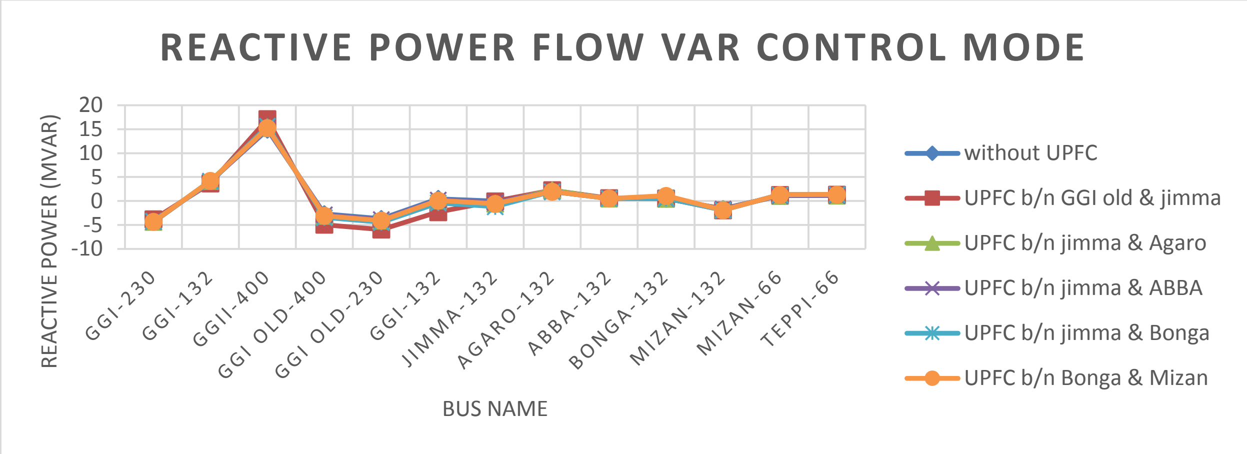

Figure 5.24: Reactive power flow without UPFC and With UPFC at different location when shunt converter is Var control mode

From figures 5.23 and 5.24, it can be observed that the Reactive power flow in lines changes by incorporating the UPFC. The best location of UPFC is in line 3, between GGI old132-bus and Jimma-bus.

The real power losses and reactive power losses are shown in figure 5.25, figure 5.26, figure 5.27 and figure 5.28 when the UPFC shunt converter is at voltage regulation mode and Var control mode respectively.

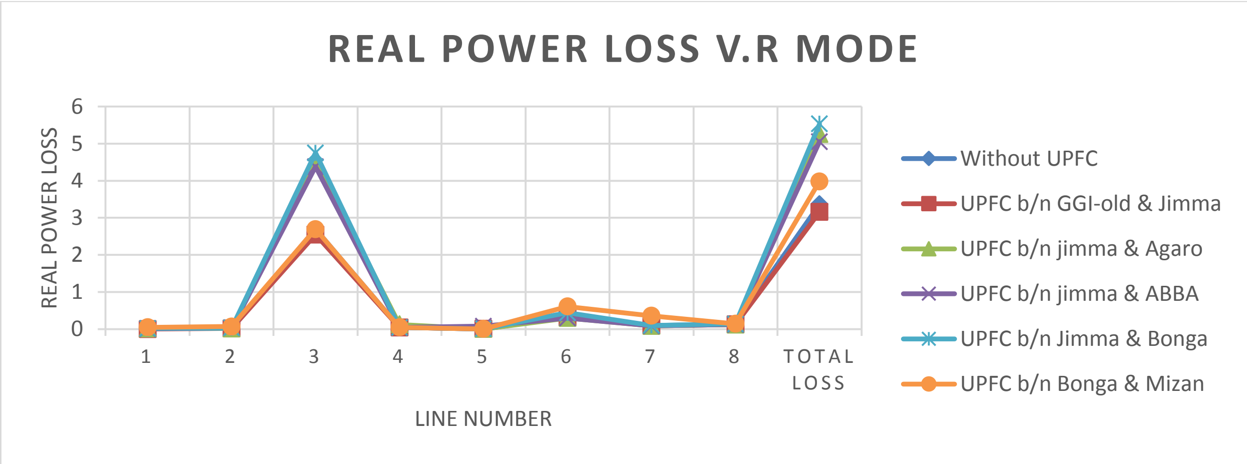

Figure 5.25: real power loss without UPFC and With UPFC at different location when shunt converter is V.R mode

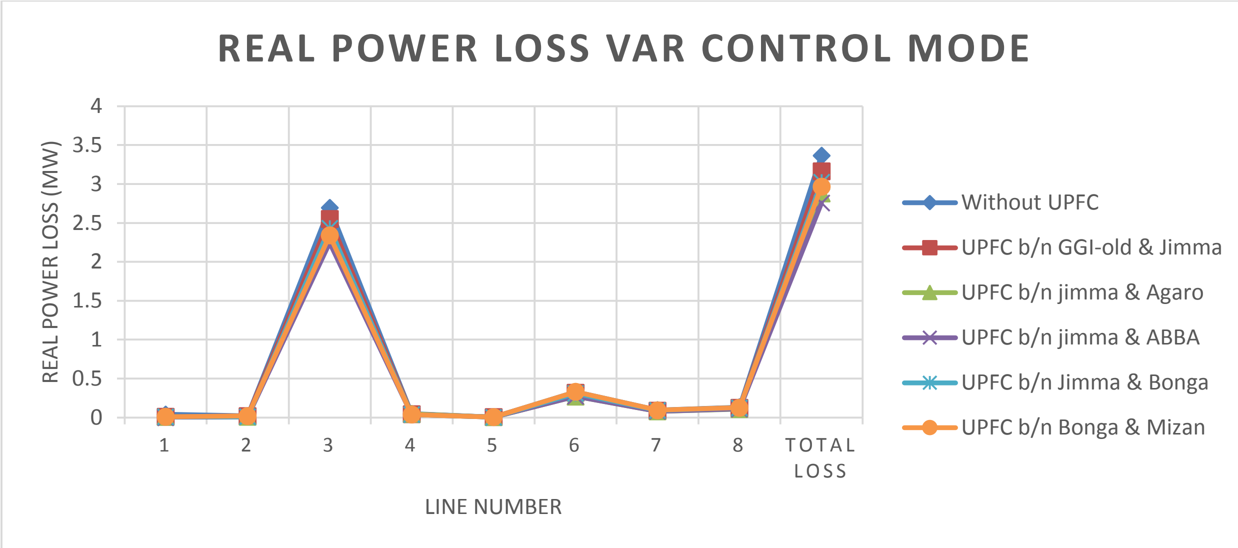

Figure 5.26: real power loss without UPFC and With UPFC at different location when shunt converter is Var control mode

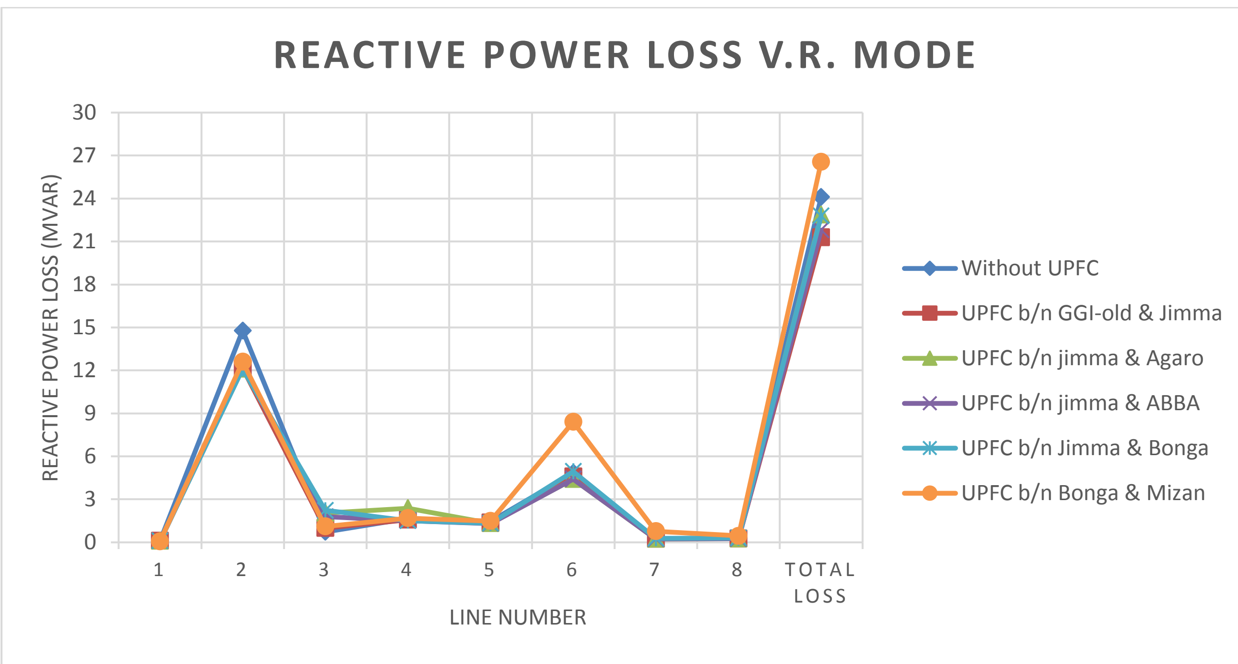

Figure 5.27: reactive power loss without UPFC and With UPFC at different location when shunt converter is V.R mode

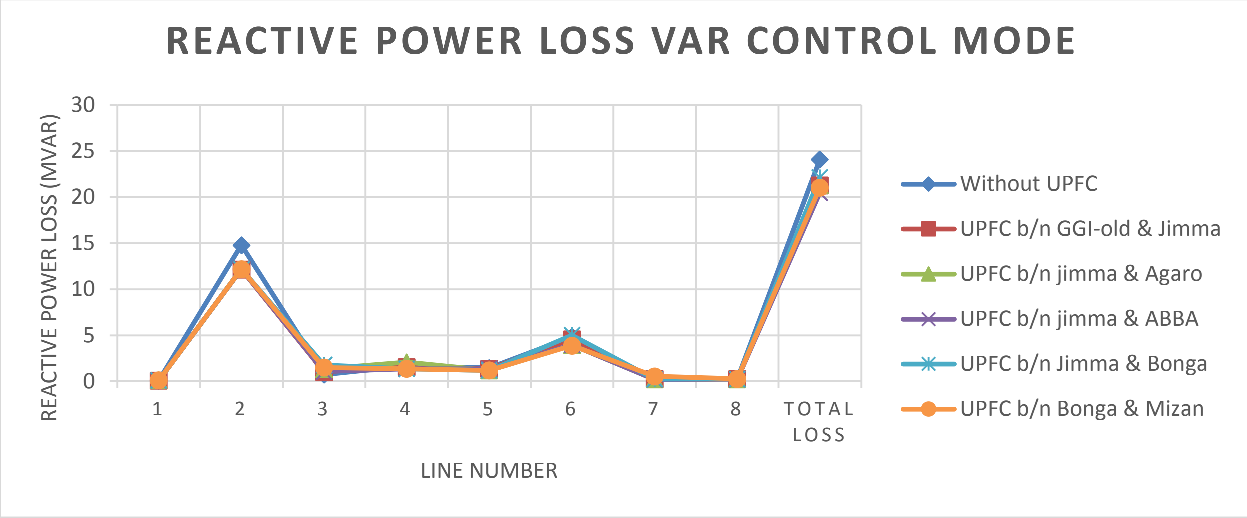

Figure 5.28: reactive power loss without UPFC and With UPFC at different location when shunt converter is var control mode

For the south western region transmission network the location that presents the lowest power losses is to connect the UPFC in line 3, between GGI old132-bus and Jimma-bus. The figure 5.33 shows that the total real power losses get decreased from 3.3667MW to 3.156MW, accounts 6.54% of the generated power, with 6.26% losses reduction when the UPFC shunt converter is operated as voltage regulation mode. The reactive power losses reduced from 24.0994 to 21.2872, with 11.67% losses reduction. But when the UPFC shunt converter is operated in Var control mode the total real power losses decreased from 3.3667MW to 3.166MW, accounts 3.57% of the generated power, with 5.96% losses reduction. The reactive power losses reduced from 24.0994 to 21.287, with 11.67% losses reduction.

This thesis present a clear study of the transmission line loss minimization and system voltage regulation of south western region transmission network of EEU by locating UPFC optimal place. The simulation was carried out by placing UPFC on various locations, all the possible cases were examined using a MATLAB/Simulink. Then the optimal location of UPFC was determined, at which the transmission line loss was minimized and the best improved bus voltage profile and power flow was obtained. Therefore, the optimal location of UPFC was in line 3, between GGI old132-bus and Jimma-bus.

CHAPTER SIX
CONCLUSION AND RECOMMENDATION

6.1. Conclusion

This study covered the effect of incorporating UPFC on transmission line losses, bus voltage profile and power flow study, determination of power loss shares of each transmission lines of south western region transmission network, selecting the optimal location of UPFC at which the losses are minimized and bus voltage profile and power flow was improved.

The simulation result of the existing transmission network of south western region of EEU with the current peak load condition delivered power having total transmission line real power loss of 3.3667 MW. This makes up 7.96% of the total generation capacity. The reactive losses in each voltage level became more positive as the voltage levels decreases. This dictates a network becomes more inductive as the voltage level decreases. Thus, for lower and higher voltages, the UPFC are incorporated to keep the voltage profile, improve power flow and reduce the losses.

The simulation result showed that optimal location of UPFC present the best benefit on power losses minimization, improvement of bus voltage profile and power flow. The numerical results for the south western region transmission network of EEU have been presented with and without UPFC and the comparative analysis was made. At the optimal placement of UPFC the real power loss is decreased to 3.156MW that accounts 6.54% of generated power when UPFC shunt converter is used as voltage regulation mode and 3.166MW that accounts 6.57% when UPFC is used as Var control mode. It was also observed that in the south western region transmission network, without UPFC the power transfer capacity is only 77.85%, whereas in case of UPFC the power transfer capability is increased to 88.99%.

Generally, this study shows that minimizing transmission line loss and regulating system voltage is advantageous in terms of balancing the demand and supply. And also it has an advantage of using the existing transmission line rather than constructing new transmission line which requires long time planning and high investment cost. The result of this study encourages EEU to take advantages of incorporating UPFC in to the transmission network of Ethiopia.

6.2. Recommendation

The electrical energy consumption of Ethiopia is increasing rapidly due to the country is on the way of growth and transformation plan-II. The existing transmission network of EEU will be incapable to handle the increasing demand efficiently, reliability problems of the transmission line and security problem. Thus, EEU, the sole utility company of the country, should have to implement power electronics based equipment's in order to reduce losses and improve system voltage.

In this study UPFC based south western region transmission network is recommended to minimize the losses and regulate system voltage. This device is less known in developing utility companies, the next step should have to be implemented by EEU to have minimum transmission line losses, voltage profile improvement and increasing power flow for the smokeless fuel of the country. UPFC satisfies the needs of almost all requirements of modern power networks. The cost of this device is relatively higher and it is compensated by their multi objective advantages as agreed by many researchers.

This thesis work shows only the steady state power flow of the transmission network of south western region of Ethiopia and it doesn't represent the overall grid interconnection of the country. Thus, future works should include the cost analysis of this method, comparative analysis of different loss minimization techniques in order to select the better method to implement and dynamic controlled power flow by using different FACTS devices.

REFERENCES

[1] Malathi Kalyani, "*Diminishing of losses in a transmission line by using UPFC*", ISSN: 2347-6982, "International Journal of Industrial Electronics and Electrical Engineering", Volume 2, 2014.

[2] A. Anbarasan, M.Y. Sanavullah and S. Ramesh., "*Transmission Line Loss Minimization in Power System Network Using TCSC and UPFC.*" Aust. J. Basic & Appl. Sci., 8(3): 564-569, 2014.

[3] S.V. Ravi Kumar and A. Siva Nagaraju, "*Loss minimization by incorporating of UPFC in load flow studies", "International Journal of Electrical and power Engineering*" Medwell publication, 2007.

[4] M. Kowsalya et.al, "*Loss Optimization for Voltage Stability Enhancement Incorporating UPFC Using Particle Swarm Optimization*", "Journal of Electrical Engineering & Technology", Vol. 4, No. 4, pp.492 - 498, 2009.

[5] Mark Ndubuku Nwohu, "*Optimal location of unified power flow controller (UPFC) in Nigerian Grid system*" ISSN: 1990-7958, "International Journal of Electrical and power Egineering" Medwell publication, 2010.

[6] D. BalaGangi Reddy and M. Suryakalavathi, "*Modeling, Analysis and Optimal Location of UPFC for Real Power Loss Minimization*", "International journal on Recent Trends in Engineering and Technology", Vol. 6, No. 2, 2011.

[7] Thomas John, "*Line loss minimization and voltage regulation using UPFC" ISSN: 2229-712x, "Elixir international journal*" Elixir publisher, 2011.

[8] Sreerama Kumar R. et. al, "*Optimal Placement of Unified Power Flow Controller for Minimization of Power Transmission Line Losses*", "International Journal of Computer Theory and Engineering", Vol. 6, No. 5, 2014.

[9] Engr.Alumona T. L, et al, "*Overview of Losses and Solutions in Power Transmission Lines*", ISSN 2224-610X, Network and Complex Systems, Vol.4, No.8, 2014.

[10] Mohsin Mahmood et al, "*Real Time Study on Technical Losses in Distribution System*", ISSN: 2320-3765, "International Journal of Advanced Research in Electrical, Electronics and Instrumentation Engineering", Vol. 3, Special Issue 1, 2014.

[11] J.P Navani, N.K Sharma and Sonal Sapra, "*Technical and Non-Technical Losses in Power System and Its Economic Consequence in Indian Economy*", ISSN: 2277-1956, "International Journal of Electronics and Computer Science Engineering".

[12] Shahzad Sarwar Bhatti et al, "*Electric Power Transmission and Distribution Losses Overview and Minimization in Pakistan*", ISSN 2229-5518, "International Journal of Scientific & Engineering Research", Vol 6, 2015.

[13] Frances Ngozi Obafemi, "*Non-Technical Losses, Energy Efficiency and Conservative Methodology in the Electricity Sector of Nigeria: The Case of Calabar, Cross River State*", ISSN: 2146-4553, "International Journal of Energy Economics and Policy", Vol. 3, No. 2, pp.185-192, 2013

[14] M. C. Anumaka, "*Analysis of technical losses in electrical power system*", IJRRAS, Vol12 Issue2, 2012.

[15] Bhushan Wane and Avinash Chandra Verma "*Power loss calculation of transmission line with consideration of voltage stability*", ISSN: 2319-7463, "International Journal of Enhanced Research in Science Technology & Engineering", Vol. 2 Issue 9, pp. 38-43, 2013.

[16] Omorogiuwa Eseosa and Elechi Promise, "*Economic Effects of Technical and Non-Technical Losses in Nigeria Power Transmission System*", e-ISSN: 2278-1676, "IOSR Journal of Electrical and Electronics Engineering", Volume 10, Issue 2, PP 89-100, 2015.

[17] Manisha Jaswani et al, "*A study of reactive power compensation in Transmission system*", E-ISSN2249–8974, "International Journal of Advanced Engineering Research and Studies", Innovations for National Development, 2015.

[18] D.M. Larruskain et al, "*Power transmission capacity upgrade of overhead lines*", Plaza de la Casilla, no. 3.

[19] Roberto Rudervall, J.P. Charpentier and Raghuveer Sharma, "*High voltage Direct Current (HVDC) Transmission system Technology Review paper*", Energy Week, Washington D.C, 2000.

[20] Ranjit Kumar, "*A Review of Benefits of FACTS Devices in Power System*", ISSN: 2249-8958, "International Journal of Engineering and Advanced Technology", Volume-3, Issue-4, 2014.

[21] M.Karthik and P.Arul, "*Optimal Power Flow Control Using FACTS Devices*", ISSN: 2319-6378, "International Journal of Emerging Science and Engineering", Vol.-1, Issue-12, 2013.

[22] C.Anitha and P.Arul, "*New Modeling of SSSC and UPFC for Power Flow Study and Reduce Power Losses*", ISSN: 2319-6386, "International Journal of Science and Modern Engineering", Vol.-1, Issue-11, 2013.

[23] Bindeshwar Singh et al, "*Introduction to FACTS controllers: A Technological Literature Survey*", "International Journal of Automation and Power Engineering", Vol. 1, Issue-9, 2012.

[24] Qazi Waqar Ali and Azzam ul Asar, "*Smart Power Transmission System Using FACTS Device*", ISSN: 2252-8792, "International Journal of Applied Power Engineering", Vol. 2, No. 2, pp. 61-70, 2013.

[25] Sunil Kumar et al, "*Transmission Loss Allocation and Loss Minimization by Incorporating UPFC in LFA*", ISSN: 2249-6645, "International Journal of Modern Engineering Research", Vol.1, Issue.1, pp. 236-245.

[26] T. Nireekshana, et. al, "*Modelling and Control Design of Unified Power Flow Controller for Various Control Strategies*", "International Journal of Engineering Science and Technology", Vol. 2(11), 2010.

[27] Ch. Chengaiah, G. V. Marutheswar and R. V. S. Satyanarayana, "*Control setting of unified power flow controller through load flow calculation*", ISSN 1819-6608, "Journal of Engineering and Applied Sciences", Asian Research Publishing Network, vol. 3, no. 6, 2008.

[28] P. Vijayapriya et. al., "*Increasing the loadability and minimizing the losses using UPFC*", "International Journal of Engineering Science and Technology", Vol. 2 (12), 2010.

[29] D. Bala Gangi Reddy, M. Suryakalavathi, "*Modeling, Analysis and Optimal Location of UPFC for Real Power Loss Minimization*", "Int. J. on Recent Trends in Engineering and Technology", Vol. 6, No. 2, 2011.

[30] Youcef DJILANI KOBIBI et al, "*Study of UPFC Optimal Location Considering Loss Reduction and Improvement of Voltage Stability and Power Flow*" ISSN 1583-0233, Leonardo Journal of Sciences, Issue 24, 2014, pp. 85-100.

[31] A. Kumaran, A. Allirani "*Location of FACTS devices for Real and Reactive Power Flow Control*" "International Conference on Signal, Image Processing and Applications", IACSIT Press, vol. 21, 2011.

[32] M. Z. EL-Sadek et al, "*Injection power UPFC model for incorporation of unified power flow controller in load flow studies*", "Journal of Engineering Sciences", Assiut University, Vol. 35, No.1, pp. 207-224, 2007.

APPENDICES

Appendix A:

Table A.1: EEU transmission line data

Node 1	Node 2	L [km]	r [Ohm/km]	x [Ohm/km]	c [nF/km]	Vn [kV]	fn (Hz)	r0 [Ohm/km]	x0 [Ohm/km]	c0 [nF/km]
ADAMITULU 132	BUTAJIRA 132	46.78	0.1835	0.4237	8.6	132	50	0.3681	1.3395	5.4
ADAMITULU 132	ASELA 132	50.964	0.1906	0.4333	8.4	132	50	0.3725	1.3232	5.6
ADDIS EAST I 45	COTOBIE 45	5.96	0.5451	0.4132	8.7	45	50	0.6902	1.4889	4.8
ADDIS EAST II 132	DC ADDIS EAST II COTOBIE	1.236	0.1835	0.4237	8.6	132	50	0.3681	1.3395	5.4
ADDIS EAST II 132	DC ADDIS EAST II ADDIS NORTH	1.236	0.1835	0.4237	8.6	132	50	0.3681	1.3395	5.4
ADDIS NORTH 132	DC ADDIS EAST II ADDIS NORTH	8.707	0.1835	0.4237	8.6	132	50	0.3681	1.3395	5.4
ADDIS WEST 45	SEBETA 45A	6.81	0.5451	0.4132	8.7	45	50	0.6902	1.4889	4.8
Adigala	Adigala	1	0.0918	0.3206	11.4	230	50	0.2676	1.1005	6.9
Adigala	PK 12	162	0.0918	0.3206	11.4	230	50	0.2676	1.1005	6.9
ADWA 66	ENDASELASIE 66	66.4	0.2676	0.4009	9	66	50	0.4533	1.4268	5.3
AGARO 132	JIMMAI I 132	34.82	0.1905	0.4373	8.4	132	50	0.4155	1.2481	6.5
AGARO230KV	BEDELE230KV	81.558	0.0591	0.3155	11.6	230	50	0.2294	1.1356	6.9
AGARO230KV	BEDELE230KV	81.558	0.0591	0.3155	11.6	230	50	0.2294	1.1356	6.9
Akaki 230	KOKA 230	66.4	0.0739	0.4142	8.9	230	50	0.2466	1.2614	5.9
Akaki 230	KOKA 230	66.4	0.0739	0.4142	8.9	230	50	0.2466	1.2614	5.9
Akaki 230	KALITI I 230 BB1	1	0.0739	0.4142	8.9	230	50	0.2466	1.2614	5.9
Akaki 230	KALITI I 230 BB1	1	0.0739	0.4142	8.9	230	50	0.2466	1.2614	5.9
AKAKI I 45	ABA SAMUEL 45	18	0.5451	0.4132	8.7	45	50	0.6902	1.4889	4.8

AKAKI I 45	DUKEM 45	15.05	0.5451	0.4132	8.7	45	50	0.6902	1.4889	4.8
Akaki II 132	N2223	28.54	0.1906	0.4264	8.6	132	50	0.3678	1.3413	5.6
Akaki II 132	DEBRE ZEIT II 132 TP	28.54	0.1906	0.4264	8.6	132	50	0.3678	1.3413	5.6
Akaki II 132	KOKA 132 BB1	61	0.1906	0.433	8.4	132	50	0.3717	1.3245	5.5
Akaki II 132	KALITI I 132 BB1	1	0.1906	0.4264	8.6	132	50	0.3678	1.3413	5.6
ALABA 132 TP	ALABA 132	0.05	0.1941	0.4308	8.4	132	50	0.3765	1.3206	5.6
ALABA 132 TP	SHASHEMENE 132	63.23	0.1941	0.4308	8.4	132	50	0.3765	1.3206	5.6
ALAMATA 230	cOMBOLCHA 230KV	170.6	0.0919	0.3167	11.6	230	50	0.2593	1.115	6.4
ALAMATA 230	cOMBOLCHA 230KV	170.6	0.0919	0.3167	11.6	230	50	0.2593	1.115	6.4
ALAMATA 66	LALIBELA 66	104.86	0.4262	0.4155	8.7	66	50	0.6119	1.4414	5.2
ALAMATA 66	MAYCHEW 66	48	0.4262	0.4155	8.7	66	50	0.6119	1.4414	5.2
ALAMATA 66	SEKOTA 66	80	0.4262	0.4155	8.7	66	50	0.6119	1.4414	5.2
ALEMAYA 66	DC ALEMAYA DIRE DAWA I	2.105	0.4261	0.4208	8.7	66	50	0.5703	1.4628	5.6
ALEMAYA 66	DC ALEMAYA HARAR II	2.105	0.4261	0.4208	8.7	66	50	0.5703	1.4628	5.6
ASEBE TEFERI 66	BEDESA 66	24	0.5219	0.4231	8.6	66	50	0.6669	1.4643	4.9
ASEBE TEFERI66KV	ASEBE TEFERI 66	3	0.5219	0.4231	8.6	66	50	0.6669	1.4643	4.9
Ashekoda Wind230	MEKELE SHR	10	0.0918	0.3193	11.4	230	50	0.2704	1.1513	6.9
AWASA 132	SHASHEMENE 132	21.6	0.1906	0.4333	8.4	132	50	0.3725	1.3232	5.6
Awash 7 230	KOKA 230	128.84	0.0725	0.4089	8.9	230	50	0.2517	1.2465	5.9
AWASH 7 KILO 132	Asebe Teferi 132	201.49	0.1906	0.4273	8.5	132	50	0.3734	1.3343	5.5
AWASH 7 KILO 66	AMIBARA 66	42.6	0.5219	0.4231	8.6	66	50	0.6669	1.4643	4.9
AWASH II 132 BB1	ASELA 132	51.2	0.1906	0.4333	8.4	132	50	0.3725	1.3232	5.6
AWASH II 132 BB1	AWASH III 132 BB1	1.45	0.1906	0.4156	8.8	132	50	0.3651	1.3652	5.5
AWASH II 132 BB1	AWASH III 132 BB1	1.45	0.1906	0.4156	8.8	132	50	0.3651	1.3652	5.5
BABILE 45	JIJIGA I 45	93	0.5171	0.4012	9	45	50	0.6624	1.5077	4.8

Bahir Dar 400KV	Beleas 400KV	62.8	0.0209	0.3096	12	400	50	0.2017	1.0341	7.7
Bahir Dar 400KV	Beleas 400KV	62.8	0.0209	0.3096	12	400	50	0.2017	1.0341	7.7
Bahir Dar 400KV	D/Markos 400KV	193.77	0.0209	0.3034	12.2	400	50	0.2219	1.0075	7.9
BAHIR DAR I 45	TIS ABAY I 45	30.02	0.2601	0.3928	9.2	45	50	0.4513	1.4297	5.4
BAHIR DAR I 66	BAHIR DAR II 66	4.52	0.522	0.4192	8.6	66	50	0.7075	1.4412	5.2
BAHIR DAR II 132	TIS ABAY II 132	28.96	0.1836	0.4228	8.7	132	50	0.3638	1.3453	5.8
BAHIR DAR II 132	TIS ABAY II 132	28.96	0.1836	0.4228	8.7	132	50	0.3638	1.3453	5.8
BAHIR DAR II 230 BB1	SHR BAHIR DAR II ALAMATA	0.01	0.0918	0.3193	11.4	230	50	0.2704	1.1513	6.9
BAHIR DAR II 230 BB1	SHR BAHIR DAR II MOTA	0.01	0.0597	0.4113	8.9	230	50	0.2369	1.2437	5.8
BAHIR DAR II 66	DANGLA 66	68.6	0.522	0.4192	8.6	66	50	0.7075	1.4412	5.2
BEDELE230KV	METU230KV	90.4	0.0919	0.3166	11.6	230	50	0.26	1.1224	7.1
BEDELE230KV	METU230KV	90.4	0.0919	0.3166	11.6	230	50	0.26	1.1224	7.1
BITCHENA 66	DEBRE MARKOS 66	65.7	0.5219	0.4231	8.6	66	50	0.6669	1.4643	4.9
BONGA 132	MIZAN 132	88.3	0.1834	0.4229	8.8	132	50	0.3267	1.3894	5.9
BONGA 132	JIMMAI I 132	102.27	0.1834	0.4229	8.8	132	50	0.3267	1.3894	5.9
CHELENKO 66	ALEMAYA 66	49.82	0.4261	0.4153	8.7	66	50	0.5707	1.4732	4.7
COMBOLCHA 132	AKISTA 132	82	0.161001	0.426824	8.514053	132	50	0.3766	1.3201	5.6
cOMBOLCHA 230KV	SEMERA230KV	177.07	0.0918	0.3206	11.4	230	50	0.2676	1.1005	6.9
COTOBIE 132	DC ADDIS EAST II COTOBIE	4.223	0.1835	0.4237	8.6	132	50	0.3681	1.3395	5.4
COTOBIE 132	lEGETAFO132KV	107.46	0.1906	0.4333	8.4	132	50	0.3732	1.3226	5.6
COTOBIE 132	KALITI NORTH 132 TP	18.65	0.1906	0.434	8.4	132	50	0.3724	1.3217	5.6
COTOBIE 132	WEREGENU 132 TP	2.45	0.1906	0.434	8.4	132	50	0.3724	1.3217	5.6
D/Markos 400KV	Sululta 400KV	215.89	0.0209	0.3096	11.9	400	50	0.2017	1.0342	6.8
D/Markos 400KV	Sululta 400KV	215.89	0.0209	0.3096	11.9	400	50	0.2017	1.0342	6.8

DABAT 66	GONDER I 66	58.41	0.522	0.4192	8.6	66	50	0.7075	1.4412	5.2
DC DIRE DAWA III DIRE DAWA I	DIRE DAWA I 132	0.324	0.1906	0.4273	8.5	132	50	0.3734	1.3343	5.5
DC DIRE DAWA III DIRE DAWA I	DIRE DAWA III 132 BB1	3.348	0.1906	0.4179	8.8	132	50	0.371	1.3553	5.7
DC DIRE DAWA III DIRE DAWA II	DIRE DAWA III 132 BB1	3.348	0.1906	0.4179	8.8	132	50	0.371	1.3553	5.7
DC HARAR II ALEMAYA	DC ALEMAYA HARAR II	12.865	0.5219	0.4231	8.6	66	50	0.6669	1.4643	4.9
DC HARAR II ALEMAYA	HARAR II 66	1.082	0.4261	0.4208	8.7	66	50	0.5703	1.4628	5.6
DC HARAR II HARAR I	HARAR I 66	1.644	0.5219	0.4231	8.6	66	50	0.6669	1.4643	4.9
DC HARAR II HARAR I	HARAR II 66	1.082	0.4261	0.4208	8.7	66	50	0.5703	1.4628	5.6
DC KOKA MODJO	KOKA 45	5.119	0.5451	0.4204	8.6	45	50	0.6897	1.4752	5.3
DC KOKA NAZRETH I	KOKA 45	5.119	0.5451	0.4204	8.6	45	50	0.6897	1.4752	5.3
DC WOLKITE GILGEL GIBE	WOLKITE 230 BB1	3.657	0.0598	0.4063	9.1	230	50	0.2354	1.2555	6.1
DC WOLKITE SEBETA	SEBETA 230 BB1	132.523	0.0597	0.4113	8.9	230	50	0.2369	1.2437	5.8
DC WOLKITE SEBETA	WOLKITE 230 BB1	3.657	0.0598	0.4063	9.1	230	50	0.2354	1.2555	6.1
DC YESU FACTORY KALITI I	KALITI I 132 BB1	0.35	0.1836	0.4181	8.8	132	50	0.3637	1.3547	5.7
DC YESU FACTORY KALITI I	YESU FACTORY 132	0.35	0.1836	0.4181	8.8	132	50	0.3637	1.3547	5.7
DEBRE BIRHAN 132	SHOA ROBIT 132	57.49	0.1906	0.4333	8.4	132	50	0.3732	1.3226	5.6
DEBRE MARKOS 230	FICTITIOUS_FIN_DEB	71.3625	0.0597	0.4113	8.9	230	50	0.2369	1.2437	5.8
DEBRE ZEIT II 132 TP	DEBRE ZEIT II 132	0.05	0.1906	0.4333	8.4	132	50	0.3732	1.3226	5.6
DEBRE ZEIT II 132 TP	ELALA GEDA DCP	14.76	0.1906	0.4264	8.6	132	50	0.3678	1.3413	5.6
DEMBI DOLO 66	GAMBELA 66	64	0.5219	0.4231	8.6	66	50	0.6669	1.4643	4.9
DESSIE 66	COMBOLCHA 66	12.69	0.522	0.4225	8.6	66	50	0.7073	1.4346	5.2
DESSIE 66	WOLDIA 66	88	0.5219	0.4231	8.6	66	50	0.6669	1.4643	4.9

DILLA 132KV	HAGEREMARIAM132KV	94.592	0.16099	0.415142	8.760153	132	50	0.3766	1.3201	5.6
DIRE DAWA DIESEL TP	DIRE DAWA DIE 132	1.896	0.1835	0.4237	8.6	132	50	0.3681	1.3395	5.4
DIRE DAWA DIESEL TP	TOWER NO 1242	0.632	0.1906	0.4273	8.5	132	50	0.3734	1.3343	5.5
DIRE DAWA I 66	DC ALEMAYA DIRE DAWA I	25.295	0.542	0.4132	8.7	66	50	0.6871	1.4889	4.8
DIRE DAWA II 132	DC DIRE DAWA III DIRE DAWA II	9.081	0.1906	0.4333	8.4	132	50	0.3732	1.3226	5.6
DIRE DAWA II 132	HARAR II 132	43.81	0.1835	0.4242	8.6	132	50	0.3679	1.3386	5.4
DIRE DAWA III 230	DIRE DAWA III 230	1	0.0725	0.4089	8.9	230	50	0.2517	1.2465	5.9
DIRE DAWA III 230	Awash 7 230	208.99	0.0725	0.4089	8.9	230	50	0.2517	1.2465	5.9
DUKEM 45	DEBRE ZEIT I 45	8.4	0.5451	0.4132	8.7	45	50	0.6902	1.4889	4.8
ELALA GEDA 132 TP	KOKA 132 BB1	22.24	0.1906	0.4264	8.6	132	50	0.3678	1.3413	5.6
ELALA GEDA 132 TP	ELALA GEDA 132	4.9	0.1906	0.4333	8.4	132	50	0.3732	1.3226	5.6
ELALA GEDA DCP	KOKA 132 BB1	22.24	0.1906	0.4264	8.6	132	50	0.3678	1.3413	5.6
endeselase230KV	N1948	229.8	0.0918	0.3234	11.3	230	50	0.2642	1.1007	6.9
FICTITIOUS_FIN_DEB	FINCHAA 230	23.7875	0.0597	0.4113	8.9	230	50	0.2369	1.2437	5.8
FICTITIOUS_GHE_GEF	GHEDO 230	33.26	0.0671	0.4272	8.7	230	50	0.2787	1.1661	6.5
FINCHA SUGAR I 66	FINCHAA 66	15.4	0.3625	0.4256	8.5	66	50	0.5537	1.3847	5.3
FINCHA SUGAR II 66	FINCHA SUGAR I 66	11	0.3625	0.4256	8.5	66	50	0.5537	1.3847	5.3
FINCHAA 230	GHEDO 230	67.19	0.0671	0.4272	8.7	230	50	0.2787	1.1661	6.5
Finchaa II	FINCHAA 230	19.44	0.0668	0.4211	8.7	230	50	0.2393	1.1985	5.8
Finchaa II	GHEDO 230	69.73	0.0668	0.4211	8.7	230	50	0.2393	1.1985	5.8
FINOTE SELAM 66	DEBRE MARKOS 66	80.02	0.5219	0.4231	8.6	66	50	0.6669	1.4643	4.9
GAMBELA 66	METU166KV	146	0.5219	0.4231	8.6	66	50	0.6669	1.4643	4.9
Gambela-Metu	Gambela 230kv	0.001	0.059	0.3098	11.8	230	50	0.2281	1.1608	6.8
Gambella-Metu	Gambela 230kv	0.01	0.059	0.3098	11.8	230	50	0.2281	1.1608	6.8
gef66kv	FITCHE 66	96	0.5219	0.4231	8.6	66	50	0.6669	1.4643	4.9

GEFARSA 132 BB1	ADDIS NORTH 132	11.11	0.1906	0.434	8.4	132	50	0.3724	1.3217	5.6
GEFARSA 132 BB1	N2426	80	0.1906	0.434	8.4	132	50	0.3724	1.3217	5.6
GEFARSA 132 BB1	SEBETA I 132 TP	10.78	0.1906	0.434	8.4	132	50	0.3724	1.3217	5.6
GEFARSA 132 BB1	KALITI I 132 BB1	24.75	0.1906	0.434	8.4	132	50	0.3724	1.3217	5.6
GEFARSA 230	SEBETA 230 BB1	10.64	0.0725	0.408	8.9	230	50	0.2519	1.248	5.8
GEFARSA 230	FICTITIOUS_GHE_GEF	99.78	0.0671	0.4272	8.7	230	50	0.2787	1.1661	6.5
GEFARSA 230	GHEDO 230	133.5	0.0669	0.4144	8.9	230	50	0.2351	1.2203	5.9
GEFARSA 230	GHEDO 230	133.5	0.0669	0.4144	8.9	230	50	0.2351	1.2203	5.9
GEFARSA 45	ADDIS ALEM 45	29.64	0.5453	0.411	8.8	45	50	0.7336	1.461	5.1
GG OLD 230KV	TOWER NO 143	65.3	0.0597	0.4113	8.9	230	50	0.2029	1.3029	6
GG OLD 230KV	N1858	1.5	0.0671	0.4272	8.7	230	50	0.2787	1.1661	6.5
GG OLD 230KV	GILGEL GIBE I 230	2.5	0.0597	0.4113	8.9	230	50	0.2029	1.3029	6
GG OLD 230KV	GILGEL GIBE I 230	2.5	0.0597	0.4113	8.9	230	50	0.2029	1.3029	6
GHEDO 132	GUDER 132	33.99	0.194	0.4308	8.4	132	50	0.3763	1.3206	5.6
GHEDO 230	N1858	130.82	0.0725	0.4089	8.9	230	50	0.2517	1.2465	5.9
GHIMBI 132	NEKEMTE 132	84.29	0.1903	0.4188	8.7	132	50	0.3345	1.3878	5.5
GHIMBI 132	MENDI132	132	0.1903	0.4188	8.7	132	50	0.3345	1.3878	5.5
GIGEL GIBE I 132	GILGEL GIBE OLD 132 BB1	2.61	0.1835	0.4486	8.2	132	50	0.3619	1.2773	5.4
Gilgel Gibe 400KV	N1853	28	0.0375	0.4259	8.7	400	50	0.286	1.0839	6.8
Gilgel Gibe 400KV	SEBETA 2 400KV	185	0.0375	0.4259	8.7	400	50	0.286	1.0839	6.8
GILGEL GIBE I 230	JImma230KV	67.21	0.0591	0.3155	11.6	230	50	0.2294	1.1356	6.9
GILGEL GIBE I 230	JImma230KV	67.21	0.0591	0.3155	11.6	230	50	0.2294	1.1356	6.9
GILGEL GIBE OLD 132 BB1	HOSAINA 132	70.62	0.1905	0.4373	8.4	132	50	0.4155	1.2481	6.5
GONDER I 66	GONDER II 66	4.31	0.522	0.4192	8.6	66	50	0.7075	1.4412	5.2
GONDER II 230	SHR GONDER II BAHIR DAR II	0.01	0.0918	0.3205	11.4	230	50	0.2709	1.1482	6.9

GONDER II 230	N2054	121	0.0918	0.3206	11.4	230	50	0.2575	1.1653	6.2
GONDER II 230	N2048	121	0.0918	0.3206	11.4	230	50	0.2575	1.1653	6.2
HARAR I 45	BABILE 45	26	0.5171	0.4012	9	45	50	0.6624	1.5077	4.8
HARAR II 132	JIJIGA II 132	95.09	0.1835	0.4242	8.6	132	50	0.3679	1.3386	5.4
hosaiena 230KV	Alaba 230KV	39.3	0.1015	0.4354	8.3	230	50	0.244	1.3021	5.3
HOSAINA 132	ALABA 132	39.6	0.1905	0.4373	8.4	132	50	0.4155	1.2481	6.5
Hurso 230	PK 12	281	0.0918	0.3206	11.4	230	50	0.2676	1.1005	6.9
Hurso 230	Adigala	121	0.0918	0.3206	11.4	230	50	0.2676	1.1005	6.9
Hurso 230	KOKA 230	313	0.0919	0.3168	11.6	230	50	0.2659	1.1619	6.9
Hurso 230	Hurso 230	1	0.0919	0.3168	11.6	230	50	0.2659	1.1619	6.9
Hurso 230	KOKA 230	313	0.0919	0.3168	11.6	230	50	0.2659	1.1619	6.9
Hurso 230	Hurso 230	1	0.0919	0.3168	11.6	230	50	0.2659	1.1619	6.9
Hurso 230	DIRE DAWA III 230	1	0.0918	0.3206	11.4	230	50	0.2676	1.1005	6.9
Hurso 230	DIRE DAWA III 230	1	0.0918	0.3206	11.4	230	50	0.2676	1.1005	6.9
JImma230KV	AGARO230KV	38.602	0.0591	0.3155	11.6	230	50	0.2294	1.1356	6.9
JImma230KV	AGARO230KV	38.602	0.0591	0.3155	11.6	230	50	0.2294	1.1356	6.9
JIMMAI I 132	N2444	71.32	0.1905	0.4373	8.4	132	50	0.4155	1.2481	6.5
JIMMAI I 132	Jimma I	7.3	0.1905	0.4373	8.4	132	50	0.4155	1.2481	6.5
KALITI I 132 BB1	ADDIS CENTER 132	14.35	0.1906	0.433	8.4	132	50	0.3717	1.3245	5.5
KALITI I 132 BB1	Akaki II 132	1	0.1906	0.4264	8.6	132	50	0.3678	1.3413	5.6
KALITI I 230 BB1	N1925	3.565	0.0725	0.408	8.9	230	50	0.2519	1.248	5.8
KALITI I 45 BB1	ADDIS SOUTH I 45	8.82	0.5451	0.4132	8.7	45	50	0.6902	1.4889	4.8
KALITI I 45 BB1	AKAKI I 45	3	0.5451	0.4132	8.7	45	50	0.6902	1.4889	4.8
KALITI I 45 BB1	AKAKI S.P FACTORY 45	6	0.5171	0.4187	8.7	45	50	0.6617	1.4735	5.6
KALITI I 45 BB1	AKAKI S.P FACTORY 45	6	0.5171	0.4187	8.7	45	50	0.6617	1.4735	5.6

KALITI II 132	KALITI I 132 BB1	6.98	0.1906	0.434	8.4	132	50	0.3724	1.3217	5.6
KALITI II 45	NEFAS SILK 45	3	0.5451	0.4204	8.7	45	50	0.6897	1.4752	5.6
KALITI NORTH 132 TP	KALITI I 132 BB1	1.5	0.1906	0.434	8.4	132	50	0.3724	1.3217	5.6
KALITI NORTH 132 TP	KALITI NORTH 132	0.44	0.1906	0.434	8.4	132	50	0.3724	1.3217	5.6
KOKA 132 BB1	WONJI TP	7.36	0.1906	0.4264	8.6	132	50	0.3678	1.3413	5.6
KOKA 132 BB1	WONJI DCP	7.36	0.1906	0.4264	8.6	132	50	0.3678	1.3413	5.6
KOKA 230	KOKA 230	1	0.0725	0.4089	8.9	230	50	0.2517	1.2465	5.9
KOKA 230	KOKA 230	1	0.0919	0.3168	11.6	230	50	0.2659	1.1619	6.9
KOKA 230	KOKA 230	1	0.0919	0.3168	11.6	230	50	0.2659	1.1619	6.9
KOKA 230	MELKA WAKENA 230	163.86	0.0739	0.4142	8.9	230	50	0.2466	1.2614	5.9
KOKA 230	MELKA WAKENA 230	163.86	0.0739	0.4142	8.9	230	50	0.2466	1.2614	5.9
lEGETAFO132KV	DEBRE BIRHAN 132	1	0.1906	0.4333	8.4	132	50	0.3732	1.3226	5.6
lEGETAFO230KV	KALITI I 230 BB1	34.5	0.0918	0.3225	11.3	230	50	0.2634	1.0946	6.9
Mehoni	ALAMATA 230	42	0.1835	0.4313	8.4	230	50	0.3581	1.2746	4.9
MEKANISSA 132	N2451	5	0.1906	0.434	8.4	132	50	0.3724	1.3217	5.6
MEKANISSA 132	KALITI I 132 BB1	16.16	0.1906	0.434	8.4	132	50	0.3724	1.3217	5.6
MEKELE 132	ADWA 132	116.74	0.1835	0.4278	8.6	132	50	0.3674	1.3319	5.5
MEKELE 132	MESSOBO 132	5.06	0.1835	0.4278	8.6	132	50	0.3674	1.3319	5.5
MEKELE 132	WUKRO TP	31.04	0.1835	0.4278	8.6	132	50	0.3674	1.3319	5.5
MEKELE 230	TEKEZE 230	103	0.0918	0.3234	11.3	230	50	0.2642	1.1007	6.9
MEKELE 230	Mehoni	100	0.0919	0.3168	11.5	230	50	0.2619	1.1675	6.7
MEKELE 230	MEKELE SHR	0.01	0.0918	0.3193	11.4	230	50	0.2704	1.1513	6.9
MELKA WAKENA YOU 66	GOBESA 66	74.2	0.4261	0.4163	8.7	66	50	0.5707	1.4713	4.8

MELKA WAKENA YOU 66	ROBE 66	72.89	0.4131	0.415	8.7	66	50	0.5986	1.437	5.2
MELKA WALKENA 132	MELKA WAKENA YOU 132	5	0.1941	0.4308	8.4	132	50	0.3765	1.3206	5.6
MENDI132	ASSOSA132	84	0.1903	0.4188	8.7	132	50	0.3345	1.3878	5.5
METEHARA TP	AWASH 7 KILO 132	29.603	0.1906	0.4273	8.5	132	50	0.3734	1.3343	5.5
METEHARA TP	METEHARA 132	0.05	0.1906	0.4273	8.5	132	50	0.3734	1.3343	5.5
METEHARA TP	NAZRETH II 132	88.238	0.1906	0.4273	8.5	132	50	0.3734	1.3343	5.5
METU 66	SOR 66	24	0.5219	0.4231	8.6	66	50	0.6669	1.4643	4.9
METU230KV	Gambella-Metu	140	0.059	0.3098	11.8	230	50	0.2281	1.1608	6.8
METU230KV	Gambela-Metu	140	0.059	0.3098	11.8	230	50	0.2281	1.1608	6.8
MIZAN 66	TEPI 66	30.15	0.4262	0.4131	8.8	66	50	0.612	1.4464	5.1
MODJO 45	DC KOKA MODJO	12.303	0.5451	0.4132	8.7	45	50	0.6902	1.4889	4.8
MOTA 230 BB1	SHR DEBRE MARKOS MOTA	111.76	0.0597	0.4113	8.9	230	50	0.2369	1.2437	5.8
N1853	GG OLD 400KV	1	0.0375	0.4259	8.7	400	50	0.286	1.0839	6.8
N1892	endeselase230KV	1	0.0918	0.3234	11.3	230	50	0.2642	1.1007	6.9
N1921	COMBOLCHA NEW132KV	1.8	0.1906	0.4333	8.4	132	50	0.3732	1.3226	5.6
N1921	COMBOLCHA 132	129.46	0.1906	0.4333	8.4	132	50	0.3732	1.3226	5.6
N1922	N1923	283.8	0.0919	0.3167	11.6	230	50	0.2593	1.115	6.4
N1922	cOMBOLCHA 230KV	1	0.0919	0.3167	11.6	230	50	0.2593	1.115	6.4
N1923	lEGETAFO230KV	1	0.0919	0.3167	11.6	230	50	0.2593	1.115	6.4
N1925	SEBETA 230 BB1	10.695	0.0725	0.408	8.9	230	50	0.2519	1.248	5.8
N1929	N1932	63.93	0.0918	0.3206	11.4	230	50	0.2676	1.1005	6.9
N1929	SEMERA230KV	1	0.0918	0.3206	11.4	230	50	0.2676	1.1005	6.9
N1932	DECHETO230KV	1	0.0918	0.3206	11.4	230	50	0.2676	1.1005	6.9
N1948	HUMERA230KV	1	0.0918	0.3234	11.3	230	50	0.2642	1.1007	6.9

N2044	Gadarif	1	0.0693	0.3206	11.4	230	50	0.2365	1.1857	6.3
N2045	Gadarif	1	0.0693	0.3206	11.4	230	50	0.2365	1.1857	6.3
N2048	Shehedi	1	0.0918	0.3206	11.4	230	50	0.2575	1.1653	6.2
N2054	N2055	1	0.0918	0.3206	11.4	230	50	0.2575	1.1653	6.2
N2223	ELALA GEDA 132 TP	14.76	0.1906	0.4264	8.6	132	50	0.3678	1.3413	5.6
N2426	MUGER 132	1	0.1906	0.434	8.4	132	50	0.3766	1.3201	5.6
N2427	danote 132Kv	1.2	0.1906	0.434	8.4	132	50	0.3724	1.3217	5.6
N2449	ALAMATA 230	129.69	0.0918	0.3193	11.4	230	50	0.2704	1.1513	6.9
N2449	Ashekoda Wind230	1	0.0918	0.3193	11.4	230	50	0.2704	1.1513	6.9
NAZRETH I 45	DC KOKA NAZRETH I	6.713	0.5451	0.4132	8.7	45	50	0.6902	1.4889	4.8
NAZRETH II 132	KOKA 132 BB1	11.485	0.1906	0.4273	8.5	132	50	0.3734	1.3343	5.5
NEKEMTE 132	BEDELE 132	73	0.1625	0.4071	8.9	132	50	0.3456	1.3708	4.7
NEKEMTE 132	Gidayana 132	94	0.1835	0.4278	8.6	132	50	0.3674	1.3319	5.5
NEKEMTE 132	GHEDO 132	115.89	0.1903	0.4188	8.7	132	50	0.3345	1.3878	5.5
PAWE 66	DANGLA 66	109	0.5219	0.4231	8.6	66	50	0.6669	1.4643	4.9
PK 12	PK 12	1	0.0918	0.3206	11.4	230	50	0.2676	1.1005	6.9
PK 12	PK 12	1	0.0918	0.3206	11.4	230	50	0.2676	1.1005	6.9
sawla 132KV	key Afer132KV	105	0.1834	0.4237	8.6	132	50	0.3267	1.3877	4.9
SEBETA 2 33	SEBETA 230 BB1	16	0.0597	0.4113	8.9	230	50	0.2029	1.3029	6
SEBETA 2 33	SEBETA 230 BB1	16	0.0597	0.4113	8.9	230	50	0.2369	1.2437	5.8
SEBETA 2 400KV	Sululta 400KV	46.5	0.0209	0.3096	11.9	400	50	0.2017	1.0342	6.8
SEBETA 2 400KV	Akaki 400	33	0.019	0.3291	11.1	400	50	0.2108	0.9855	7
SEBETA 45A	GEDJA 45	23.06	0.5172	0.4093	8.8	45	50	0.7056	1.4592	5.2
SEBETA 45B	ADDIS WEST 45	6.2	0.5451	0.4132	8.7	45	50	0.6902	1.4889	4.8
SEBETA 66	WOLISSO 66	98.6	0.5219	0.4231	8.6	66	50	0.6669	1.4643	4.9

SEBETA I 132	SEBETA I 132 TP	0.05	0.1906	0.434	8.4	132	50	0.3724	1.3217	5.6
SEBETA I 132 TP	MEKANISSA 132	7.81	0.1906	0.434	8.4	132	50	0.3724	1.3217	5.6
SHAKISSO 66	NEGELE BORENA 66	113.9	0.4261	0.4163	8.7	66	50	0.5707	1.4713	4.8
SHASHEMENE 132	ADAMITULU 132	76.83	0.1906	0.4333	8.4	132	50	0.3725	1.3232	5.6
SHASHEMENE 132	MELKA WAKENA YOU 132	119.19	0.1941	0.4308	8.4	132	50	0.3765	1.3206	5.6
Shehedi	N2044	292	0.0693	0.3206	11.4	230	50	0.2365	1.1857	6.3
Shehedi	N2045	292	0.0693	0.3206	11.4	230	50	0.2365	1.1857	6.3
SHOA ROBIT 132	Tap Kemise	87.4	0.1906	0.4333	8.4	132	50	0.3732	1.3226	5.6
SHR BAHIR DAR II ALAMATA	SHR2 ALAMATA BAHIR DAR II	348	0.0918	0.3193	11.4	230	50	0.2704	1.1513	6.9
SHR BAHIR DAR II MOTA	MOTA 230 BB1	81.11	0.0597	0.4113	8.9	230	50	0.2369	1.2437	5.8
SHR DEBRE MARKOS MOTA	DEBRE MARKOS 230	0.01	0.0597	0.4113	8.9	230	50	0.2369	1.2437	5.8
SHR GONDER II BAHIR DAR II	BAHIR DAR II 230 BB1	136.97	0.0918	0.3205	11.4	230	50	0.2709	1.1482	6.9
SHR1 ALAMATA BAHIR DAR II	ALAMATA 230	0.005	0.0918	0.3193	11.4	230	50	0.2704	1.1513	6.9
SHR2 ALAMATA BAHIR DAR II	SHR1 ALAMATA BAHIR DAR II	0.005	0.0918	0.3193	11.4	230	50	0.2704	1.1513	6.9
Sululta 132KV	danote 132Kv	57	0.1835	0.4237	8.6	132	50	0.3639	1.344	4.9
Sululta 230KV	GEFARSA 230	16.86	0.0599	0.4081	9.1	230	50	0.2456	1.1745	6.1
Sululta 230KV	GEFARSA 230	16.86	0.0599	0.4081	9.1	230	50	0.2456	1.1745	6.1
Sululta 230KV	lEGETAFO230 KV	21	0.0919	0.3167	11.6	230	50	0.2593	1.115	6.4
Tap Kemise	COMBOLCHA NEW132KV	34.7	0.1906	0.4333	8.4	132	50	0.3732	1.3226	5.6
Tap Kemise	Kemisse 132	0.713	0.1603	0.4229	8.7	132	50	0.3441	1.3426	5.7
Tap Kemise	Kemisse 132	0.713	0.1603	0.4229	8.7	132	50	0.3441	1.3426	5.7

TEKEZE 230	MEKELE 230	103	0.0918	0.3234	11.3	230	50	0.2642	1.1007	6.9
TEKEZE 230	N1892	1	0.0918	0.3234	11.3	230	50	0.2642	1.1007	6.9
TOWER NO 1242	DIRE DAWA III 132 BB1	2.968	0.1906	0.4455	8.2	132	50	0.3701	1.3011	5.5
TOWER NO 143	DC WOLKITE GILGEL GIBE	3.812	0.0597	0.4113	8.9	230	50	0.2369	1.2437	5.8
Welayta Sodo 400 kv	Akaki 400	267	0.0206	0.3082	12.5	400	50	0.2215	1.0163	7.1
Welayta Sodo 400 kv	Gilgel Gibe 400KV	119	0.019	0.3291	11.1	400	50	0.2108	0.9855	7
Welayta Sodo 400 kv	Gibe 3 400	51	0.0206	0.3082	12.5	400	50	0.2215	1.0163	7.1
Welayta Sodo 400 kv	Gibe 3 400	51.3	0.0189	0.3097	11.8	400	50	0.1986	1.0479	6.8
WEREGENU 132 TP	KALITI I 132 BB1	17.51	0.1906	0.434	8.4	132	50	0.3724	1.3217	5.6
WEREGENU 132 TP	WEREGENU 132	4.5	0.1906	0.434	8.4	132	50	0.3724	1.3217	5.6
WERETA 66	BAHIR DAR I 66	51.62	0.522	0.4192	8.6	66	50	0.7075	1.4412	5.2
WERETA 66	GONDER II 66	81.82	0.522	0.4192	8.6	66	50	0.7075	1.4412	5.2
WOLAYITA SODO 132	ALABA 132 TP	60.76	0.1941	0.4308	8.4	132	50	0.3765	1.3206	5.6
WOLAYITA SODO 132	Welyat sodo 132 new	1	0.1905	0.4373	8.4	132	50	0.4155	1.2481	6.5
WOLAYITA SODO 132	sawla 132KV	124	0.1905	0.4373	8.4	132	50	0.4155	1.2481	6.5
WOLAYITA SODO 132	ARBAMINCH 132	109.13	0.1905	0.4373	8.4	132	50	0.4155	1.2481	6.5
WOLISSO 66	WOLKITE 66	39.17	0.4261	0.4142	8.7	66	50	0.5707	1.4755	4.7
WOLKITE 230 BB1	hosaiena 230KV	89.3	0.1015	0.4354	8.3	230	50	0.244	1.3021	5.3
WONJI DCP	AWASH II 132 BB1	17.99	0.1906	0.4264	8.6	132	50	0.3678	1.3413	5.6
WONJI TP	AWASH II 132 BB1	17.99	0.1906	0.4264	8.6	132	50	0.3678	1.3413	5.6
WONJI TP	WONJI 132	0.57	0.1906	0.4333	8.4	132	50	0.3732	1.3226	5.6
WUKRO TP	ADIGRAT 132	56.55	0.1835	0.4278	8.6	132	50	0.3674	1.3319	5.5
WUKRO TP	WUKRO 132	1.168	0.1835	0.4278	8.6	132	50	0.3674	1.3319	5.5
YESU FACTORY 132	Akaki II 132	0.3	0.1836	0.4181	8.8	132	50	0.3637	1.3547	5.7
YIRGA ALEM 132	DILLA 132KV	38.7	0.16099	0.415142	8.760153	132	50	0.3766	1.3201	5.6

YIRGA ALEM 132	SHAKISSO 132	133.21	0.1941	0.4308	8.4	132	50	0.3766	1.3201	5.6
YIRGA ALEM 132	AWASA 132	35.09	0.1906	0.4333	8.4	132	50	0.3725	1.3232	5.6
YIRGA ALEM 45	DILLA I 45	39.71	0.5172	0.4093	8.8	45	50	0.7056	1.4592	5.2

Appendix B

Table B.1: EEU Two winding transformer data

Node 1	Node 2	Vn1 [kV]	Vn2 [kV]	Sn [MVA]	Smax [MVA]	X [%]	R [%]
ADAMITULU 132	ADAMITULU 15	132	16	12	12	11.93	0.693
ADDIS CENTER 132	ADDIS CENTER 15	132	15	25	31.5	10.3	0.4608
ADDIS CENTER 132	ADDIS CENTER 15	132	15	25	31.5	10.32	0.458
ADDIS EAST II 132	ADDIS EAST II 15	132	15	20	25	8.162	0.3304
ADDIS EAST II 132	ADDIS EAST II 15	132	15	20	25	8.148	0.3376
ADDIS NORTH 132	ADDIS NORTH 15	132	15	20	25	9.88	0.4355
ADDIS NORTH 132	ADDIS NORTH 15	132	15	20	25	9.84	0.426
AGARO 132	AGARO 15	132	15.75	6.3	6.3	8.08	0.848
ALABA 132	ALABA 15	132	16	6	6	7.4	0.621
ALABA 132	Alaba15KV	132	15	25	31.5	10.3	0.4608
ARBAMINCH 132	ARBAMINCH 15	132	15.75	12.5	12.5	8.24	0.65
ASELA 132	ASELA 15	132	16	12	12	11.93	0.693
AWASA 132	AWASA 15	132	16	12	16	11.919	0.6888
AWASA 132	AWASA 15	132	16	12	16	11.995	0.6872
AWASH 7 KILO 132	AWASH 7 KILO DIE 15	132	16	25	31.5	9.71	0.364
AWASH II 132 BB1	AWASH II 15B	132	15	20	25	8.168	0.312
BEDELE 132	BEDELE 15	132	15.75	6.3	6.3	8.2	0.85
BEDELE230KV	BEDELE 132	230	132	63	63	8.65	0.41
BEDELE230KV	BEDELE 132	230	132	63	63	10.3	0.41
COTOBIE 132	COTOBIE 15B	132	16	12	16	12.105	0.7036
danote 132Kv	Dangote 11.5kv	132	11.5	50	50	11.1	0.83
DEBRE BIRHAN 132	DEBRE BIRHAN 15	132	16	6	6	7.14	0.621
DEBRE ZEIT II 132	DEBRE ZEIT II 15	132	15	16	20	10.591	0.399
DEBRE ZEIT II 132	DEBREZIT II 15A	128	15	16	20	7.8	0.4
DIRE DAWA DIE 132	DIRE DAWA DIESEL 15	141.3	15	33	55	8.472	0.2334
DIRE DAWA I 132	MU DIESEL 15	128	16.5	12	15	6.5	0.5
DIRE DAWA I 132	MU DIESEL 15	128	16.5	12	15	6.5	0.5
DIRE DAWA II 132	DIRE DAWA II 15	128	16	16	20	7.8	0.3535
DIRE DAWA II 132	DIRE DAWA II 15	128	16	16	20	8.027	0.3497

ELALA GEDA 132	ELALA GEDA 15	132	16	12	16	11.997	0.7023
GHIMBI 132	GHIMBI 15	132	15	20	25	7.9904	0.3432
GHIMBI 132	GHIMBI 15	132	15	20	25	7.9984	0.3416
Gidayana 132	Gidayana 33	132	33	6.3	6.3	10.5	0.62
Gidayana 132	Gidayana 33	132	33	6.3	6.3	10.5	0.62
GILGEL GIBE OLD 132	GILGEL GIBE 15	132	15.75	6.3	6.3	8.1	0.85
GUDER 132	GUDER 15	132	16	12	15	7.89	0.6
GUDER 132	GUDER 15	132	16	12	15	7.89	0.6
HAGEREMARIAM132 KV	HAGEREMARIAM33 KV	132	33	20	25	10.5	0.34
HOSAINA 132	HOSAINA 15	132	15.75	6.3	6.3	8.03	0.85
HOSAINA 132	Hos 15KV	132	15	25	31.5	10.3	0.4608
HOSAINA 132	Hosana 15KV	132	15	20	25	9.39	0.3558
Jimma I	Jimma I 15KV	132	15	16	20	7.944	0.3558
Jimma I	JimmaI 15kv	132	15	16	20	7.944	0.3558
JIMMAI I 132	Jimma 15	132	15	20	25	9.39	0.3558
KALITI II 132	KALITI II 15B	132	15	20	25	8.096	0.312
KALITI NORTH 132	KALITI NORTH 15	132	15	16	20	7.81	0.344
KALITI NORTH 132	KALITI NORTH 15	132	15	16	20	7.81	0.344
key Afer132KV	Key Afer33KV	132	33	20	25	10.5	0.73
MEKANISSA 132	MEKANISSA 15	132	15	20	25	8.067	0.353
MEKANISSA 132	MEKANISSA 15	132	15	20	25	8.069	0.3528
MESSOBO 132	MESSOBO 6	132	6	16	20	8.021	0.3824
MESSOBO 132	MESSOBO 6	132	6	16	20	8.021	0.3824
MESSOBO 132	Mesobo New6.3A	132	6.3	45	55	10.5	0.41
MESSOBO 132	MESOBO6.3B	132	6.3	45	55	10.5	0.41
METEHARA 132	METEHARA 15	132	15	18	22	9.87	0.47
MUGER 132	MUGER 15	132	16	12	12	11.933	0.693
MUGER 132	MUGER 15	132	16	12	12	11.933	0.693
N2451	N2450	132	15	25	25	9.71	0.364
N2451	N2450	132	15	25	25	9.71	0.364
NAZRETH II 132	NAZARETH 15NEW	132	15	25	25	9.71	0.364
NAZRETH II 132	NAZARETH 15NEW	132	15	25	25	9.71	0.364
NEKEMTE 132	NEKEMTE 15	132	15	20	25	7.988	0.3456
NEKEMTE 132	NEKEMTE 15	132	15	20	25	7.9448	0.3424
sawla 132KV	Sawla33KV	132	33	20	25	10.5	0.73
SEBETA I 132	SEBETA 15II	132	15	18	22	11.71	0.68
SEBETA I 132	SEBETA 15II	132	15	40	50	10.3	0.29
SHASHEMENE 132	SHASHEMENE 15	132	15	20	25	8.07	0.3544
SHOA ROBIT 132	SHOA ROBIT 15	132	16	6	6	7.16	0.621
TIS ABAY II 132	TIS ABAY II 10.5 GR1	132	10.5	24	40	7.794	0.256
TIS ABAY II 132	TIS ABAY II 10.5 GR2	132	10.5	24	40	7.794	0.2566
WEREGENU 132	WEREGENU 15	132	15	16	20	8.06	0.3569
WEREGENU 132	weregenu 15KVbb1	132	15	25	25	7.948	0.3536
WEREGENU 132	Weregenu Mobile 132KV	132	15	12	16	8.06	0.3569

WONJI 132	WONJI 15	135	16	16	20	8.048	0.4656
WUKRO 132	WUKRO 15	132	15	20	25	8.096	0.312
YESU FACTORY 132	YESU FACTORY 15	132	15	10	10	8.64	0.4

Table B.2 EEU Three winding transformer data

Node 1	Node 2	Node 3	Sn12 [MVA]	Sn23 [MVA]	Sn31 [MVA]	X12 [%]	X23 [%]	X31 [%]	R12 [%]	R23 [%]	R31 [%]
ADIGRAT 132	ADIGRAT 66	ADIGRAT 15	9.6	6.4	6.4	6.552	2.272	6.912	0.3084	0.2065	0.2373
ADIGRAT 132	ADIGRAT 66	ADIGRAT 15	9.6	6.4	6.4	6.552	2.272	6.912	0.3084	0.2065	0.2373
ADWA 132	ADWA 66	ADWA 15	9.6	6.4	6.4	6.632	2.352	6.992	0.3122	0.209	0.2402
ADWA 132	ADWA 66	ADWA 15	9.6	6.4	6.4	6.568	2.288	6.928	0.3092	0.2069	0.2378
AGARO230KV	AGARO 132	AGARO15KV	63	63	23	41.44	10.03	28.4	0.001	0.001	0.001
AKISTA 132	AKISTA66	AKISTA33	20	9	20	10.32	6.4	17.8	0.1	0.15	0.46
Alaba 230KV	ALABA 132	Alba 15KV	25	15	15	2.456	4.344	5.988	0.119	0.074	0.232
Alaba 230KV	ALABA 132	Alba 15KV	25	15	15	2.456	4.344	5.988	0.119	0.074	0.232
ALAMATA 132	ALAMATA 66	ALAMATA 15A	9.6	6.4	6.4	6.6	2.48	7.12	0.3106	0.208	0.239
ALAMATA 230	ALAMATA 132	ALAMATA 15C	25	15	15	2.456	4.344	5.988	0.119	0.074	0.232
ALAMATA 230	ALAMATA 132	ALAMATA 15B	25	15	15	2.456	4.344	5.988	0.119	0.074	0.232
Asebe Teferi 132	ASEEBE TEFERI15	ASEBE TEFERI66KV	20	15	25	6.568	6.928	2.288	0.3092	0.2378	0.2069
Asebe Teferi 132	ASEEBE TEFERI15	ASEBE TEFERI66KV	20	15	25	8	8	8	0.001	0.001	0.001
AWASH 7 KILO 132	AWASH 7 KILO 66	AWASH 7 KILO 15	12	12	4	12.06	2.02	6.69	0.5	0.5	0.5
AWASH II 132 BB1	AWASH II 15A	AWASH II GR1 10.5	4.2	4.2	14	2.905	5.887	7.259	0.298	0.306	0.379
AWASH II 132 BB1	AWASH II 15A	AWASH II GR2 10.5	6	6	20	4.064	7.77	10.43	0.464	0.492	0.4322
AWASH III 132 BB1	AWASH III 15	AWASH III GR2 10.5	6	6	20	4.064	7.77	10.43	0.464	0.492	0.4322
AWASH III 132 BB1	AWASH III 15	AWASH III GR1 10.5	4.2	4.2	14	2.933	5.943	7.266	0.298	0.309	0.38
BAHIR DAR II 230 BB1	BAHIR DAR II 66	BAHIR DAR II 15A	6.3	2.7	2.7	6.309	0.933	3.827	0.889	0.8	0.8
BAHIR DAR II 230 BB1	BAHIR DAR II 132	BAHIR DAR II 15B	50	16.7	16.7	9.341	4.69	8.286	0.389	0.469	0.42

BAHIR DAR II 230 BB1	BAHIR DAR II 132	BAHIR DAR II 15B	50	16.7	16.7	9.349	4.675	8.254	0.389	0.47	0.421
BAHIR DAR II 230 BB1	BAHIR DAR II 66	BAHIR DAR II 15A	6.3	2.7	2.7	6.309	0.933	3.827	0.889	0.8	0.8
BONGA 132	BONGA 33	BONGA 15	20	9.6	9.6	8.59	5.11	15.19	0.383	0.197	0.26
BUTAJIRA 132	BUTAJIRA 33	BUTAJIRA 15	9.6	9.6	9.6	4.0896	2.546	6.893	0.4	0.423	0.409
COMBOLCHA 132	COMBOLCHA 66	COMBOLCHA 15	6	6	12	6.39	13.17	10.24	0.3	0.3	0.3
COMBOLCHA 132	COMBOLCHA 66	COMBOLCHA 15	6	6	12	6.37	13.23	10.3	0.3	0.3	0.3
cOMBOLCHA 230KV	COMBOLCHA NEW132KV	COMBOLCHA NEW33KV	63	63	23	41.44	10.03	28.4	0.001	0.001	0.001
COTOBIE 132	COTOBIE 45	COTOBIE 15A	12	12	4	12	1.64	5	0.08	0.06	0.22
DEBRE BIRHAN 132	DEREBERE HAN15B	DEREBERE HAN33	20	20	25	17	6.5	10.42	0.001	0.001	0.001
DEBRE MARKOS 230	DEBRE MARKOS 66	DEBRE MARKOS 15	6.3	2.7	2.7	6.415	0.939	3.85	0.889	0.8	0.8
DEBRE MARKOS 230	DEBRE MARKOS 66	DEBRE MARKOS 15	6.3	2.7	2.7	6.383	0.9324	3.851	0.889	0.8	0.8
DEBRE ZEIT II 132	debreziet II15Kv	DEBREZIET II33KV	16	8	8	8.4	6.82	2.16	0.3917	0.2394	0.1886
DEMBI DOLO 66	Denbidolo 33	DEMBI DOLO 15	9.6	9.6	5	6.375	2.285	5.8	0.4	0.4	0.4
DILLA 132KV	DILLA33KV	DILLA15B	20	20	12.5	10.5	6.3	17.6	0.4	0.4	0.4
DIRE DAWA I 132	DIRE DAWA I 66	DIRE DAWA I 15	20	20	20	7.88	5.7	14.76	0.451	0.359	0.456
DIRE DAWA III 230	DIRE DAWA III 132 BB1	DIRE DAWA III 15	37.8	11.34	11.34	4.54	2.238	3.8	0.139	0.167	0.148
DIRE DAWA III 230	DIRE DAWA III 132 BB1	DIRE DAWA III 15	37.8	11.34	11.34	4.54	2.238	3.8	0.139	0.167	0.148
endeselase230KV	N1889	N1888	40	20	20	18.02	6.39	11.3	0.001	0.001	0.001
FINCHAA 230	FINCHAA 66	FINCHAA 15A	12.02	12.02	24.2	4.702	1.293	6.944	0.8	0.8	0.868
Finchaa II	Finchaa II 33KV	Finchaa II 15KV	20	10	10	22	8	13.93	0.001	0.001	0.001
Gambela 230kv	GAMBELA 66	GAMBLA33KV	32	16	16	11.94	11.64	11.56	0.001	0.001	0.001
GAMBELA 66	Gambela 33	GAMBELA 15	9	4.8	4.8	6.375	2.285	5.8	0.4	0.4	0.4
GEFARSA 132 BB1	GEFARSA 45	GEFARSA 15A	15	15	15	6.078	3.57	13.125	0.34	0.33	0.38
GEFARSA 132 BB1	GEFARSA 45	GEFARSA 15B	18	6	6	11.44	1.51	5.71	0.477	0.22	0.228

GEFARSA 132 BB1	gef66kv	gef 15kv	20	20	20	7.88	5.7	14.76	0.451	0.359	0.456
GEFARSA 132 BB1	gef33KVNEW	GEF15UEAP	28	8	20	10	6.3	17.6	0.4	0.4	0.4
GG OLD 230KV	GILGEL GIBE OLD 132 BB1	GGOLD33	40	40	12	11.7	30.9	47.7	0.001	0.001	0.001
GG OLD 230KV	GILGEL GIBE OLD 132 BB1	N2441	40	40	12	11.7	30.9	47.7	0.001	0.001	0.001
GHEDO 230	GHEDO 132	GHEDO 15	16	4	4	7.36	3.94	1.876	0.356	0.145	0.102
GHEDO 230	GHEDO 132	GHEDO 15	16	4	4	7.27	3.927	1.89	0.349	0.145	0.109
GHEDO 230	GHEDO 132	GHEDO 15	37.8	11.34	11.34	4.54	2.238	3.8	0.139	0.167	0.148
GONDER II 230	GONDER II 66	GONDER II 15	16	16	16	4.672	4.01	9.02	0.3286	0.3202	0.2914
HARAR II 132	HARAR II 66	HARAR II 33	20	9.6	9.6	8	2.408	6.896	0.384	0.17	0.24
HARAR II 132	HARAR II 66	HARAR II 33	20	9.6	9.6	8	2.4	6.928	0.379	0.167	0.239
HUMERA230KV	HUMERA15KV	HUMERA33KV	25	12.5	12.5	17.87	6.42	11.2	0.275	0.262	0.25
JIJIGA II 132	JIJIGA II 33	JIJIGA II 15	20	9.6	9.6	8.4	2.16	6.82	0.3917	0.1886	0.2394
KALITI I 132 BB1	KALITI I 45 BB1	KALITI I 15	18	12	6	11.34	1.56	5.88	0.5088	0.2133	0.2833
KALITI I 132 BB1	KALITI I 45 BB1	KALITI I 15	18	6	6	11.49	1.515	5.69	0.476	0.226	0.276
KALITI I 132 BB1	KALITI I 45 BB1	KALITI I 15	20	20	8	11.016	1.7536	6.7776	0.512	0.2637	0.2812
KALITI II 132	KALITI II 45	KALITI II 15A	20	8	8	10.984	1.744	6.8064	0.5208	0.2658	0.2842
Kemisse 132	Kemisse 33	Kemisse 15	20	20	12.5	10.39	6.42	17.5	0.4	0.4	0.4
KOKA 132 BB1	KOKA HYDRO 10.5 GR1	KOKA HYDRO 15	18	6	6	9.629	8	3.94	0.5364	0.4763	0.433
KOKA 132 BB1	KOKA 45	KOKA 15	12	4	4	12.37	4.97	18.57	0.569	0.799	0.966
KOKA 132 BB1	KOKA HYDRO 10.5 GR2	KOKA HYDRO 15	18	6	6	9.548	8	3.955	0.5311	0.4797	0.436
KOKA 132 BB1	KOKA HYDRO 10.5 GR3	KOKA HYDRO 15	18	6	6	9.615	8	3.959	0.5238	0.453	0.43
lEGETAFO 230KV	lEGETAFO132KV	LEGTAFO15KV	63	63	23	41.44	10.03	28.4	0.001	0.001	0.001
MEKELE 230	MEKELE 132	MEKELE 15	25	15	15	2.456	4.344	5.988	0.119	0.074	0.232
MEKELE 230	MEKELE 132	MEKELE 15	25	15	15	2.456	4.344	5.988	0.119	0.074	0.232
MELKA WAKENA YOU 132	MELKA WAKENA YOU 66	MELKA WAKENA YOU 15	6	6	6	10.1	7.08	15.06	0.828	0.7	0.681

MELKA WAKENA YOU 132	MELKA WAKENA YOU 66	MELKA WAKENA YOU 15	6	6	6	10.11	7.09	15.08	0.83	0.7	0.705
METU230 KV	METU166KV	METU15KV	40	20	20	22.49	8.16	13.82	0.001	0.001	0.001
MIZAN 132	MIZAN 66	MIZAN 33	20	9.6	9.6	8.632	2.496	7.265	0.6348	0.2912	0.4021
MUGER 132	MUGER NEW33KV	MUGER NEW15	28	8	20	10	6.3	17.6	0.4	0.4	0.4
NEGELE BORENA 66	NEGELE BORENA 33	NEGELE BORENA 15	9	4.8	4.8	6.375	2.285	5.8	0.4	0.4	0.4
SEBETA 230 BB1	SEBETA I 132	SEB NEW TR115kv	63	63	21	9.349	4.675	8.254	0.389	0.469	0.42
SEBETA 230 BB1	SEBETA I 132	SEBTRA215 kv	63	63	21	9.349	4.675	8.254	0.385	0.469	0.42
SEBETA I 132	SEBETA 45A	SEBETA 15III	20	8	8	11	1.79	6.78	0.328	0.16	0.216
SEBETA I 132	SEBETA 45B	SEBETA 15I	12	4	4	12.485	4.78	18.45	0.558	0.795	0.966
SHAKISSO 132	SHAKISSO 66	SHAKISSO 15	6	6	6	10.14	7.08	15.06	0.82	0.7	0.775
SHAKISSO 132	SHAKISSO 66	SHAKISSO 15	6	6	6	10.09	7.08	15.06	0.816	0.7	0.775
Sululta 132KV	Sululta 33	SULULTA 15	50	25	25	17.68	6.96	10.32	0.001	0.001	0.001
TEKEZE 230	TEKEZE66KV	TEKEZE6.6 KV	20	20	20	13.9	8	8	0.5	0.4	0.5
TEPI 66	TEPI 33	TEPI 15	9.6	5.04	5.04	7.34	4.07	12.57	0.3869	0.2121	0.2683
WOLAYITA SODO 132	WOLAYITA SODDO 66	WOLAYITA SODDO 15	6	6	6	10.06	7.06	14.98	0.772	0.7	0.681
WOLKITE 230 BB1	WOLKITE 66	WOLKITE 33	16	16	16	5.56	2.756	8.68	0.2456	0.252	0.246
YIRGA ALEM 132	YIRGA ALEM 45	YIRGA ALEM 15	12	12	4	12.2	12.1	7.3	0.5	0.5	0.5
YIRGA ALEM 132	YIRGALEM33KV	YIRGALEM 15B	20	20	12.5	10.39	6.42	17.5	0.4	0.4	0.4

Appendix C

UPFC series converter injected voltage, real and reactive power at different location

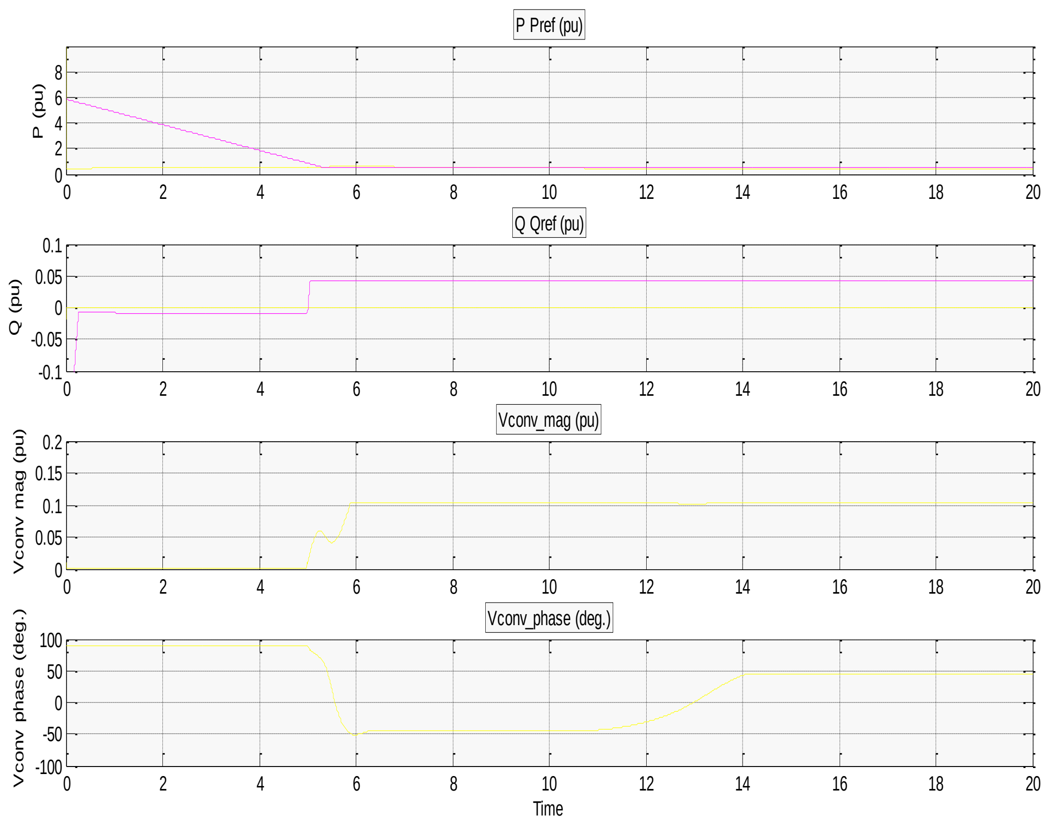

Figure C.1: UPFC series converter injected voltage, real and reactive power for UPFC between GGI old132 and Jimma

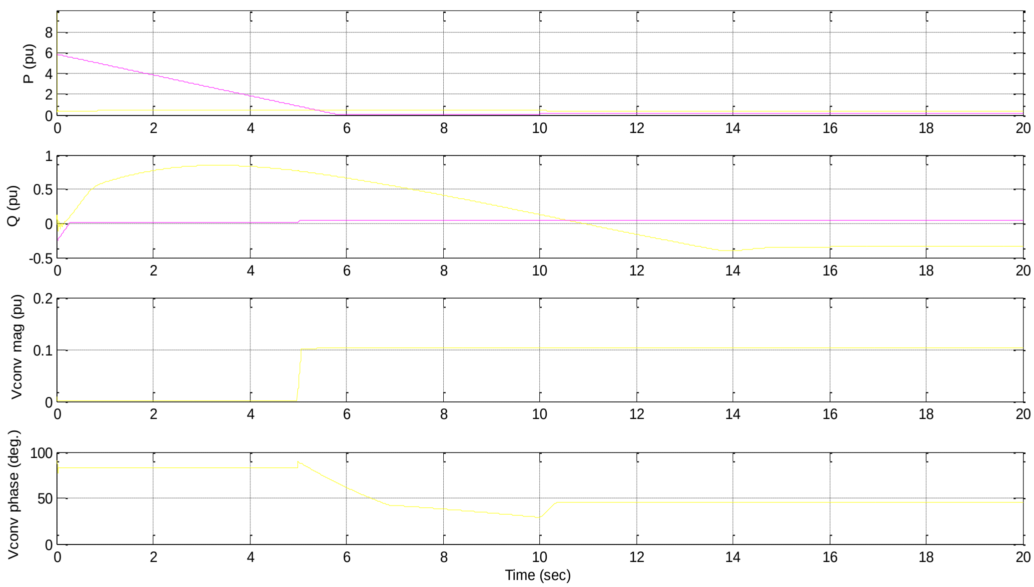

Figure C.2: UPFC series converter injected voltage, real and reactive power for UPFC between Jimma and Agaro operated with voltage regulation mode

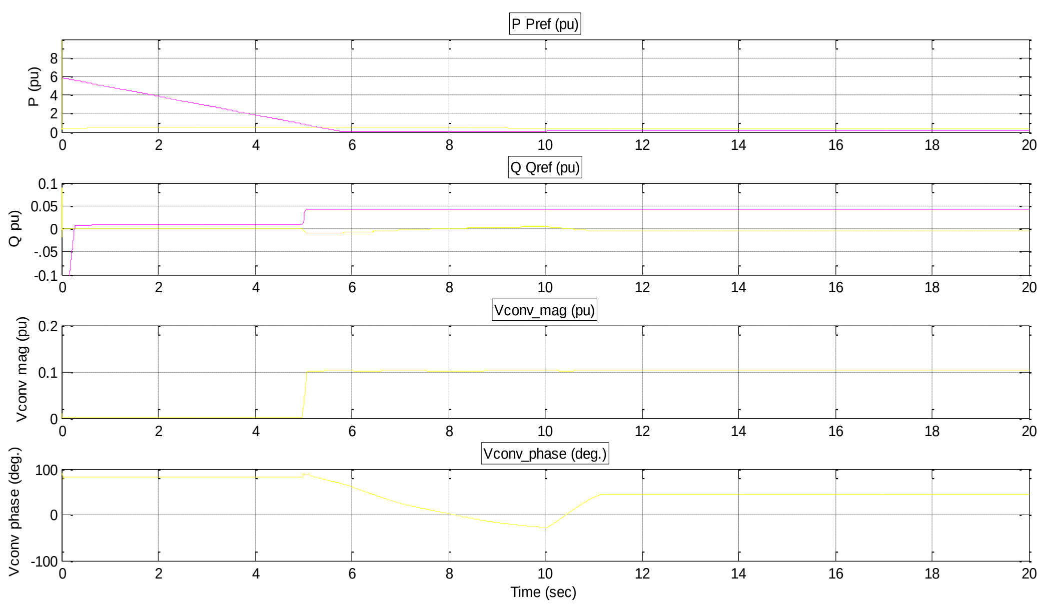

Figure C.3: UPFC series converter injected voltage, real and reactive power for UPFC between Jimma and Agaro operated with var control mode

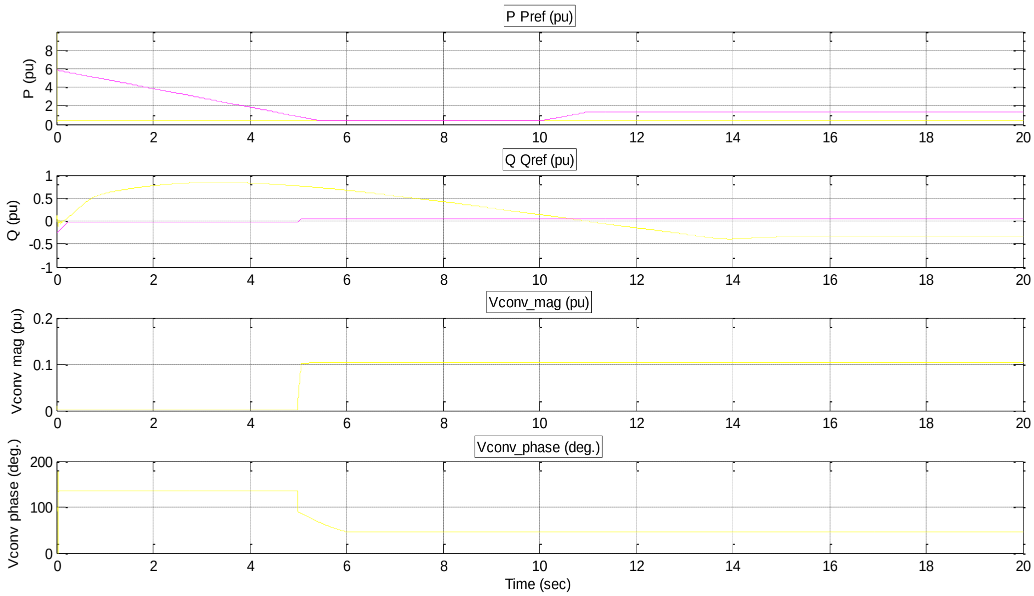

Figure C.4: UPFC series converter injected voltage, real and reactive power for UPFC between Jimma-bus and ABBA-bus operated with voltage regulation mode

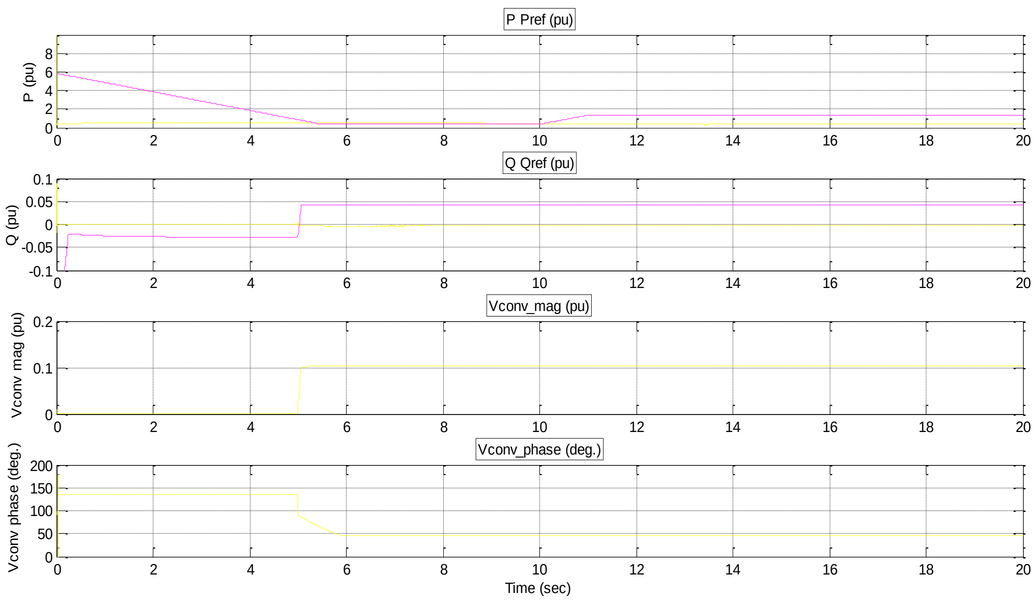

Figure C.5: UPFC series converter injected voltage, real and reactive power for UPFC between Jimma-bus and ABBA-bus operated with var control mode

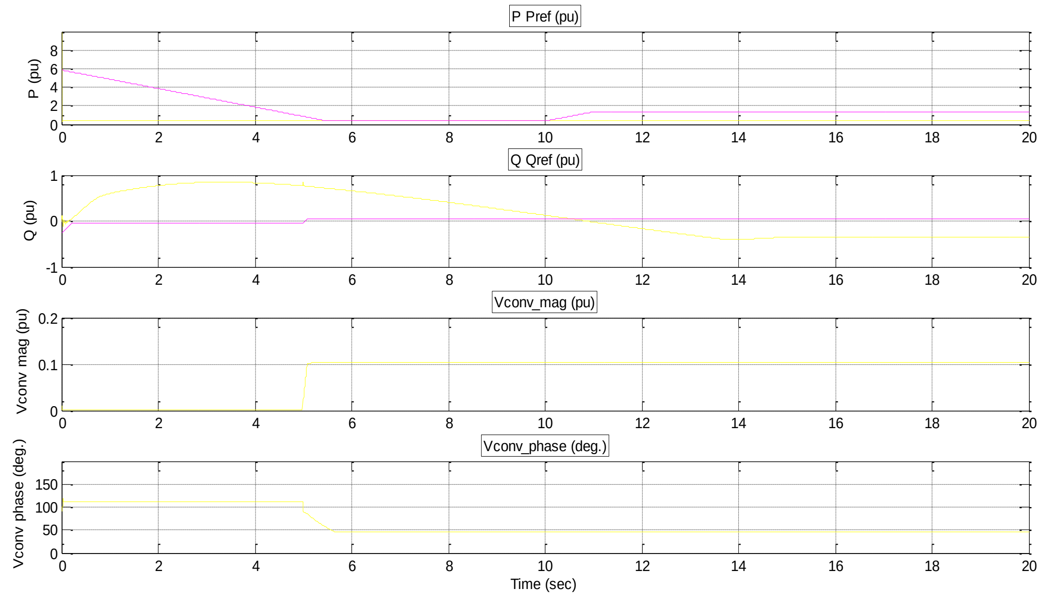

Figure C.6: UPFC series converter injected voltage, real and reactive power for UPFC between Jimma-bus and Bonga-bus operated with voltage regulation mode

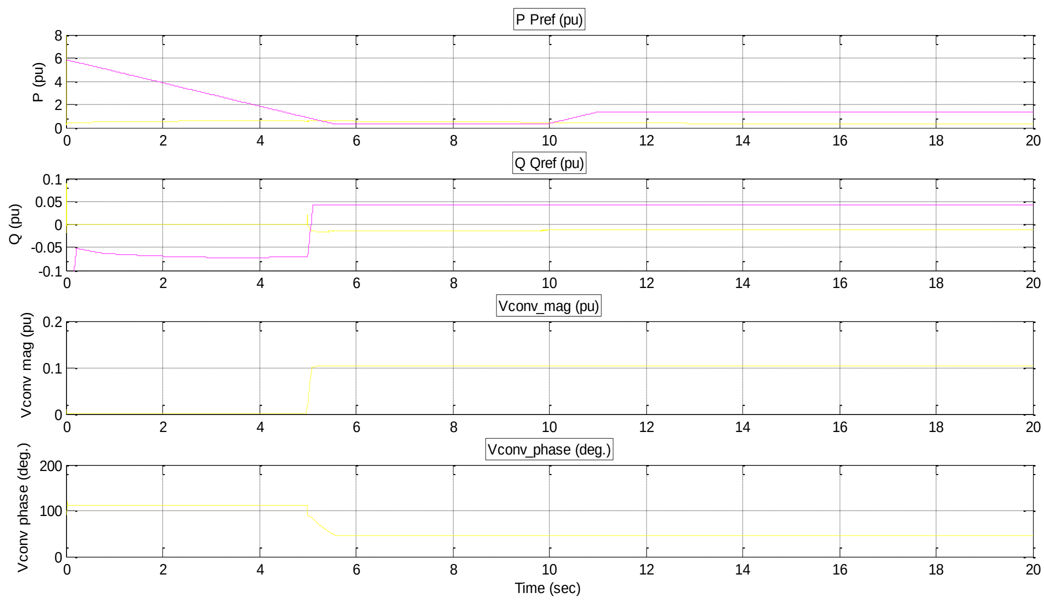

Figure C.7: UPFC series converter injected voltage, real and reactive power for UPFC between Jimma-bus and Bonga-bus operated with var regulation mode

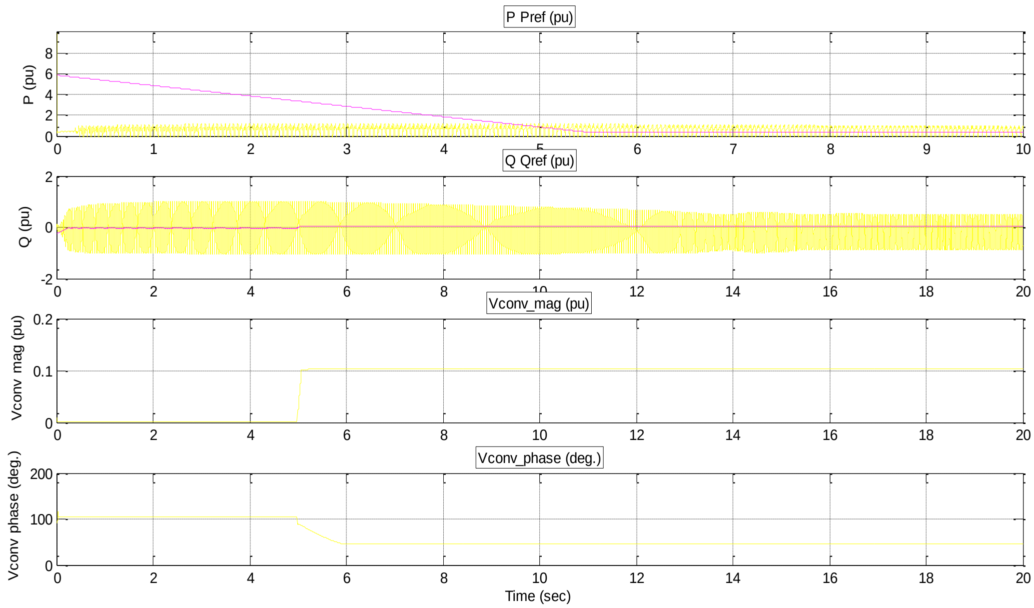

Figure C.8: UPFC series converter injected voltage, real and reactive power for UPFC between Bonga-bus and Mizan-bus operated with shunt converter voltage regulation mode

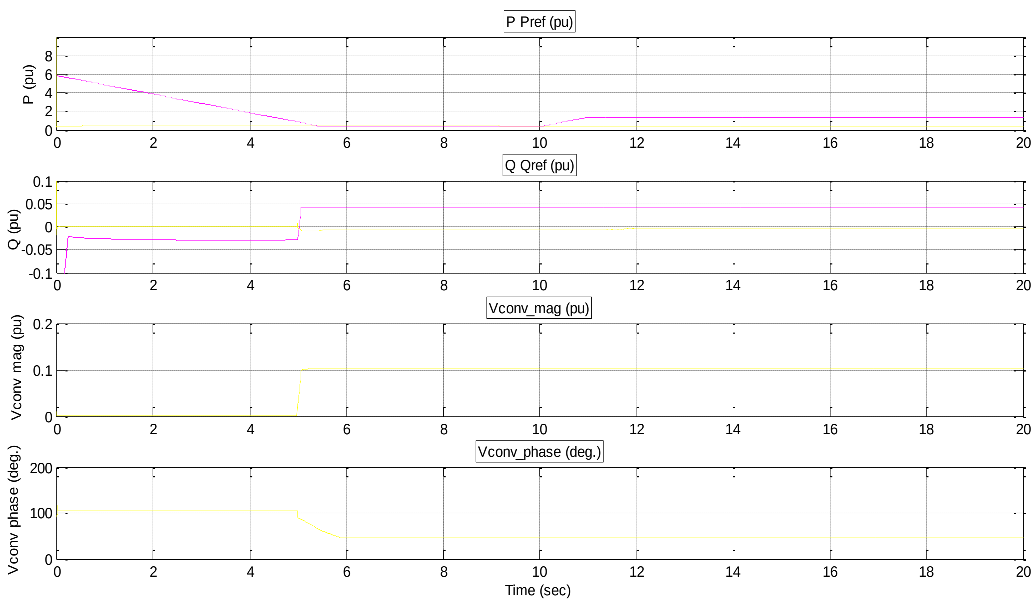

Figure C.9: UPFC series converter injected voltage, real and reactive power for UPFC between Bonga-bus and Mizan-bus operated with shunt converter var control mode